INFORMATION TO USERS

The most advanced technology has been used to photograph and reproduce this manuscript from the microfilm master. UMI films the text directly from the original or copy submitted. Thus, some thesis and dissertation copies are in typewriter face, while others may be from any type of computer printer.

The quality of this reproduction is dependent upon the quality of the copy submitted. Broken or indistinct print, colored or poor quality illustrations and photographs, print bleedthrough, substandard margins, and improper alignment can adversely affect reproduction.

In the unlikely event that the author did not send UMI a complete manuscript and there are missing pages, these will be noted. Also, if unauthorized copyright material had to be removed, a note will indicate the deletion.

Oversize materials (e.g., maps, drawings, charts) are reproduced by sectioning the original, beginning at the upper left-hand corner and continuing from left to right in equal sections with small overlaps. Each original is also photographed in one exposure and is included in reduced form at the back of the book. These are also available as one exposure on a standard 35mm slide or as a 17" x 23" black and white photographic print for an additional charge.

Photographs included in the original manuscript have been reproduced xerographically in this copy. Higher quality 6" x 9" black and white photographic prints are available for any photographs or illustrations appearing in this copy for an additional charge. Contact UMI directly to order.

U·M·I

University Microfilms International
A Bell & Howell Information Company
300 North Zeeb Road, Ann Arbor, MI 48106-1346 USA
313/761-4700 800/521-0600

Order Number 8906886

Multicomponent flow injection analysis and quantitative infrared emission spectroscopy: Chemometric applications

Erickson, Brice Carl, Ph.D.

University of Washington, 1988

U·M·I
300 N. Zeeb Rd.
Ann Arbor, MI 48106

MULTICOMPONENT FLOW INJECTION ANALYSIS AND QUANTITATIVE INFRARED EMISSION SPECTROSCOPY: CHEMOMETRIC APPLICATIONS

by

BRICE CARL ERICKSON

A dissertation submitted in partial fulfillment
of the requirements for the degree of

Doctor of Philosophy

University of Washington

1988

Approved by _____

(Chairperson of Supervisory Committee)

_____

_____

_____

Program Authorized
to Offer Degree Chemistry

Date August 18, 1988

In presenting this dissertation in partial fulfillment of the requirements for the Doctoral degree at the University of Washington, I agree that the Library shall make its copies freely available for inspection. I further agree that extensive copying of this dissertation is allowable only for scholarly purposes, consistent with "fair use" as prescribed in the U.S. Copyright Law. Requests for copying or reproduction of this dissertation may be referred to University Microfilms, 300 North Zeeb Road, Ann Arbor, Michigan 48106, to whom the author has granted "the right to reproduce and sell (a) copies of the manuscript in microform and/or (b) printed copies of the manuscript made from microform."

Signature Brian Erickson

Date August 18, 1988

University of Washington

Abstract

MULTICOMPONENT FLOW INJECTION ANALYSIS AND QUANTITATIVE INFRARED EMISSION SPECTROSCOPY: CHEMOMETRIC APPLICATIONS

by Brice Carl Erickson

Chairperson of the Supervisory Committee: Professor Bruce R. Kowalski
Department of Chemistry

Chemometrics involves the use of mathematical and statistical methods to provide maximum information from chemical data. A number of methods and algorithms have been developed which have been found useful in the analysis of chemical data. The developments in this volume include the use of chemometric methods in two areas which have generally been overlooked in the past. The first is the use of flow injection analysis (FIA) methods for mixtures using non-specific detectors. The Self-Modeling Curve Resolution method of Lawton and Sylvestre is used to distinguish analytes from background absorber in the sample using a UV/Visible absorbance detector. The second is infrared emission spectroscopy which, although currently used in a few applications, should become a much more generally useful tool when combined with the power of multivariate calibration methods. The Partial Least Squares method is applied to emission spectra for estimation of sample composition, thickness and temperature.

Table of Contents

List of Figures

List of Tables

ACKNOWLEDGEMENTS

Many people deserve thanks for the impact they have had on the completion of this work.

I wish to express my appreciation to Professor Bruce Kowalski for his guidance, and for making sure "philosophy" is an integral part of the "Doctor of Philosophy" degree in chemistry.

The Center for Process Analytical Chemistry and the many industrial sponsors must be acknowledged for financial support for much of this work.

I would especially like to thank Randy Pell for sharing the responsibilities and accomplishments, as well as the frustrations, of research. Thanks to other members of the Laboratory for Chemometrics--Dave Haaland, Pat Carey, Scott Ramos, Sandy Moore, Eugenio Sanchez, Ken Beebe, Bruce Wilson, Walter Lindberg, Avi Lorber, David Veltkamp, Peter Schlagel, Larry Wangen and Mary Beth Seasholtz--for providing a supportive and creative atmosphere. Others deserving thanks for their involvement in these projects include Professors Ruzicka and Callis.

"Thanks" can never sufficiently convey what should be expressed to those special people whose love, faith, support and commitment have shaped all that I am and do--my parents, Reynold and Marian Erickson, and my wife Shirley and son Jared.

Soli Deo Gloria!

To Shirley

and Jared

Introduction

According to the International Chemometrics Society, chemometrics has been defined as "the chemical discipline that uses mathematical and statistical methods, (a) to design or select optimal measurement procedures and experiments; and (b) to provide maximum chemical information by analyzing chemical data. In the field of Analytical Chemistry, Chemometrics is the chemical discipline that uses mathematical and statistical methods for the obtention in the optimal way of relevant information on material systems."[1] The development and use of chemometric methods has been closely tied to the development and availability of the computer power necessary for its use, and both have greatly expanded in the last few years. A number of methods and algorithms have been developed which have been found useful in the analysis of chemical data. While chemometric methods have been applied to several analytical methods, the number of applications will undoubtedly continue to grow as new algorithms and creative uses and adaptations of current methods are developed.

In fact, whole new areas of chemical analysis are being opened up by the use of chemometrics. Perhaps the most notable example has been the use of multivariate calibration methods in near infrared (NIR) spectroscopy, which due to the complexity of its spectra had not previously been found useful for chemical analysis.

The developments in this volume include the use of chemometric methods in two additional areas which have generally been overlooked in the past. The first is the use of flow injection analysis (FIA) methods using non-specific detectors. The second is infrared emission spectroscopy which, although currently used in a few applications, should become a much more generally useful tool when combined with the power of multivariate calibration methods.

Chapter 1. Flow Injection Analysis

1.1 Introduction

Flow injection analysis (FIA) was introduced by Ruzicka and Hansen in 1975.[2] A typical FIA system is shown in figure 1.1.1. A carrier or reagent solution is pumped through narrow bore tubing, generally with an i.d. of around 0.5 mm. A small amount of sample is then injected into the flowing stream of carrier using a valve or syringe. The sample is allowed to disperse into the carrier stream under controlled conditions. The analyte or a product of the reaction of analyte with a reagent in the carrier is detected at a point downstream. The main advantages of FIA are its speed, simplicity, low reagent consumption and reproducibility, which account for the great popularity the technique has gained in just over a decade. These advantages are due mainly to the fact that all samples are treated identically, so that reaching a steady-state is not necessary.

The types of data obtained from most Flow Injection Analysis experiments as currently practiced therefore are also relatively simple. The output is typically a single peak for each sample with a reproducible shape, varying only in size from one sample to the next so that peak height, area or width can be related to concentration. Resolution of a particular analyte from a mixture or solution in colorimetric FIA procedures has generally depended either on the specificity of the chemical reaction between analyte and reagent in the flowing stream, or the specificity of the detector. These operational parameters must be chosen very carefully to avoid interferences from other components of the sample.

FIA methods have therefore generally been restricted to detection of a single analyte where chemical reaction with a reagent is involved. Alternatively, FIA may be used as a sample handling technique for other instrumentation capable of resolving multiple

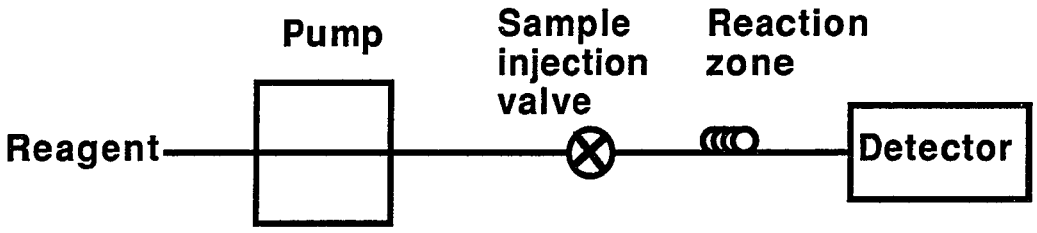

FIGURE 1.1.1. Typical flow injection analysis system. The sample loop of the injection valve may either be filled manually or by a second tube line from a pump.

analytes, such as flame emission spectroscopy [3] or inductively coupled plasma/atomic emission spectroscopy,[4] or solving a sytem of equations using the same number of wavelengths as analytes.[5, 6]

As a result, when several analytes are to be determined by colorimetric FIA methods, each generally requires a separate FIA channel, including pump channel, injection loop or valve, reaction zone and detector. In addition, where colorimetric detection is used it is often difficult to distinguish the product of the reaction of analyte with reagent from background color which may be present in the sample due to unknown components. This requires adequate sample preparation to assure that no interfering species are present.

In this work a method is presented for determining multiple analytes or an analyte in the presence of a background absorber based on varying peak shapes. This is accomplished by creating gradients which result in varying ratios of reagent to analyte, or varying conditions such as pH, over the zone of injected sample. Chemometric methods of data analysis are used to resolve the data. While a number of chemometric methods are available which might be applied to various types of experiments, such as Partial Least Squares regression or the Generalized Rank Annihilation Method, the method used here involves Curve Resolution methods of Lawton and Sylvestre. This is an important first step in opening up the use of FIA for multiple analyte detection using non-specific reagents and/or detectors.

1.2 History

In order to optimize the experimental conditions for the gradients necessary for the use of these methods, a basic understanding of the dynamics of flowing systems on the scale of FIA systems is necessary.

Continuous Flow Analysis (CFA) methods are used for the automated chemical analysis of a number of analytes in a variety of types of samples. A sample is incorporated in a flowing stream, usually caused to mix and react with one or more reagents, and the resulting product is detected. In designing such a system there are two criteria which must be satisfied having to do with mixing: the sample must be adequately mixed with the reagent(s) to produce the desired product, yet consecutive samples must be adequately separated so that they can be distinguished from one another.

In early attempts to use flow systems for analysis under laminar flow conditions, samples were pumped continuously into the stream and mixed sequentially with reagents to produce a detectable product. Due to the long times necessary to flush the sample out of the system under laminar flow, analysis rates were about 10-15 samples per hour.

The AutoAnalyzer technology originally developed by Skeggs in the 1950's and used extensively since that time, especially in clinical laboratories, was able to increase analysis rates by partitioning the stream into small segments using air bubbles.[7] Samples and reagents are merged into the stream through T type fittings, and the friction at the wall which causes currents to be set up within each segment, along with gravitational effects as the segments move through mixing coils, assure complete mixing. While there is some movement of solution from one segment to the segment behind by capillary action at the walls, a short wash between samples is generally sufficient to be able to distinguish between samples at rates of 20 or more samples per hour. There are a number of drawbacks, however, to including air bubbles in the flowing stream. These include the need for surfactants to maintain flow and avoid "pulsing" due to pressure drops in the system, the need to wait for a steady-state signal

due to poor reproducibility of sampling, long start-up times, and the need to remove the bubbles before detection.

Flow Injection Analysis (FIA) as developed by Ruzicka and Hansen [2] which uses small diameter tubing (usually around .5mm) does not include air bubbles in the stream. The sample is injected, rather than continuously pumped, into a carrier stream, usually by means of a valve. The sample disperses into the carrier and is allowed to react with reagent(s) either present in the carrier or added through mixing T's. Steady-state readings are not required due to the reproducibility of the injection and flow systems. When properly configured, these systems generally use far less reagent than the AutoAnalyzer systems, and are often capable of analyzing 120 or more samples per hour.

1.3 Flow Dynamics

In an attempt to explain the results obtained by FIA methods, and to optimize system design, there have been a few attempts to outline the theory of the hydrodynamic principles which affect the dispersion of the sample into the flowing stream.[8,9,10,11] These are generally based on earlier work in the chemical engineering literature,[12,13,14] especially impulse-response experiments to study residence time distributions in chemical reactors, and more recent work on chromatographic systems.[15,16]

In ideal chemical reactors, either perfectly mixed batch reactors or plug flow tubular reactors, each atom of material spends the same amount of time in the reactor. This rarely being the case, chemical engineers have developed methods to model nonideal systems. These models of flowing systems serve as a good starting point for developing the theory of FIA. Rather than simply referring to the mean time atoms

spend in the reactor, T, which is the reactor volume divided by the flow rate, it is useful to discuss the residence time distribution (RTD) of a system, which is the relative proportions of fluid elements that remain in the system various lengths of time. This is determined experimentally by injecting a tracer into the reactor and monitoring its concentration in the effluent over time. In a pulse input experiment an amount of tracer is injected into the stream in as short a time as possible. The effluent concentration curve over time, C(t), is referred to as a C curve, as seen in figure 1.3.1 for ideal plug or mixed flows, and an arbitrary flow. The E(t) curve is referred to as the resident time distribution function and is simply the C(t) curve normalized for the amount of tracer injected, or the area under the curve.

Alternatively, a step injection may be used where an inert input flow is suddenly replaced by a constant flow of tracer. In a negative-step tracer experiment a constant flow of tracer is suddenly replaced by the inert flow. The output concentration over time is then called an F curve, and as can also be seen in figure 1.3.1, will appear as the integral of the C curve.

In general, pulse experiments are most like FIA experiments.

If sample dispersion is to be minimized a desirable situation would be turbulent flow, where the path of an individual molecule is random as streamlines in the solution cross causing rapid mixing, which would approach plug flow. In a straight tube this is assumed to begin to occur when the system has a Reynolds number (Re) above about 2000 (although turbulence at higher Re can be suppressed with proper system geometry) where

$$Re = 4 \rho q / \pi d \phi$$

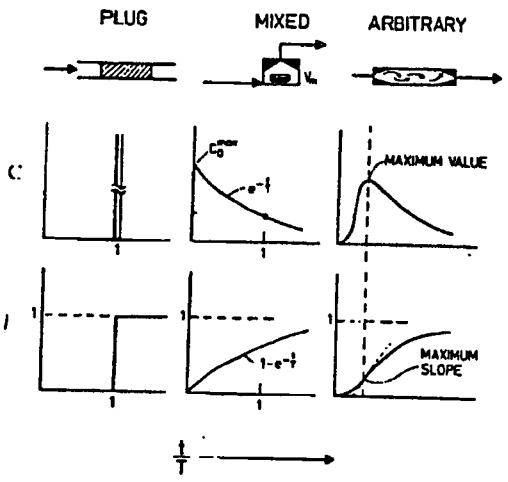

FIGURE 1.3.1. Residence Time Distribution Curves. [8]

and ρ is density in g/ml, q is flow rate in ml/sec, d is channel diameter in cm and ϕ is the fluid viscosity in poise. But the pressures necessary for turbulent flow preclude the use of the simple instrumentation which is one of the main advantages of FIA. Re for typical FIA systems are generally in the range of 20 to 130, so turbulent flow conditions do not apply.

If a straight cylindrical tube under laminar flow conditions with constant flow is assumed, a parabolic flow velocity distribution is set up within the tubing with flow rate at the center double the average flow rate, and flow velocity of zero at the wall (figure 1.3.2) where

$$F_i = 2F(1 - r_i^2/R^2)$$

and F_i is the flow velocity at distance r_i from the center of tubing with radius R and F is average flow velocity. If no additional mixing effects are assumed there are obvious problems in that mixing with the reagent in the stream will be minimal, and some of the sample will remain at the wall and will never be completely washed out of the system.

An additional parameter affecting the concentration profile within the tubing of actual systems is molecular diffusion. This results in the stationary sample adjacent to the wall eventually diffusing away from the wall to the faster moving portion of the stream in the center, and sample in the faster portion is able to diffuse into the slower portion. Tubing diameter is important: the narrow bore tubing used in most FIA systems (around 0.5 mm) minimizes the distance a molecule must diffuse for effective radial mixing. Therefore the "infinite" washout times predicted by laminar flow alone are not observed.

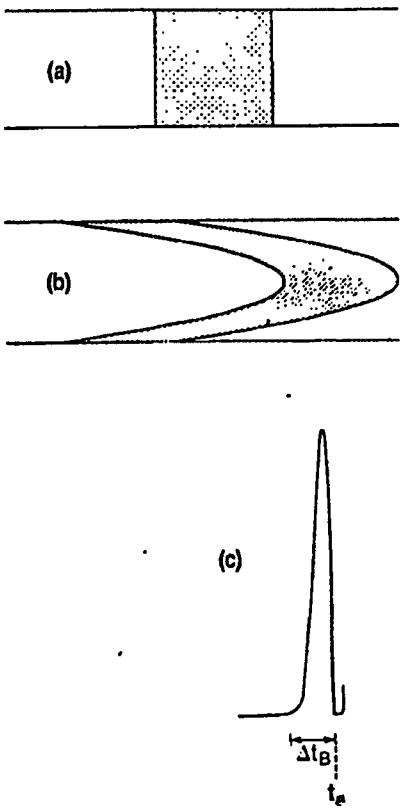

FIGURE 1.3.2. Parabolic flow velocity under laminar flow conditions. Bolus shapes (a) at injection and (b) after injection. (c) Peak shape observed at detector.[11]

Where there is sufficient radial mixing in the tubing, the system may be modeled as a series of continuously stirred tanks (tanks-in-series model). For one tank, the normalized C curve is expressed as

$$C(t) = (1/t_i)\, e^{(-t/t_i)}$$

where t_i is the mean residence time of the material in one tank, which is equal to the tank volume divided by flow rate. Mixing chambers, as in the center of figure 1.3.1, have been used in FIA, especially where peak width measurements are desired, such as in titrations, and are modeled well by this expression. For a series of N tanks, the normalized C curve is

$$C(t) = (1/t_i)\, (t/t_i)^{N-1}\, [1/(N-1)!]\, e^{(-t/t_i)} = \{t^{N-1} / [(N-1)!\, t_i^N]\}\, e^{(-t/t_i)}$$

For large N, this curve approaches a Gaussian shape; it is increasingly skewed as N decreases as seen in figure 1.3.3. The variance of the curve

$$\sigma^2 = N\, t_i^2 = T^2/N$$

where $T = N\, t_i$ is the mean residence time in the entire system. If $N \geq 10$ so that a Gaussian distribution is achieved, σ^2 is related to sample dispersion by

$$\sigma^2 = 2\, \delta$$

where the dispersion number, δ, is dimensionless

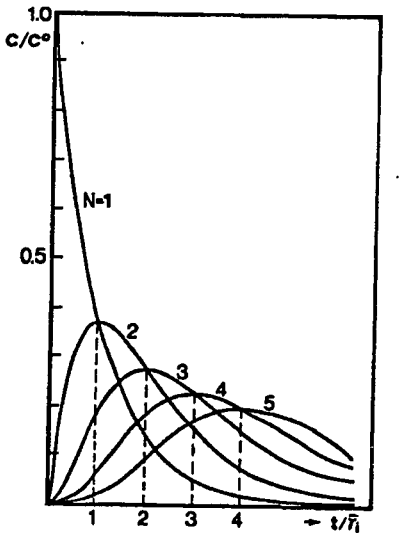

FIGURE 1.3.3. Tanks in series model. C-curves observed for 1, 2, 3, 4, and 5 tanks in series.[8]

$$\delta = D/FL$$

and D is the axial dispersion coefficient in cm^2/sec, F is mean linear flow velocity and *L* is tube length. So

$$\delta = (1/2)(T^2/N)$$

indicating that if the mean residence time, T, is held constant while the number of mixing chambers, N, is increased then dispersion is decreased, eventually approximating a plug flow.

The mixing efficiency of a system can be expressed (in analogy to chromatographic plate height) by the height of an imaginary mixing stage expressed as a volume,

$$H_V = V_r/N$$

time,

$$H_t = T/N$$

or length

$$H = L/N = L(\sigma)_t^2/T^2.$$

It may also be expressed by the radial mass transfer constant, *a*, which is the reciprocal of the mean residence time in a single tank

$$a = 1/t_i = Q/V_i = F/H = N/T$$

where Q is flow rate, V_r and V_i are volumes of the total system and a single tank, respectively. Therefore a smaller H or larger a value indicates more efficient radial mixing.

One might expect that increasing flow rate would be the best way to increase mixing (and therefore N) and decrease dispersion since this eventually leads to turbulent flow, as is generally done in chemical reactor engineering. But the dispersion number is dependent on the linear flow velocity. Axial dispersion is mainly due to the parabolic axial velocity profile, where the liquid in the center of the tubing travels at twice the mean velocity; thus an increase in flow rate will actually increase axial dispersion unless it is accompanied by additional mixing, for example due to turbulent flow. If, on the other hand, flow velocity is reduced, radial mixing which is due to molecular diffusion will begin to dominate and break down the parabolic profile caused by the flowing liquid. Figure 1.3.4 shows the effective mixing height at various flow rates in a typical FIA system with straight tubing; the decrease in H with decreasing flow rate indicates that dispersion will be minimized at lower flow rates. According to Taylor's studies, radial diffusion will affect velocity profiles if residence time $T=r^2/3.8^2D_c$ where D_c is the molecular diffusion coefficient. For values typical for FIA, this is about 6.2 sec for .5mm i.d. tubing, but increases rapidly to 25 sec for 1mm i.d. tubing; considering the large size of chemical reactors, it is obvious why this effect has generally not been found useful in chemical engineering applications. A minimum is seen at about Re = 0.1 where the molecular diffusion nearly compensates

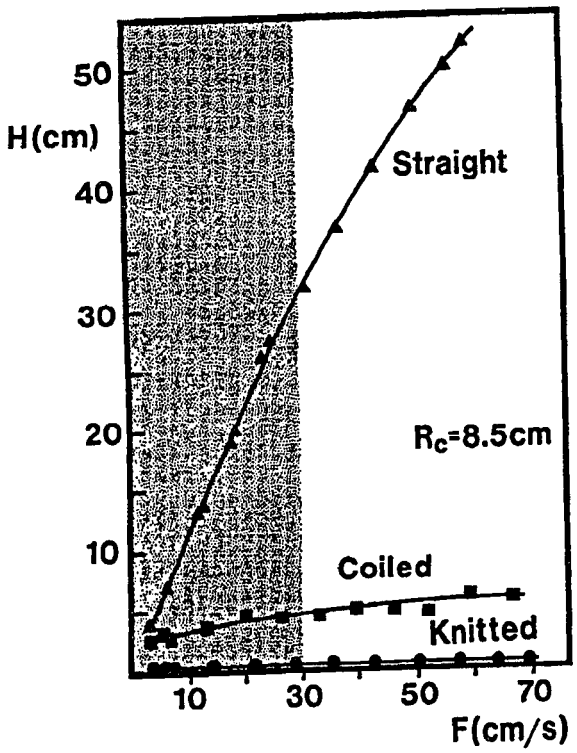

FIGURE 1.3.4. Mixing height vs. flow rate. Dispersion expressed as mixing height for straight, coiled and knitted tubing as a function of linear flow velocity, F (cm/s). Tubing length is 10 m; inside diameter is 0.56 mm. Shaded area covers flow velocities typical for FIA.[9]

for the velocity profile, although this is too slow to be practical in real systems.

The above discussion using the tanks-in-series model is generally applicable for systems with sufficient mixing length (high N), and small injection volume, so that Gaussian peak shapes are obtained. However complex changes are observed between the time of injection and obtaining a Gaussian shaped peak. Again straight open tubes will be assumed. It is useful to discuss observations in terms of reduced time,

$$\tau = (D_m/R^2)\, t$$

and reduced length,

$$L^* = (D_m/R^2F)\, L = (D_m/R^2)\, T$$

where t is time since injection and D_m is the molecular diffusion coefficient in cm^2/sec. Vanderslice *et al.* have calculated the bolus shapes at various times. Figure 1.3.5 shows the bolus shapes and the C curves observed at selected times. For $\tau < 0.01$, convection (parabolic flow velocity profile) dominates the dispersion of solute giving a sharp rise followed by exponential decay (similar to the single tank model). For $\tau > 0.1$, diffusion effects dominate giving near-Gaussian shaped peaks (as in high N tanks-in-series model). But for $0.01 \leq \tau \leq 0.1$ a double peak (or shoulder) is expected; the rounded peak begins to dominate with increasing τ as dispersion effects begin to dominate. Note that this is quite different from the skewed single peaks that would be expected from the tanks-in-series model with low N.

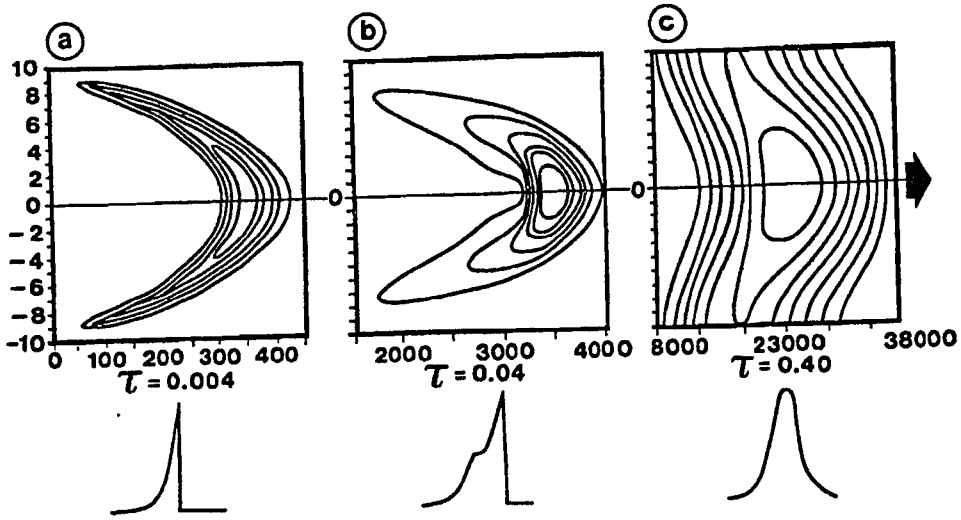

FIGURE 1.3.5. Bolus shapes. Dispersion of a sample plug in a straight tubular channel as affected by molecular diffusion with increasing residence time (top) and corresponding RTD curves (bottom). From left to right $\tau = 0.004$, $\tau = 0.04$, and $\tau = 0.40$.[9]

Other radial mass transfer and convection effects will influence dispersion when the system no longer consists of straight tubing. Coiled tubing reactors have been used extensively, initially for convenience. But centrifugal forces in these systems also set up radial secondary flows, perpendicular to the main axial flow. The flows provide convective transport across the channel, and also bisect the channel so that diffusion distances are cut in half (figure 1.3.6). This increase in radial mixing results in reduced axial dispersion of the sample, which in a typical FIA system provides moderate improvement in performance by reducing peak width and thus increasing sample throughput.

A variety of other system geometries (see examples in figure 1.3.7) have been used which result in sudden changes in the direction of flow to increase radial mass transfer, and therefore reduce axial dispersion. One of the most effective methods involves use of reactors filled with inert beads. Packed beds are generally avoided due to high pressure drops which complicate the equipment involved. However, single bead string reactors, where the bead diameter is greater than half the channel diameter, have been used. The changes in flow direction in this case are much more random than for coiled tubing resulting in far less axial dispersion of the sample. Unfortunately there are a number of drawbacks to using packed or bead reactors, including the tendency to trap bubbles, and the increase in surface area which can be a problem if the sample tends to adsorb to surfaces.

Another way to incorporate a random flow patterns is by "coiling" the tubing in a more random fashion. This has been done by "knitting" or knotting the tubing, resulting in more random flow patterns. The effect on mixing height by coiling and knitting are also shown in figure 1.3.4; note that H remains nearly constant for the knitted reactor with an average of .47 cm over the range of flow rates used. In pressed

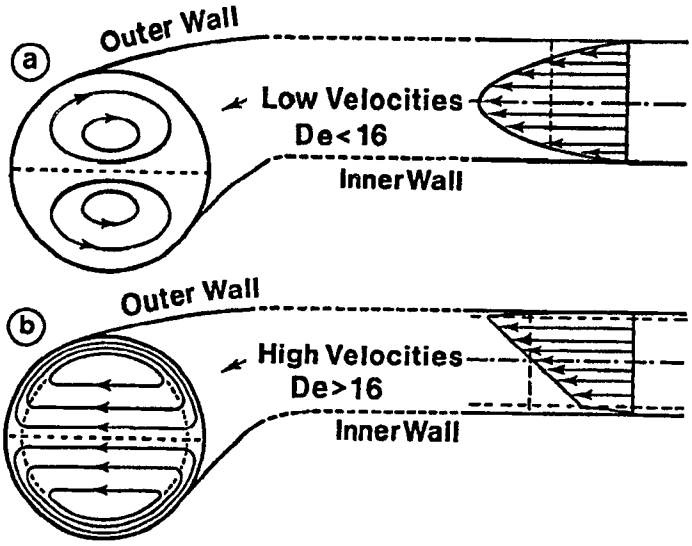

FIGURE 1.3.6. Secondary flow in coiled tubing. Secondary flow patterns and velocity profiles in coiled tube at (a) low and (b) high flow velocities.[9]

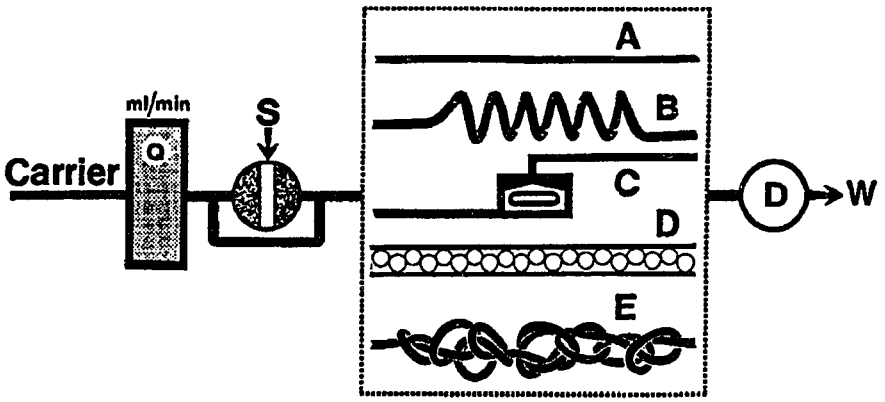

FIGURE 1.3.7. Reactor geometries. Microreactor geometries most frequently used in FIA: A. straight open tube; B. coiled tube; C. mixing chamber; D. single-bead string reactor; and E. knitted reactor.[9]

microconduits as developed by Ruzicka [17] this can be done by imprinting the channels with meandering or "zigzagging" flow paths. In each case the random flow decreases axial dispersion of the sample, decreasing peak widths which increases analysis rates or allows additional reaction time without degrading the peak.

Since axial dispersion is dependent on the rate of molecular diffusion (to varying degrees, depending on system geometry), slightly different peak shapes would be expected for different solutes. This effect has been observed by Hungerford, shown in figure 1.3.8. Peak shapes shown are for $KMnO_4$, bromothymol blue and glucose oxidase with diffusion coefficients 2.0×10^{-5}, 5.4×10^{-6} and 2.2×10^{-7} cm^2/sec respectively. Diffusion rate differences show the greatest effect on peak shape for straight tubes, but minimal effect in the knotted reactor as would be expected from the above discussion.

Another deviation of real FIA systems from the models above is the size of the sample injection. Injected samples may be very small or very large, essentially covering the range from pulse to step experiments. Typical FIA peaks resulting from various size injections are seen in figure 1.3.9.

The dispersion, D, in FIA has been defined as

$$D = C°/C$$

where $C°$ is the original concentration at injection and C is the (expected) concentration (due to dispersion, assuming no reaction). A value of $D = 2$ indicates the sample is half the original concentration, etc. C^{max} and D^{max} are then the values at peak maximum. The D^{max} for a particular system can be important, for example, in determining the concentration of reagent necessary in the carrier stream to assure an excess is available

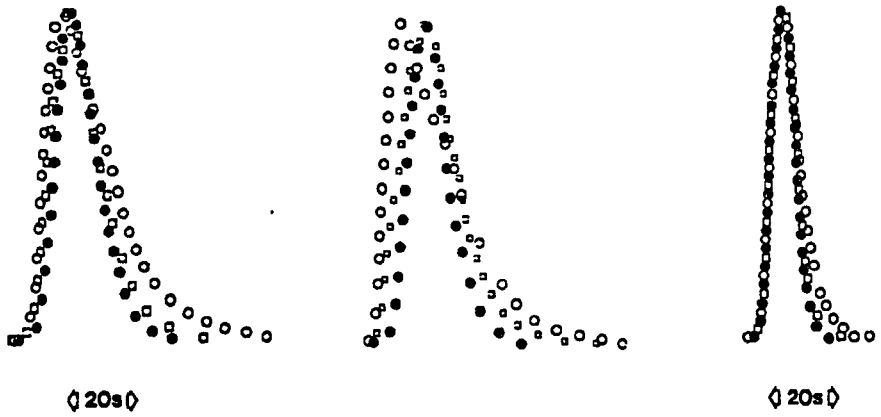

FIGURE 1.3.8. Dispersion of solutes of varying diffusion coefficients. Peaks obtained from dispersion of three solutes in straight (left), coiled (middle) and knotted (right) reactors. o - glucose oxidase, □ - bromothymol blue, • - $KMnO_4$.[10]

to react with the analyte in the sample. An injection parameter, $\alpha = S_V/V_r$, relates the sample volume to the reactor size. Again using the tanks-in-series model assuming a single tank,

$$C = C^{init} e^{(-t/T)}$$

Since C^{init} will be approximated by dilution of the injected sample concentration and volume by the reactor volume, taken at the peak maximum,

$$C^{max} = (C^\circ S_V / V_r)\, e^{(-t/T)} = (C^\circ S_V / V_r)\, e^{(-tQ/V_r)}$$

and

$$C^{max} / C^\circ = \alpha\, e^{(-tQ/V_r)} = 1/D^{max}.$$

Mixing actually begins in the sample injection loop in real FIA systems, so the calculated V_r includes the actual reactor volume and approximately half of the sample loop; V_r can only be considered constant for a given injection volume.

Alternatively, the problem can be viewed as a step experiment for a single tank with the F curve (figure 1.3.1)

$$C / C^\circ = 1 - e^{(-t/T)}$$

Note that this holds and the value increases as long as injected sample continues to enter the tank. Once all of the sample plug has entered, the tank is diluted by additional

flow, so the peak maximum will be seen as the last of the sample enters the tank, at which point

$$t / T = S_v / V_r$$

so

$$C^{max} / C^\circ = 1 - e^{(-S_v / V_r)}$$

If we wish to find $S_{1/2}$ which is the S_v which gives maximum concentration (C^{max}) of half the original concentration (C°)

$$C^{max} / C^\circ = .5 = 1 - e^{(-S_{1/2} / V_r)}$$

$$S_{1/2} / V_r = .693$$

$$S_{1/2} = .693\ V_r$$

Then the problem can be stated in terms of $S_{1/2}$ and S_v as

$$C^{max} / C^\circ = 1 - e^{(-.693\ S_v / S_{1/2})} = 1/D^{max}$$

The problem can also be stated as tank-in-series with high N, where a Gaussian shape would be expected from an infinitely narrow injection. Looked at qualitatively, the Gaussian peak will increase in height as sample injection width increases until it

reaches a plateau, at which point the peak width continues to increase (figure 1.3.9a). In a single line FIA system this generally means that the sample is undiluted by the carrier stream in the plateau region, and therefore has no chance to react with reagent present in the carrier. The result is that reaction product will only be seen at the edges of the sample zone and a double peak will be observed. (Please note that this is the configuration which will be used and discussed later in section 1.5.) Sternberg and Schifreen *et al.* have described the output expected with a plug input as

$$C / C^\circ = 1/2 \{erf[(at - N) / (2N)^{1/2}] - erf[(at - a\xi - N) / (2N)^{1/2}]\}$$

and

$$C^{max} / C^\circ = erf[2 \alpha N^{1/2}(2^{1/2})] = 1/D^{max}$$

where ξ is the normalized injection parameter ($\alpha N/a$) and erf is the error function. The result is a plug input broadened by a Gaussian operator, with the center of the peak shifted from that expected from an infinitely narrow injection by half the sample injection width (figure 1.3.10). The peak width at half height (expressed as a volume) is approximately equal to the injection volume, S_V, when injection volume is greater than 3σ (expressed as a volume).

For small $\alpha N^{1/2}$

$$C^{max} / C^\circ = \alpha (N/2\pi)^{1/2}$$

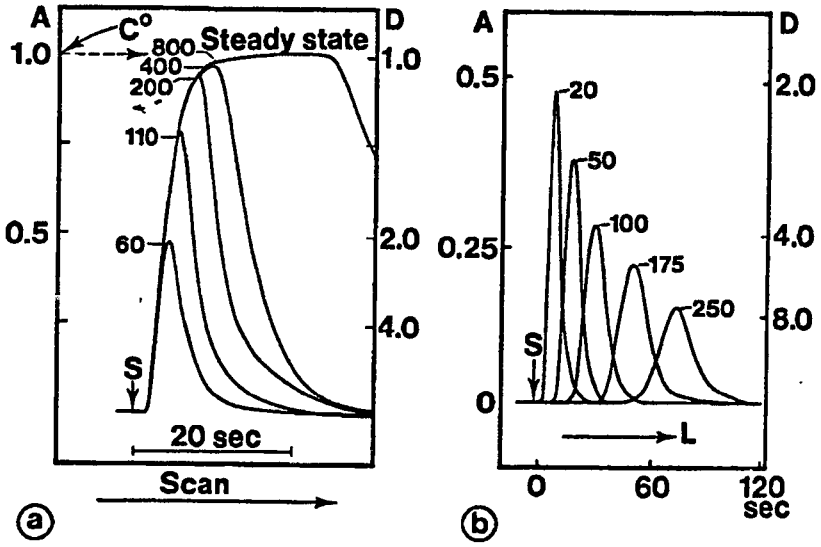

FIGURE 1.3.9. Response curves as a function of injection volume and tube length.[9]

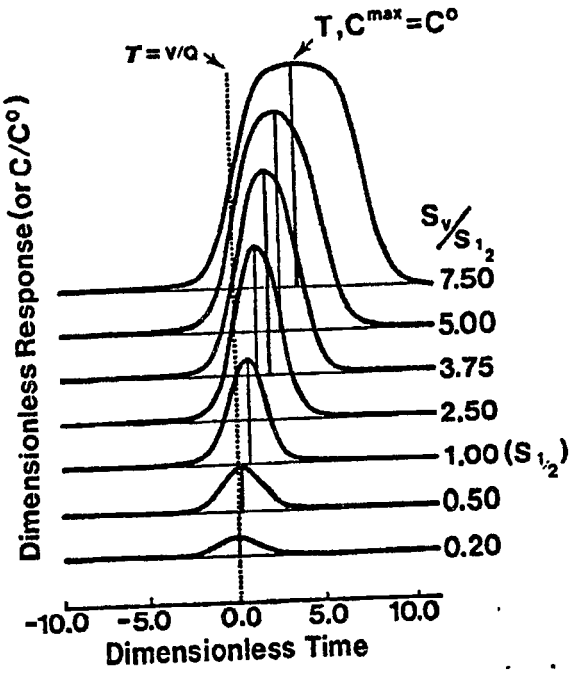

FIGURE 1.3.10. Response as a function of injection volume.[9]

which agrees with the observation that for $S_v < S_{1/2}$ peak height increases linearly with injection volume. Figure 1.3.11 summarizes the expected peak heights based on injection volume and N.

While this certainly is not an exhaustive study of flow dynamics in FIA systems, hopefully it has given an adequate overview of the major effects and mathematical models that have been developed to explain them. These models have generally been developed for "ideal" systems, and while they should be helpful for constructing FIA systems for specific purposes or explaining generally the phenomena occuring in FIA systems, the additional complexity of real systems precludes the development of precise models for individual systems. For this reason, calibration of systems for quantitative analysis and for actual values of C^{max}, D, peak shapes, etc. are necessary.

1.4 Injection Valve Design

In order to make use of the principles of dispersion in FIA to form the desired gradients, an injection valve was needed which would allow a variety of patterns of injection of sample(s), reagents(s) and carrier. A particular valve design used in the laboratory was found with slight modification to be capable of a variety of injection modes.[18] Like the flow injection method itself, the valve is very simple, inexpensive and versatile; it should therefore prove useful in a variety of applications and variations on the basic FIA method which have been developed over the years.[19]

The most commonly used valve in FIA is the six-port rotory valve diagrammed in figure 1.4.1. The sample loop is filled in the "load" position, and then placed in the reagent stream when turned to the "inject" position.

The valve design used here is similar, having six ports on the front rotor. But rather than simply connecting adjacent pairs of these ports on the back plate, all six also are

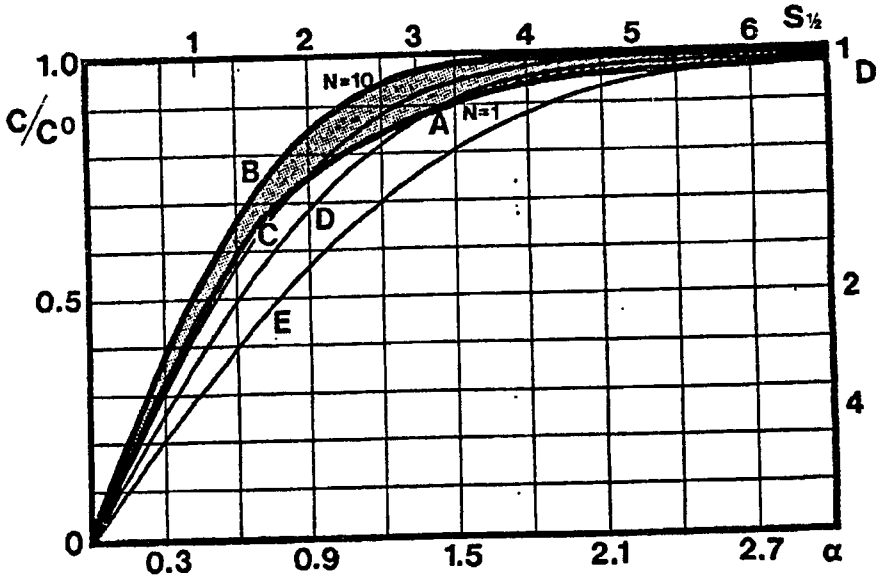

FIGURE 1.3.11. Theoretical curves for peak height as a function of injection volume.[9]

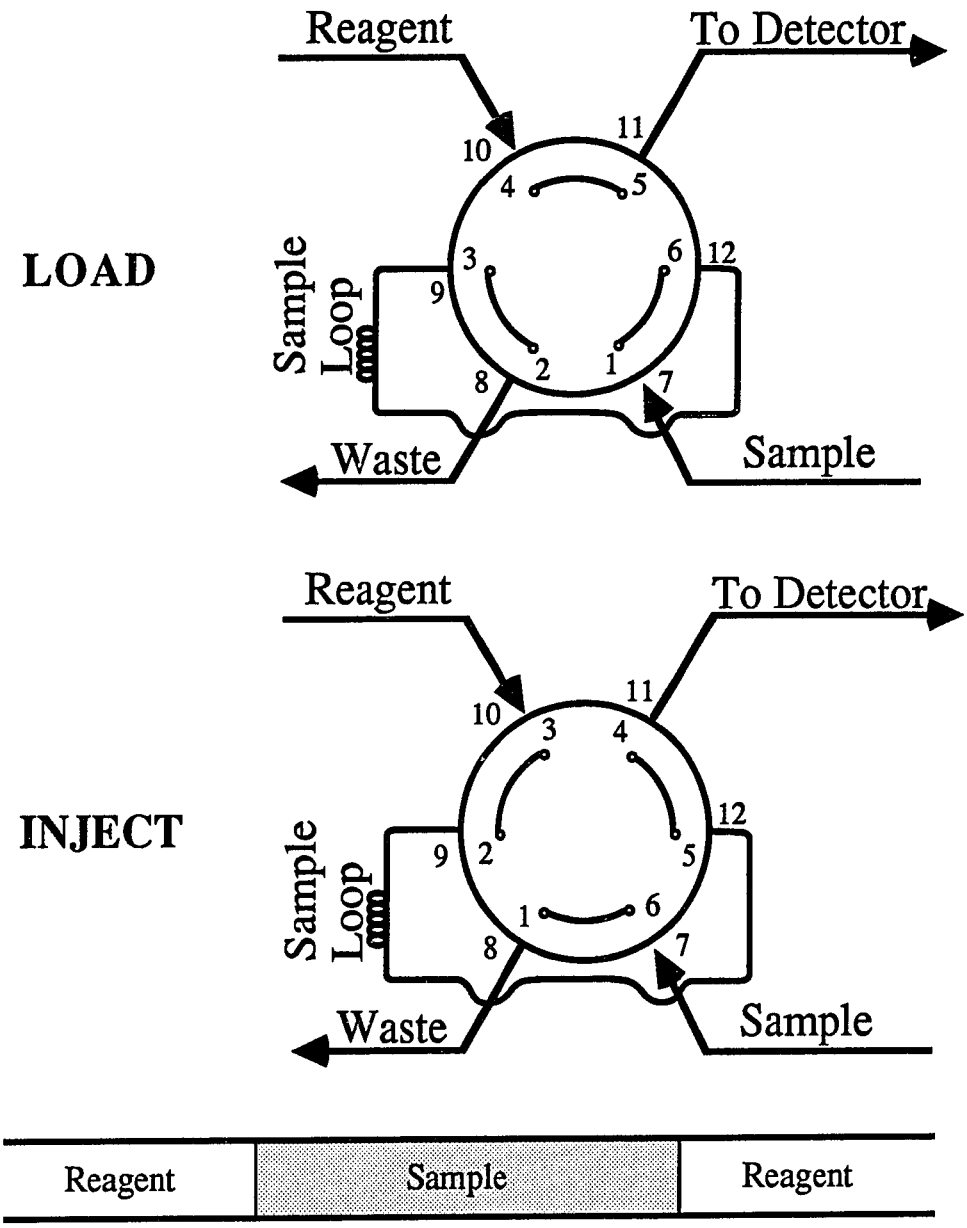

FIGURE 1.4.1. Six-port Injection Valve. The valve configurations are shown in LOAD and INJECT positions. Lower diagram shows the resulting injection in the reagent stream.

individually accessible giving a total of twelve ports which provide a wide range of options in its configuration.

The valve shown in figure 1.4.2 is constructed by bolting a solid Teflon cylinder (1.75cm diameter and 1 cm. thick) with six evenly spaced holes on a PVC plate 1 cm. thick. Matching holes are made through the plate, and channels are imprinted on the bottom of the plate to additional holes away from the rotating disk. For convenience, additional channels may be imprinted on the same plate to be used for reaction coils, merging zones, sequential reagent additions, etc.[20] Short pieces of tubing are inserted into the exposed holes on the top of the plate and in the disk. Connections are made by simply fitting with sleeves of slightly larger tubing. The bottom of the plate is sealed, leaving the impressed channels open for flow. A lever on the disk allows it to be turned from one position to the other, with stops on the plate assuring that the holes in disk and plate are aligned in either the LOAD or INJECT position. The valve is normally operated manually, but has also been automated. Sample and/or reagent loops may be filled manually by syringe, by aspiration, or by peristaltic pump (usually by drawing on the waste line); if the pump used to fill the loop(s) is separate from the carrier pump (which runs constantly), sample or reagent may be conserved by running it only when the valve is in the LOAD position and stopping it in the INJECT position.

The standard six-port arrangement shown in figure 1.4.1 can be formed by simply connecting pairs of ports on the rotor (or on the plate). Alternatively for a simple injection the valve can be configured as shown in figure 1.4.3.

While FIA methods greatly reduced reagent consumption in comparison to most previous methods, it was discovered that a further reduction could be accomplished by simultaneously injecting reagent and sample, then merging the two streams as shown by Mindegaard [21] and Bergamin *et. al.*[22] Toei and Baba have also designed a valve

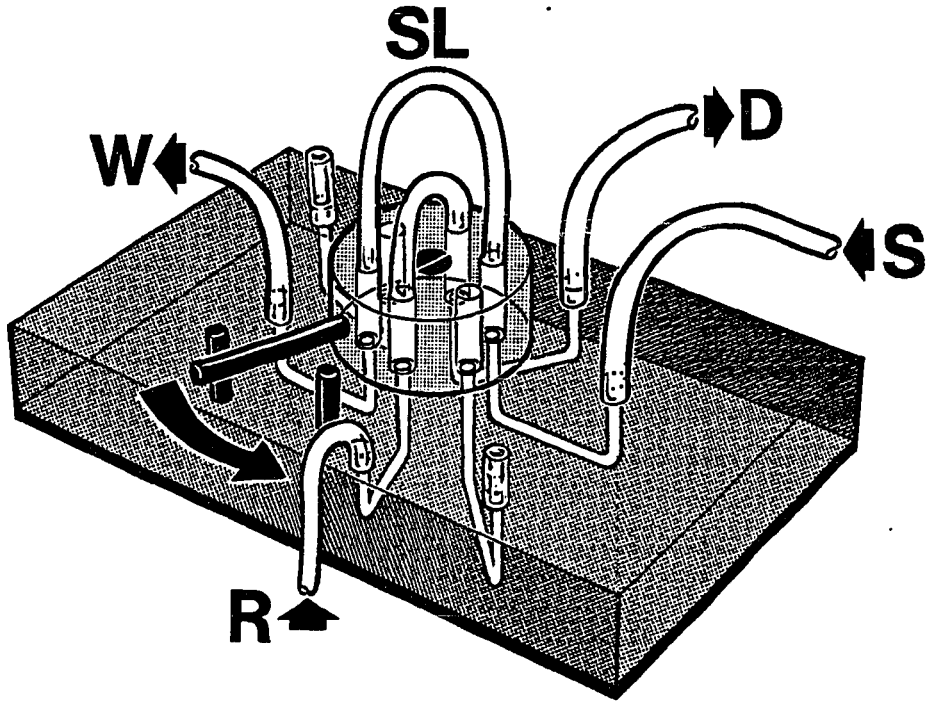

FIGURE 1.4.2. Valve Construction. See description in text.

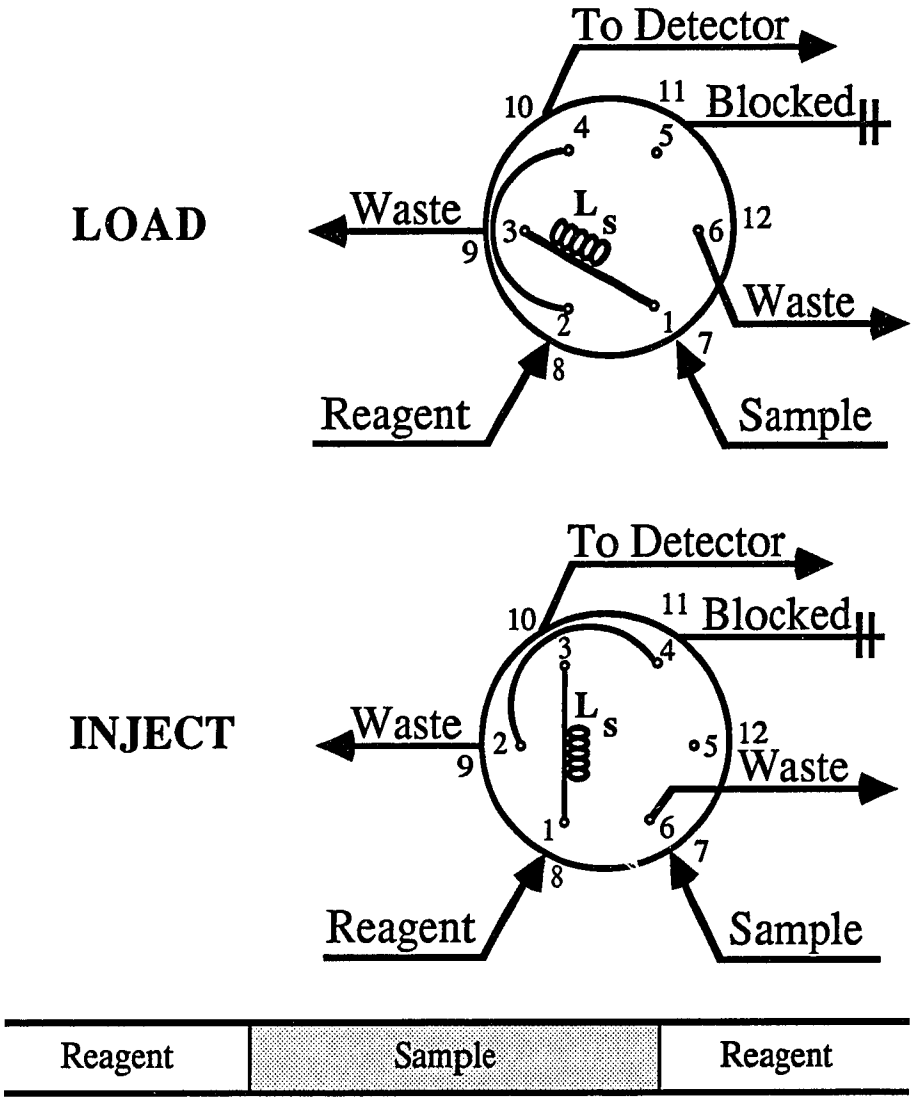

FIGURE 1.4.3. Alternate Sample Injection. Simple injection configuration for alternative valve. L_S is the sample loop.

which is capable of either simultaneous sample and reagent injection, or simple sample injection.[23]

The valve configured as in figure 1.4.4 allows simultaneous sample/reagent injection after filling the two loops. Note that the two carrier inlets may be propelled by a single pump tube by splitting the line from the pump as in the Toei design, or by separate pump tubes, which is preferable since flow rates through both loops do not need to be hydrodynamically balanced in order to assure reproducible injections--as is the case in Toei's design.

Rios and coworkers recently proposed a two-valve system which allows injection of a plug of reagent (at a different pH than the reagent stream) in the center of the sample plug.[24] This allows more sensitive multiple analyte detection of the pH-sensitive products formed in the resulting pH gradient by the method originally proposed by Betteridge and Fields.[25] We propose that this type of injection can also be accomplished with a single valve configured as shown in figure 1.4.5. A second application of this configuration involves reversing sample and reagent lines: a plug of sample can be "sandwiched" between two reagent plugs in an unreactive carrier to conserve reagent in a single line system.

Another alternative which may be useful for the Betteridge and Fields method is shown in figure 1.4.6A. This allows injection of sample followed by reagent (or vice versa). An information rich assymmetrical double pH gradient is created over the sample zone, rather than the information redundant symmetrical double gradient which is observed when the reagent is injected in the center of the sample zone as in figure 1.4.5A. The same configuration might also be used for the gradient scanning standards addition method proposed by Fang *et. al* [3] by replacing the reagent in the reagent loop with a standard solution of the analyte. By injecting a sample plug immediately

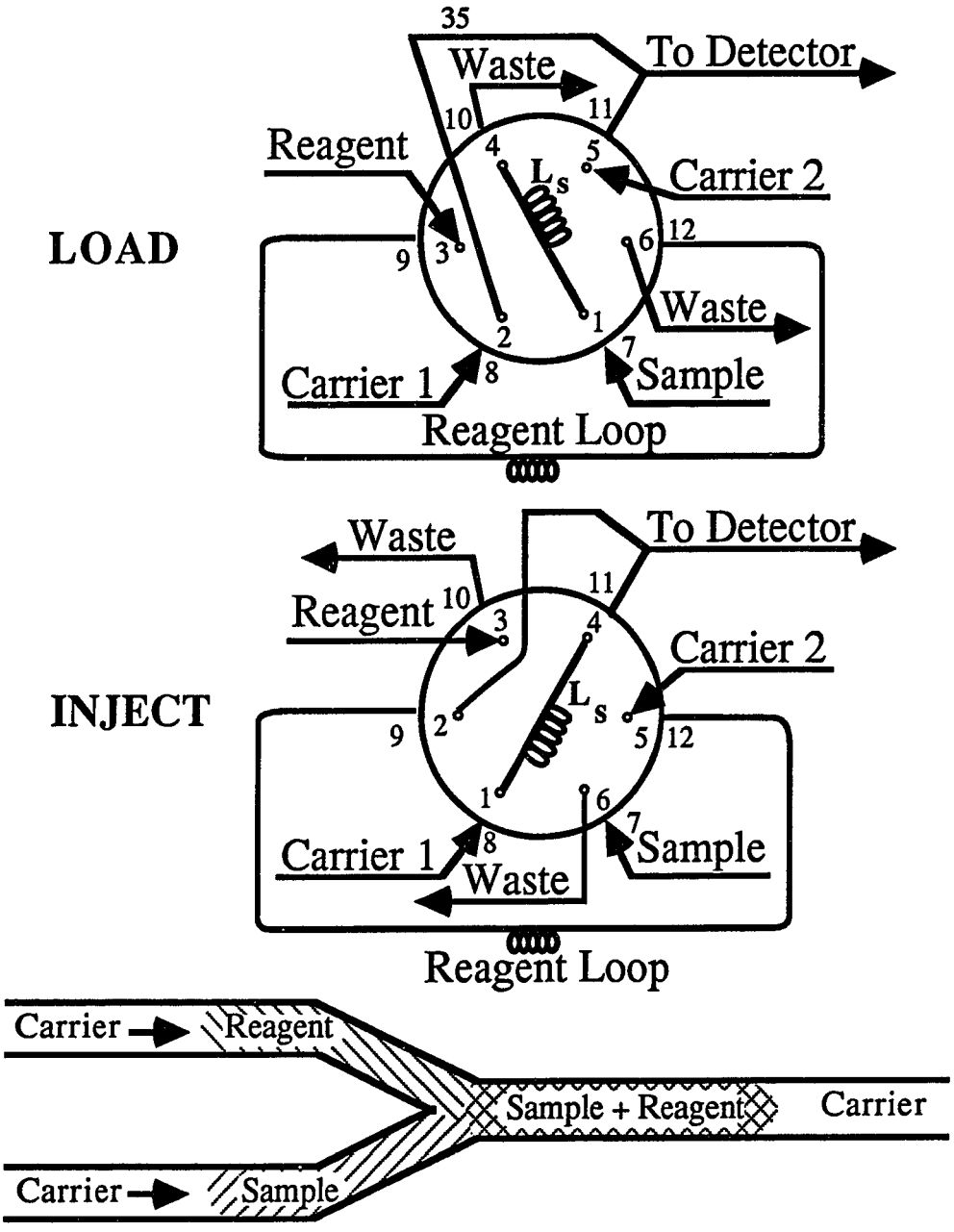

FIGURE 1.4.4. Simultaneous Injection. Sample and reagent are injected simultaneously into separate streams which are merged downstream. L_S is the sample loop.

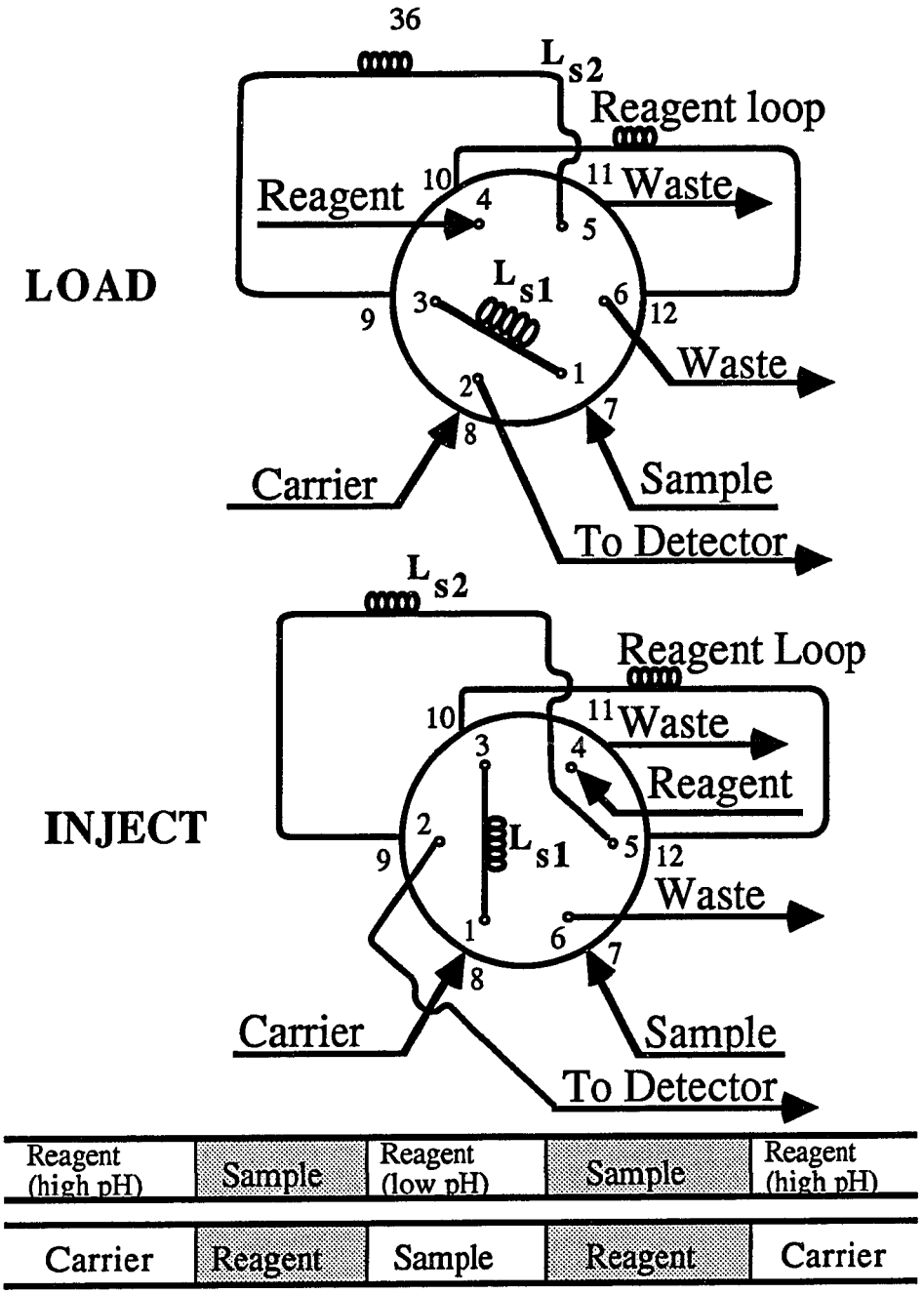

FIGURE 1.4.5. Gradient Injection. (A) Reagent of different pH than reagent stream is injected between two plugs of sample. L_{s1} and L_{s2} are sample loops. (B) By reversing sample and reagent loops, sample can be injected between two plugs of reagent in an unreactive carrier, minimizing reagent consumption.

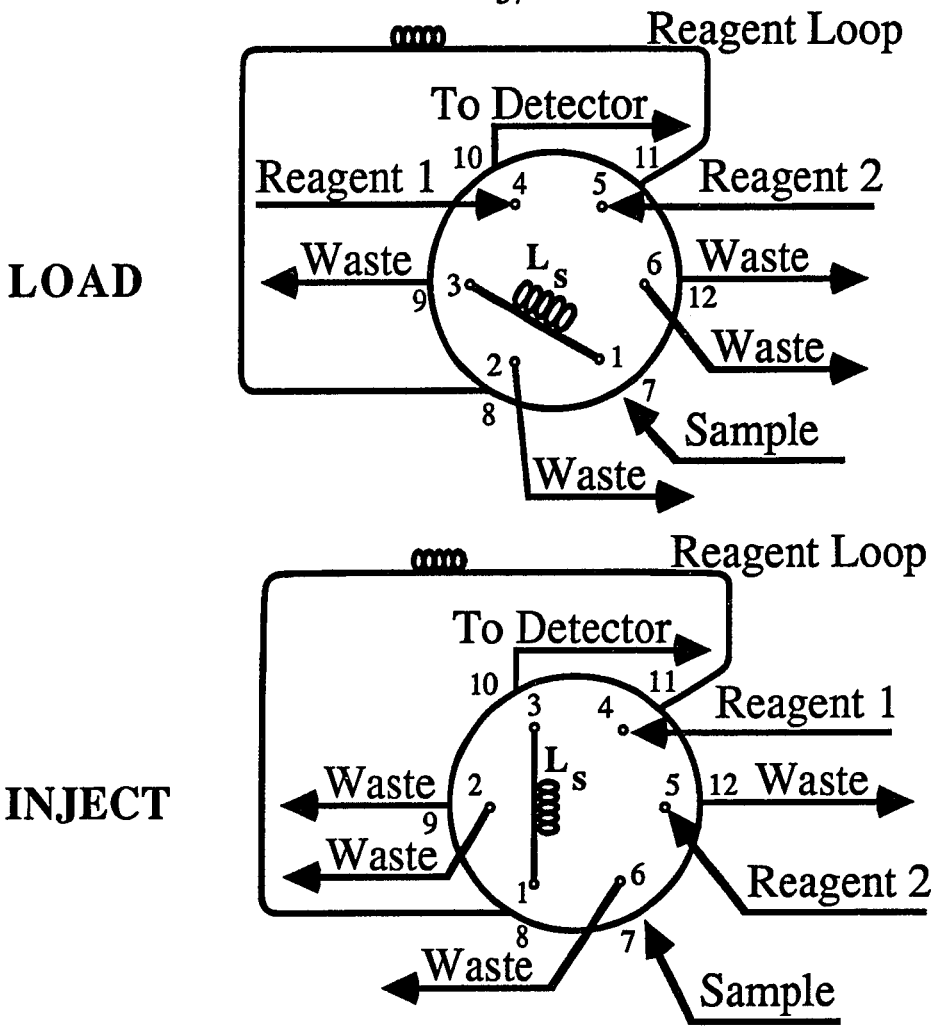

FIGURE 1.4.6. Gradient Injection. Sample in L_S is injected adjacent to a plug of (A) reagent for gradient studies, (B) standard for gradient scanning standards additions or (C) potential interferent to observe effects at various concentration ratios.

followed by a plug of standard into the carrier stream (and then merging with a reagent stream if necessary), response can be observed at times corresponding to various sample/standard concentration ratios. This valve configuration can also be used for interference studies where the sample plug is immediately followed by a plug of potential interferent. The interferent partially disperses into the sample plug while both mutually disperse into the carrier stream, which may merge with reagent downstream, again allowing observation of response at times corresponding to various concentration ratios.[26]

Another configuration is shown in figure 1.4.7, which results in a double injection of sample separated by a plug of the reagent stream which can result in two separate peaks. By using sample loops of different volumes, the dynamic range of the system can be increased by calibrating high concentrations from the smaller injection volume and low concentrations by the larger injection volume. A fiagram (output concentration profile) identical to that obtained with a split stream manifold [27] will be obtained, but since the present method does not rely on hydrodynamic balance of split streams, reproducible results over extended dynamic range and time periods will be observed. The reagent loop can also be replaced by a packed reactor. An example of the use of this configuration is the analysis of nitrate and nitrite. The reagent loop is replaced by a copper/cadmium reaction column as used by Anderson.[28] Two loops are filled with the sample. When injected, the first sample passes directly to the reaction manifold where it is merged with reagent and nitrite is detected. The second, however, first passes through the copperized cadmium reduction column converting nitrate to nitrite, allowing measurement of total nitrate plus nitrite. Nitrate concentration can then be calculated by difference. Note that each peak position must be calibrated separately, since the second peak travels a greater distance causing additional dispersion. Figure

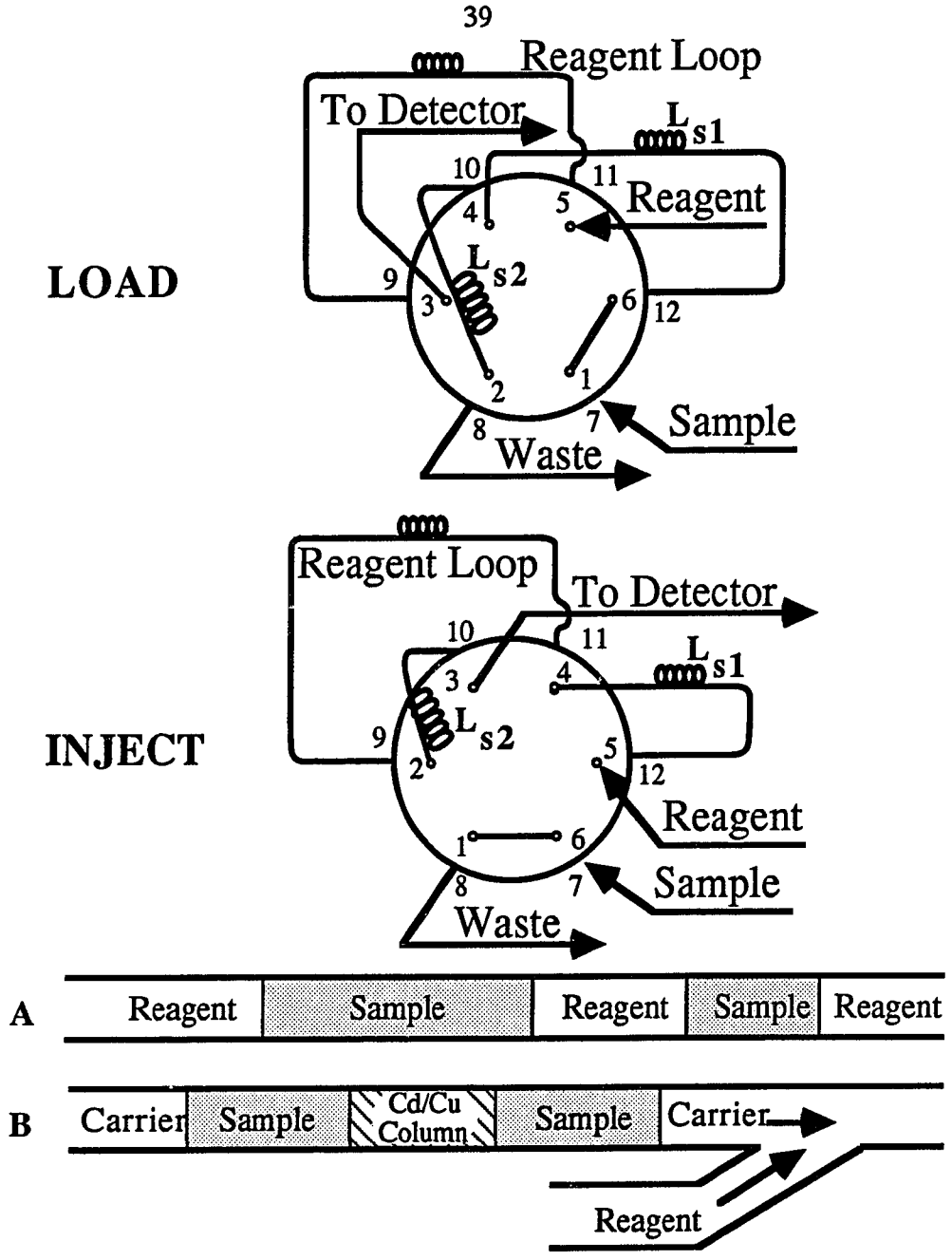

FIGURE 1.4.7. Double Sample Injection. Two plugs of the same sample in L_{s1} and L_{s2} are injected either (A) with different sample volumes or (B) separated by a reaction column.

1.4.8 shows a similar arrangement which allows injection of two separate samples. It may also be used for injections similar to those shown in figure 1.4.6 but where a small plug of the carrier is placed between the sample and reagent, standard or interferent.

Finally, figure 1.4.9 shows a method for continuous filling of sample loops. Two sample loops are used. They may be matched or of different sizes. While one loop is being filled with sample, the other is injected into the carrier stream. When the valve is turned, the filled loop is injected into the carrier as the other loop is refilled with sample.

1.5 Curve Resolution in FIA

1.5.1 Introduction

When a sample to be analyzed is a pure substance, it can usually be identified and its purity verified by its physical, spectral and chemical properties. When the sample is a mixture or solution containing several chemical species, additional steps may be necessary for identification and quantitation of analytes. While a great deal of data can be easily collected about the sample as a whole, the problem is to get information about individual chemical species (analytes) within the sample. Information from the sample must therefore be resolved into its component parts to determine the individual contributions of the analytes of interest. This resolution step is an implicit part of any qualitative or quantitative analysis done on a mixture sample. In this section, a novel approach to resolution of analytes in mixtures using flow injection analysis with multiple sensor detection and chemometric data analysis techniques is presented.

"Resolution" implies separating or distinguishing component parts of a multicomponent system. It may take on a number of meanings in scientific applications, such as resolution of adjacent channels in a spectrophotometer, or resolution of peaks in chromatography. Unless chromatographic resolution is specifically referred to,

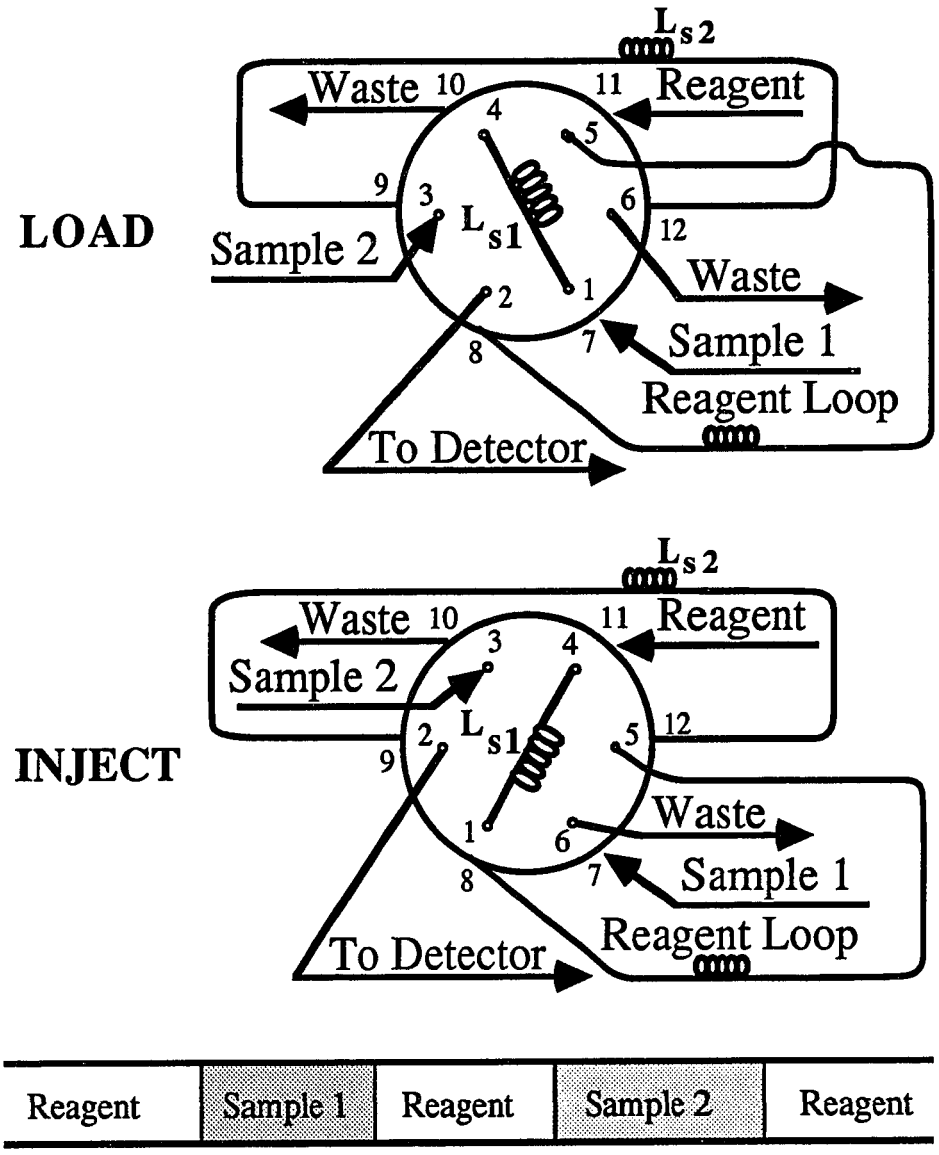

FIGURE 1.4.8. Double injection. Two separate loops L_{s1} and L_{s2} are filled with distinct samples (similar to figure 7). Alternatively, sample in L_{s2} may be injected with reagent, standard or interferent (similar to figure 6) in L_{s1} separated by a small plug of the carrier.

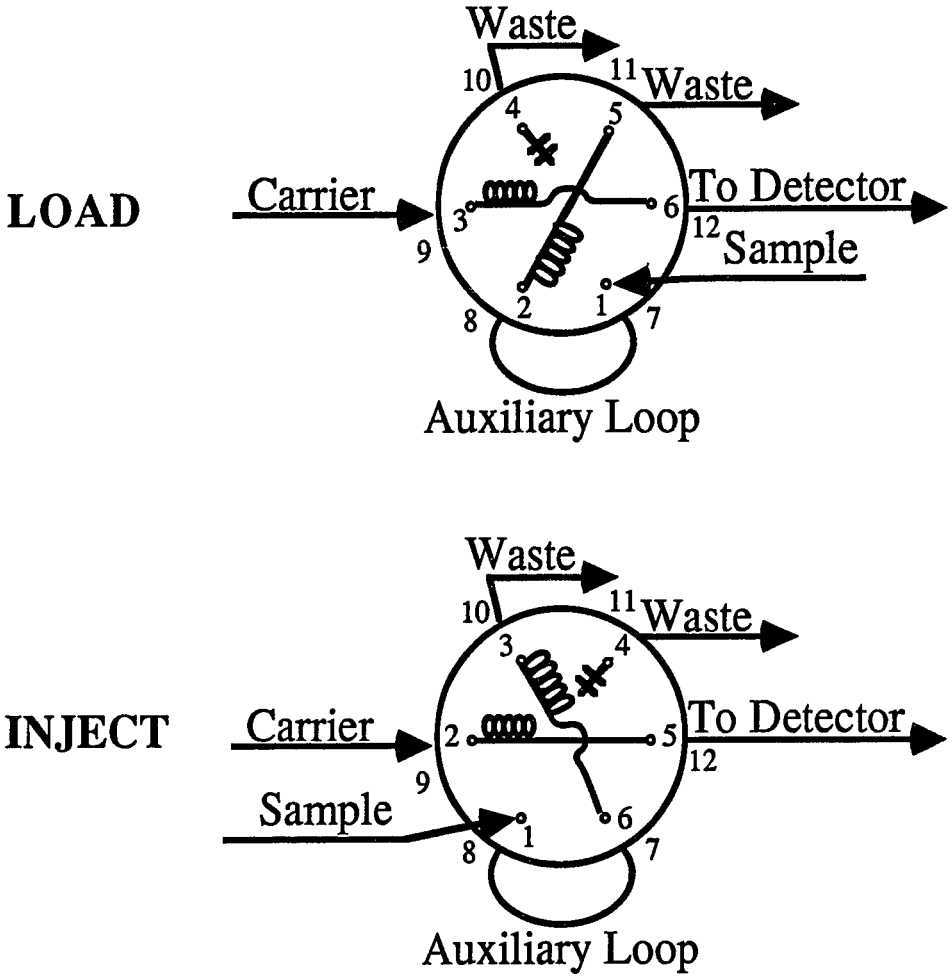

FIGURE 1.4.9. Alternating injection. Two separate loops L_{s1} and L_{s2} are alternately filled and injected.

"resolution" in this paper refers generally to the ability of any method to distinguish individual chemical species from one another in a chemical mixture or solution.

Several tools for resolution are available to the chemist in the form of various instruments, chemical procedures and methods. Most analytical methods to accomplish such resolution fall into one of three categories, or some combination of these three: physical separation methods, spectral discrimination, and selective chemical reaction methods. Physical properties such as boiling point, melting point, refractive index, etc. are useful in identifying pure samples, but since they measure properties of the sample nonselectively they are less useful for mixtures and solutions unless a separation step is applied first.

The most obvious way to isolate information for a particular analyte is to physically separate the analyte from the rest of the sample. This might be done, for example, by a series of extractions, crystallizations, distillations, filtrations, etc. More commonly some form of chromatography is used: if the relative affinities of two analytes for the mobile and stationary phases are sufficiently different and the path length is adequate, they will essentially be completely separated. Detection in this case may be by any of a number of non-specific detectors. The identity and quantity of a given analyte may be determined by its concentration profile: the size, shape and position of its peak in the chromatogram. In this way, several components can be detected by their individual peaks in the concentration profile (chromatogram). The major emphasis in developing a new analysis scheme must then be maximizing the separation (chromatographic resolution) of components.

Resolution, however, does not necessarily require a physical separation of sample components. Unique spectral information may adequately resolve the analyte from the rest of the sample by giving information due only to one analyte. For example, a

colored analyte is easily detected in an otherwise colorless sample due to its absorption in the visible light range. In fact, any unique wavelength of absorption or emission for an analyte may be useful for pinpointing the analyte of interest for analysis.

When broad bands are encountered with some spectroscopic techniques it is difficult to find information about individual analytes in mixtures due to spectral overlap. In these cases a physical separation is generally done first , and the spectral methods are used to confirm the identity of the pure components thus obtained. This may be done on-line using the spectrometer as the detector for a chromatographic system; note, however, that here the resolution is due to the separation step.

The third set of analytical methods involve the way analytes react with other chemical or electrochemical species, and can be called kinetic methods. Most commonly, a reagent is chosen which reacts specifically with the analyte (or group of analytes) of interest resulting in a product species which is more easily or uniquely detected. Methods have been developed, for example, for the colorimetric determination of chemical species which, upon addition of a selective reagent, yield a colored product which can easily be monitored at a certain wavelength. In titrations, an indicator may be added to show more distinctly when a quantitative reaction has reached a selected endpoint. These "wet chemical" methods were the backbone of analytical chemistry for well over a century, until recent domination by chromatographic and spectral methods of analysis. A resurgence of interest in these traditional approaches is now occurring with the development of flow injection analysis (FIA), which facilitates automation and exploitation of kinetics, and ensures greater precision and reproducibility.[20]

For cases where complete resolution is not possible using a traditional resolution method, various mathematical techniques have been developed to extract more information from the collected data.[29] For example, when the spectra of all

components in a mixture are known, least-squares regression may be used to find the best fit of the known reference spectra of the analytes to the measured spectrum of the mixture, thereby giving an estimate of the concentrations of the individual components. In chromatography, assumptions about reproducible peak shapes can be used to find the best fit of peaks to the chromatogram.[30,31,32]

Several algorithms which are much more powerful are available for data where instrument response depends on two orders ("dimensions") simultaneously. For example, the entire UV/visible spectrum (rather than a single wavelength) of the effluent in liquid chromatography can be constantly monitored. A response will be recorded at a given wavelength at a given time only if an analyte is present in the chromatogram at that time and if the analyte absorbs at that wavelength.

For example, if two components are not adequately separated by chromatography they may appear as a single peak and be difficult to quantitate (figure 1.5.1). If there exists a wavelength at which one component absorbs while the other does not, that component can be isolated by monitoring the unique wavelength. If each component has a unique wavelength, both may be detected in this way. In cases where the spectral absorbances of the components are not known or where no unique absorbances exist, this method, which depends on spectral resolution, will not be useful. But when partial resolution is available in both orders simultaneously, more complete resolution can often be calculated mathematically. For example, the self-modeling curve resolution technique of Lawton and Sylvestre [33] is a method by which the spectra and chromatograms of two overlapping components can be estimated without any previous information about the samples. The method has been applied successfully to gas chromatography/mass spectral [34] and liquid chromatography/UV-visible absorbance [35] data. Thus chemometric methods are able to take the partial resolution available

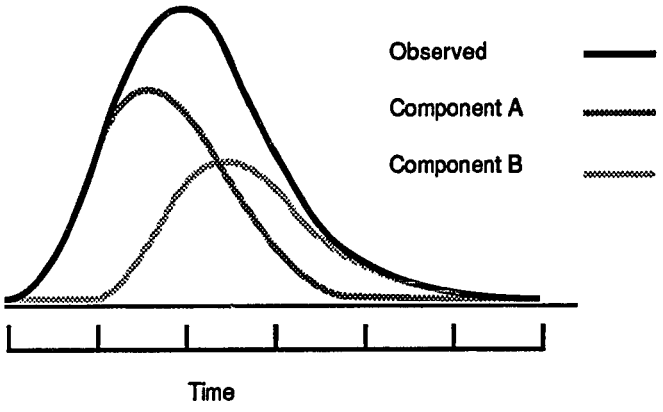

FIGURE 1.5.1. Two partially resolved chromatographic peaks may appear as a single peak.

from spectral and separation resolution methods and mathematically extract a more complete resolution of species.

Applications of chemometric methods to FIA have been limited to date. Some applications have been developed for FIA which result in more complex peak shapes. Dyke and Fernando have confounded the output of a FIA system by running at high sampling rates which results in overlapping peaks, and used deconvolution techniques to improve sample throughput. Vithanage and Dasgupta have shown the usefulness of FIA with a UV/vis photodiode array detector for studies of chemical equilibria in proton-ligand (acid/base indicator) and metal-ligand systems by monitoring absorbances at an isosbestic wavelength,and the lmax for each form of the system. Equilibrium constants were then calculated by solving simultaneous equations. Other than these applications, chemometric methods applied to FIA have generally been limited to optimization of operational parameters for experiments, or filtering of data from the detector while essentially using FIA as a sampling system.

In the simplest FIA system, the sample is injected into a flowing stream of reagent; additional tubing, usually coiled, allows the sample to disperse into the reagent stream and react to form a detectable product before reaching the flow-through detector (figure 1.5.2). The output is typically a single, smooth peak whose height, area or width can be related to analyte concentration. Its main advantages over other automated chemical systems or manual analyses are speed, simplicity of the system, and reproducibility.[19] Until now, FIA methods have relied on the specificity of the chemical reactions and/or detection systems for resolution of a given analyte in a mixture. (One exception would be the work of Betteridge and Fields who have subjected samples to a pH gradient along with a complexing reagent whose response to various metals is pH dependent, allowing simultaneous determination of binary mixtures of metal ions at different points on the

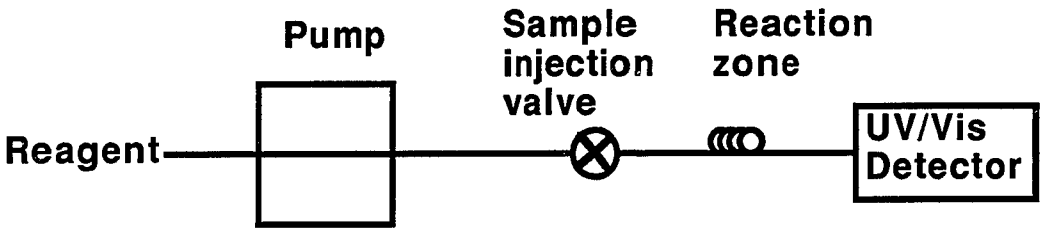

FIGURE 1.5.2. Single-line flow injection analysis system.

profile. However this method requires creation of a gradient such that the two components can be distinctly observed.)

As the sample disperses into the reagent carrier, the sample and carrier will have mirror image concentration profiles when plotted as the fraction or per cent of their original concentrations, since they are "diluting" one another. Figure 1.5.3 shows how these profiles change as the sample is propelled along the tubing by the carrier. To assure that all of the analyte in the sample reacts to yield detectable product, channel dimensions and geometry, flow rate, sample volume and reagent concentration are selected so that an excess of reagent is present throughout the sample zone before reaching the detector. This is done by allowing sufficient dispersion of the reagent into the sample zone (figure 1.5.3E) by using a small sample volume and relatively long reaction coil, so that even at the minimum concentration of reagent--which corresponds to the maximum analyte concentration--the reagent is in excess. Alternatively, a two line system, merging sample and reagent lines, may be used so that reagent concentration is constant throughout the sample zone; however the single line mode is often preferred for its simplicity, especially in on-line process analysis situations. Differentiation of analytes in a sample by their concentration profiles has not been possible since the peak position and shape for all analytes is assumed to be identical, varying only in size from one sample to the next.

If, however, a single line system is used with a larger sample size and limited dispersion before reaching the detector, there will be a region in the center of the sample zone where the reagent is deficient or absent as in figure 1.5.3C, and shown in more detail in figure 1.5.4. Reaction of analytes in the sample with the reagent may vary in this region, resulting in differing concentration profile shapes. While FIA workers in the past have vigorously avoided this situation, it can reveal a great deal of additional

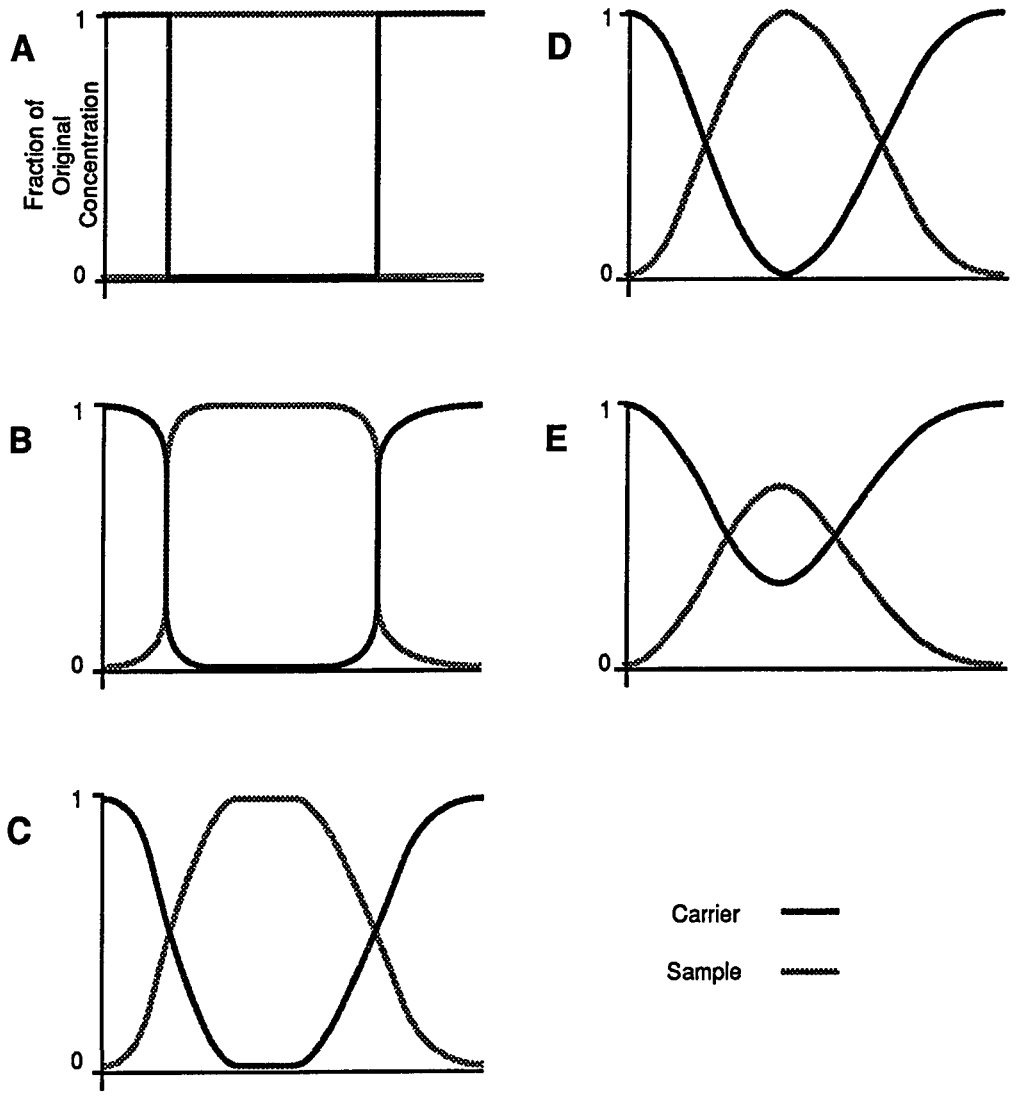

FIGURE 1.5.3. FIA sample dispersion over increasing length of reaction tubing. A. Initial injection of sample as a plug in reagent stream. B, C, D. Dispersion of sample into carrier. E. Reagent from carrier present throughout sample zone.

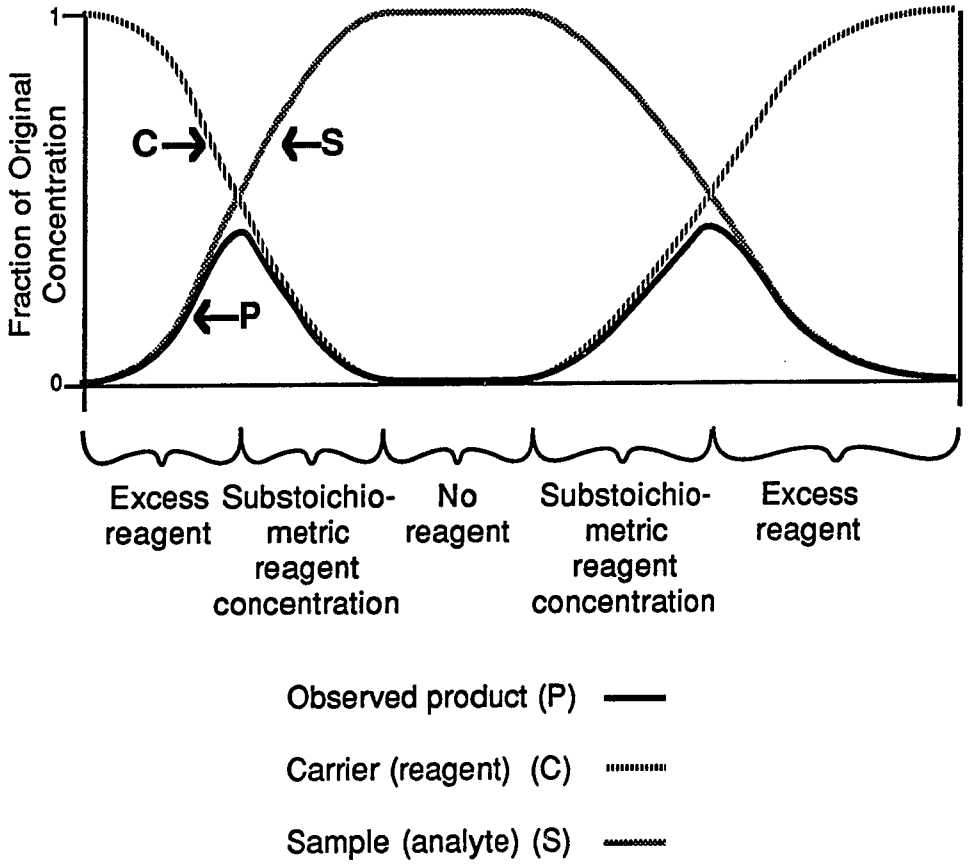

FIGURE 1.5.4. Relative concentrations of sample and carrier with observed concentration of reaction product. Where reagent is in excess, essentially all analyte will be found as reaction product if sufficient reaction time has elapsed. Where analyte is present in substoiciometric amounts, some product will be observed, but not all analyte is converted to product. Where no reagent is present, no product can be formed.

information about the sample. For example, a colored component present in the sample which is not affected by the reagent (sample background absorbance) will have a smooth peak shape with a single maximum plateau (figure 1.5.4S), while a colorless analyte which forms a colored product (figure 1.5.4P) when reacted with the reagent will have two peak maxima at the outer edges of the sample region where both analyte and reagent are present, but a valley between where the reagent (figure 1.5.4R) is deficient or absent. Note that differences now exist between the components in both the spectral and concentration domains. The self-modeling curve resolution technique can now be applied successfully to the FIA system with UV/vis multiple wavelength spectral detection to mathematically extract a more complete resolution of species.

1.5.2 Experimental

Figure 1.5.2 shows the FIA system used for the analysis. A peristaltic pump is used with a flow rate of 0.7 ml./min. The single line system uses an injection valve [18] with a 500 microliter sample loop and 0.5 mm i.d. tubing with a 20 cm reaction zone. A UV/vis spectrum from 328 - 600 nm at 4 nm intervals is acquired every two seconds throughout the experiment by a Hewlett Packard 1040A detector. Data files are then transferred to a VAX computer for data analysis by the Self Modeling Curve Resolution program.[36]

The model system used for this study included various mixtures of methyl violet and phenolphthalein with concentrations in the 0 - 20 ppm (parts-per-million) range. Samples and carrier contained 5% methanol to minimize adsorption on the tubing; they were also buffered with 5 mM acetic, boric and phosphoric acids, with samples then adjusted to pH 6 and carrier adjusted to pH 11 to provide a gradual pH gradient as the sample disperses into the carrier. Methyl violet does not change color over this pH

range, and can be considered the background interferent, with phenolphthalein as the analyte to be quantitated as it reacts with base in the carrier.

1.5.3 Results and Discussion

The absorbance profile observed at the detector for a mixture of 10 ppm phenolphthalein and 5 ppm methyl violet, shown in figure 1.5.5, has three maxima as might be expected from the above discussion for a limited dispersion FIA system.

The Self-Modeling Curve Resolution (SMCR) algorithm is used to determine spectra and concentration profiles for the two components. No knowledge of the spectra or profile shapes is necessary. Spectra obtained during the experiment are assumed to be linear combinations of the two component spectra. Factor analysis of the data matrix confirms that two principle eigenvectors contain essentially all of the information associated with the chemical components. Each of the n-dimensional spectral vectors where n = number of wavelengths used can then be expressed as a point in a two-dimensional (factors' loadings) space, as seen in figure 1.5.6. If the spectra are normalized to unit area, their representative points in the factors' loading space fall on a line, as in figure 1.5.7. One of the spectra of each of the two pure components must then fall on the line somewhere within each of the shaded regions; the inner boundaries of the regions are determined by the extreme measured spectra, and outer boundaries are determined by the requirement that spectral absorbances must be non-negative.

The resulting bands of possible solutions for the spectra seen in figure 1.5.8A compare favorably with the actual spectra in 1.5.8B and 1.5.8C measured on pure samples of the two components. We can further restrict the result by knowledge we have of the system. Assuming that there is some point in the center of the peak which

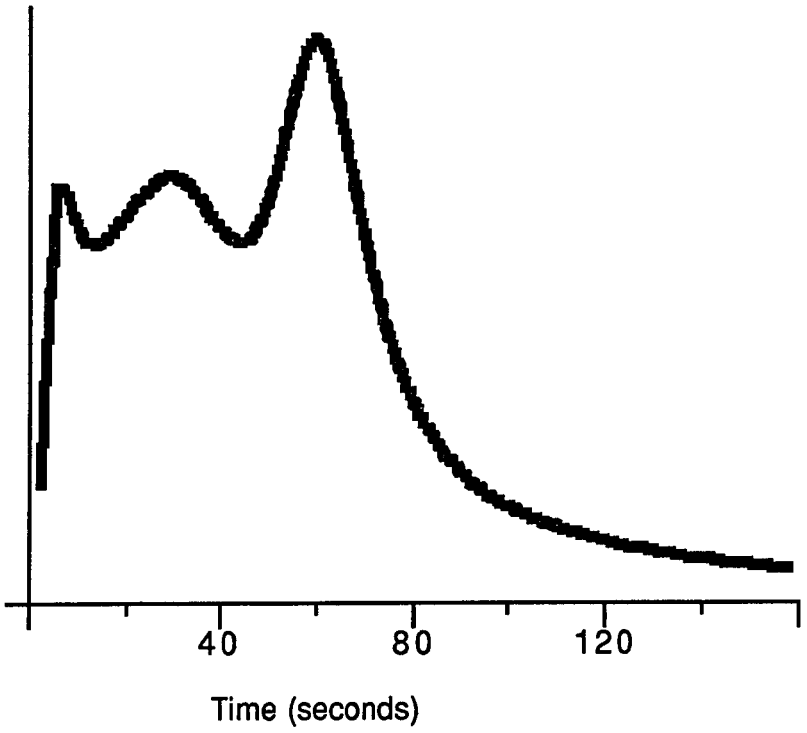

FIGURE 1.5.5. FIA concentration profile of double peaks from product (outer peaks) superimposed on background absorbance.

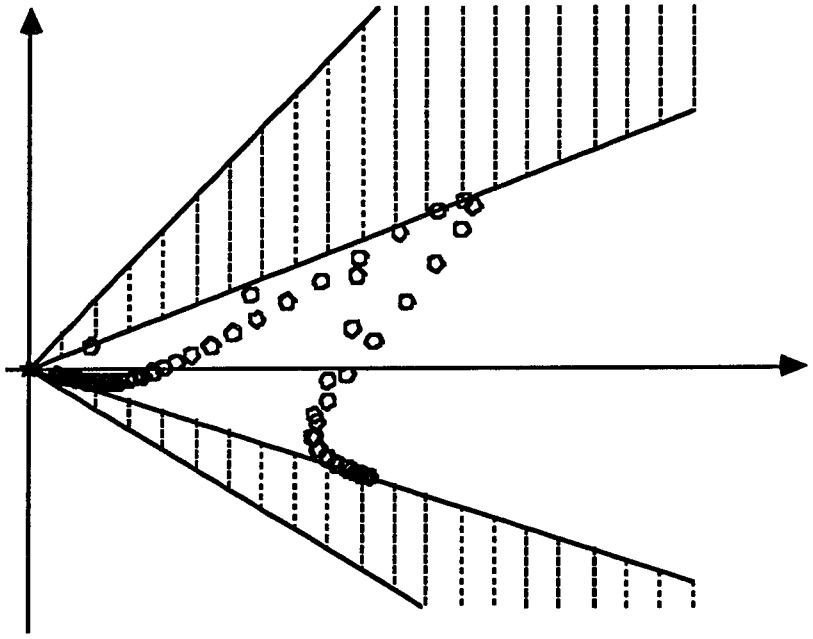

FIGURE 1.5.6. Projection of measured spectral vectors onto plane determined by first two eigenvectors.

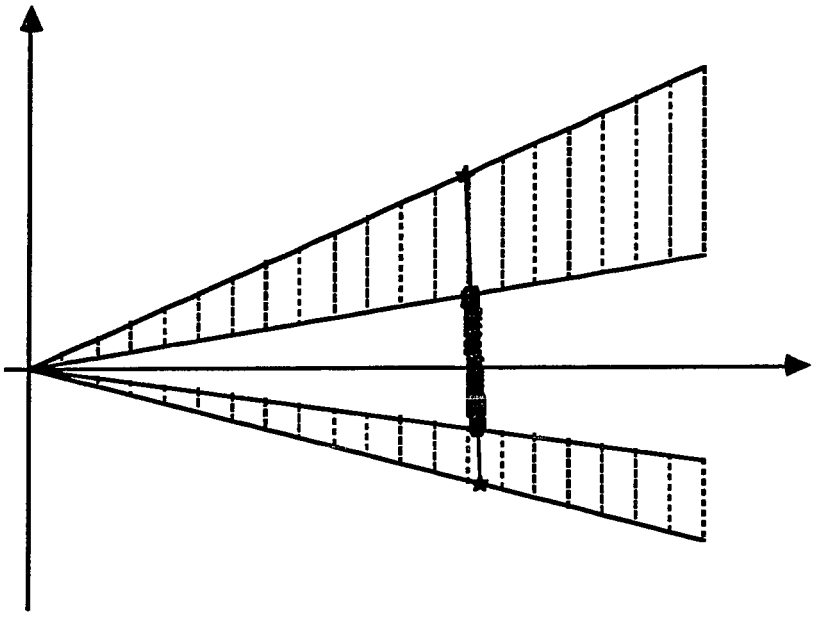

FIGURE 1.5.7. Projection of normalized spectral vectors onto plane determined by first two eigenvectors. Inner bounds determined by extreme measured spectra, outer bounds determined by non-negativity restraint.

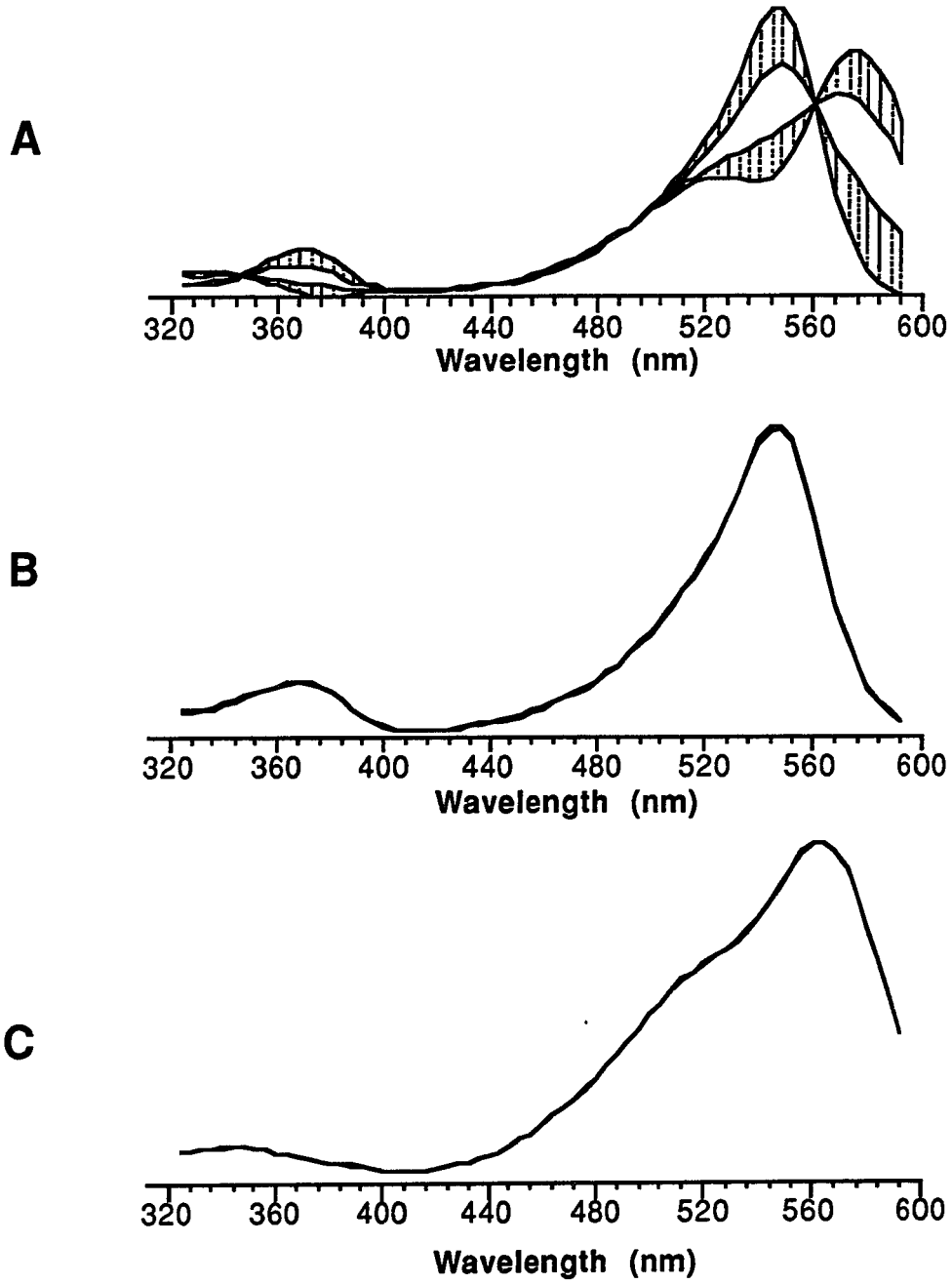

FIGURE 1.5.8. A. Solution bands for spectra of the two components from SMCR. B. Pure phenolphthalein spectrum. C. Pure methyl violet spectrum.

contains only background and no analyte results in choosing the inner boundary condition for the background spectrum. Assuming that the analyte reaction product has an absorbance near zero at some point in its spectrum results in choosing the outer boundary for the analyte spectrum; since the background absorber is present throughout the region where the reaction product is observed, the inner boundary would not be an appropriate choice.

Using these estimated spectra, the concentration profiles ("fiagrams") for the analyte reaction product and background absorber can be estimated by finding the multivariate least-squares solution (figure 1.5.9). Trailing of the methyl violet peak is due to adsorption on the tubing walls. Areas for the double peaks due to the analyte product (phenolphthalein) in the mixtures are calculated from the profiles determined by SMCR; concentration estimates are calculated by univariate linear least-squares regression with corresponding areas from injections of standard solution of 0, 5, 10, 15 and 20 ppm phenolphthalein. The results shown in table 1.5.1 imply good predictive ability of the method for quantitation at lower concentrations, with much larger errors at higher concentrations of sample and background. Mixture samples at these higher concentrations have absorbances in excess of 1.5 absorbance units at some wavelengths, which may result in non-linearities in the detector. Thus care must be taken to stay within the linear range of the detector for concentrations used.

Note that the analyte has been quantitated in spite of the fact that it has a spectrum very similar to the background absorber. No physical separation of the analyte from the sample matrix is necessary. This removal of the background limitation in spectrometry is crucially important for the analysis of real samples [37]

Chemometric methods of data analysis have in the past been shown to increase resolution where separation or spectral methods alone are inadequate. It has been

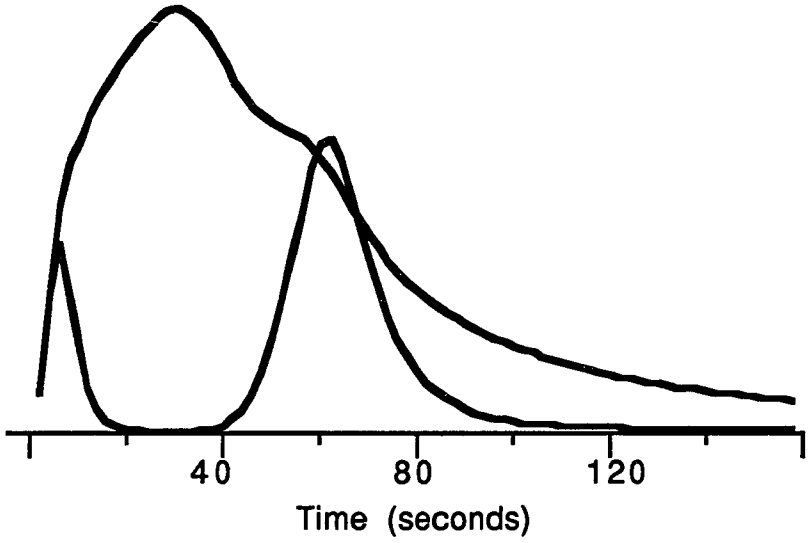

FIGURE 1.5.9. FIA concentration profiles for reaction product of analyte with reagent (double peak) and background determined by SMCR.

TABLE 1.5.1. Predicted concentrations for FIA.

Sample	Bckgd (Methyl Voilet) conc. (ppm)	Analyte (Phenolphthalein) conc. (ppm)	Estimated analyte conc.
1	5	5	5.1
2	5	10	9.7
3	5	20	15.3
4	10	20	17.4

shown that chemometric methods are also useful in the similar situation when traditional chemical methods are performed in a concentration gradient using FIA combined with multi-wavelength spectral detection, where FIA or spectroscopy alone do not provide adequate resolution. This method is useful for separating sample components when the concentration profiles can be made to differ.

Conceptually the present approach represents a further step away from traditional methods such as gravimetry, titrimetry or even chromatography since the analyte is not separated quantitatively from the sample material. The analyte is not even quantitatively reacted with the reagent, and it is this incomplete reaction which gives additional information about the sample. A nonhomogeneous yet reproducible concentration gradient is formed from a sample zone which was homogeneous prior to injection. Multiple readouts are obtained for all sample components, since each spectrum of the dispersed sample zone yields different information due to difference in sample/reagent ratio and elapsed reaction time. Thus physical resolution of sample components has been replaced by a combination of kinetic (FIA), spectral and mathematical (chemometric) methods. This opens up an entirely new and exciting area to the analytical chemist for the chemical analysis of mixtures.

Chapter 2. Infrared Emission Spectroscopy

2.1 Introduction

The interaction of electromagnetic radiation with matter has been of interest to scientists for well over a century. The basic principles involved are fairly well understood, and used extensively in many branches of science. The interaction of matter with radiation in the mid-infrared (IR) region has been of significant interest; two of its major applications are the measurement of IR emission for temperature estimation, and measurement of IR absorption spectra for qualitative (and quantitative) analysis of chemical composition.

Samples which absorb IR radiation also emit at the same wavelengths. This implies that the information in an absorbance or transmission spectrum used for chemical analysis should also be present in the emission spectrum of the sample when it is heated. While there have been a few applications of infrared emission spectroscopy (IES) for chemical analysis, they have been rather limited due to (a) lack of suitable instrumentation of requisite sensitivity to detect the small amount of radiation available from relatively low temperature samples, and (b) difficulty in deriving quantitative information from the observed spectra.[38,39] Emission spectra are much more complex than transmission spectra since they are affected not only by sample composition, but by several other effects as well such as background black body radiation, internal reflection and self-reabsorption, refractive index, sample thickness and geometry, temperature and temperature gradients[40]. The recent availability of reliable and relatively inexpensive computer-controlled Fourier transform infrared (FTIR) spectrometers with cooled detectors has solved many of the instrumentation problems of sensitivity and data collection, while chemical quantitation and spectral

interpretation have remained a challenge. In this work, the use of multivariate calibration methods, specifically the Partial Least Squares (PLS) algorithm, is presented as an aid to the use of IR emission spectra for quantitative analysis.

The emphasis of this work is on the usefulness of the IES methods in process analysis. Currently in most manufacturing plants quality control is accomplished by testing the product in a laboratory after it is made, often with a delay of hours or even days. Off-specification materials must then be discarded, reprocessed or reworked, or sold as a lower grade. In contrast, process analysis methods allow the product quality to be monitored as it is being made. In this way, the process can be corrected immediately if the product does not meet quality standards. This minimizes cost and waste due to off-specification product, and results in a larger quantity of higher quality product being made at lower overall cost.

In a recent review of process analytical chemistry, non-invasive, remote methods of analysis were identified as highly desirable.[41] Infrared emission spectroscopy (IES) is obviously such a technique. Many products made by the chemical industry are above ambient temperatures at some or all points in the manufacturing process. Some of these products are considerably higher in temperature as they are produced such as glass, polymers, metal and synthetic fibers. A method of monitoring the composition or quality of the product would be desirable, but conditions and hazards in the plant environment may make absorbance or reflectance measurements difficult to obtain. Emission spectroscopy, on the other hand, may have several advantages over transmission spectroscopy in such situations. Multivariate calibration methods should help to make IES a useful analysis tool in a number of process analysis applications. While the main emphasis in this work will be on process analysis, the methods will undoubtedly find application in other areas.

The objective of this project is therefore to demonstrate the feasibility of extracting chemical and/or physical property information from infrared emission spectra by use of the appropriate chemometric data analysis techniques. Chemometric methods show promise in developing calibration models that can accurately analyze for individual components in the presence of interferences from the other sample components as well as other factors (e.g., temperature) for certain sample types.

2.2 Theory of Infrared Radiation

2.2.1 Early Discoveries in Infrared Radiation

The existance of infrared radiation was first noted by Herschell around 1800 by observing an alcohol thermometer in the solar spectrum outside of the visible range.[42] Once the thermocouple was invented in 1822, it could be blackened for use as a radiation detector. Maxwell's theory of electromagnetic waves spurred research after 1870.

Planck was the first to successfully explain the spectral distribution of radiation intensities with temperature by requiring that radiation modes at various frequencies could only be excited to discrete energies at integral multiples of $h\nu$ where h is Planck's constant and ν is the frequency. For a black body, which is a perfect absorber and ideal radiator, the Planck distribution can be expressed in a number of ways, for example in terms of specific luminance over frequency,

$$L_\nu = \frac{2h\nu^3}{c^2 (e^{h\nu/kT} - 1)}$$

specific luminance per cm^{-1} ($\bar{\nu}$ indicates wavenumbers),

$$L_{\bar{\nu}} = \frac{2hc\,\bar{\nu}^3}{e^{hc\,\bar{\nu}/kT} - 1}$$

or per unit wavelength

$$L_\lambda = \frac{2hc^2}{\lambda^5(e^{hc/\lambda kT} - 1)}.$$

The resulting emission intensities over wavelength are shown in figure 2.2.1 for a variety of temperatures. Emission intensities reach a maximum, then drop off at higher energies or shorter wavelengths. As temperature increases, emission intensities increase at all wavelengths, but the distribution and its maximum are shifted toward higher energies or shorter wavelengths.

2.2.2 General Infrared Theory

The definition of a black body is that it is a perfect absorber of radiation. But the truth of the matter is that real objects are generally not black bodies, although some objects can be made which approach black body behavior. Thus when incident radiation strikes an object, it may be absorbed, reflected or transmitted by the object. The total of these three effects, however, must account for all of the incident radiation, that is

$$R + T + A = 1$$

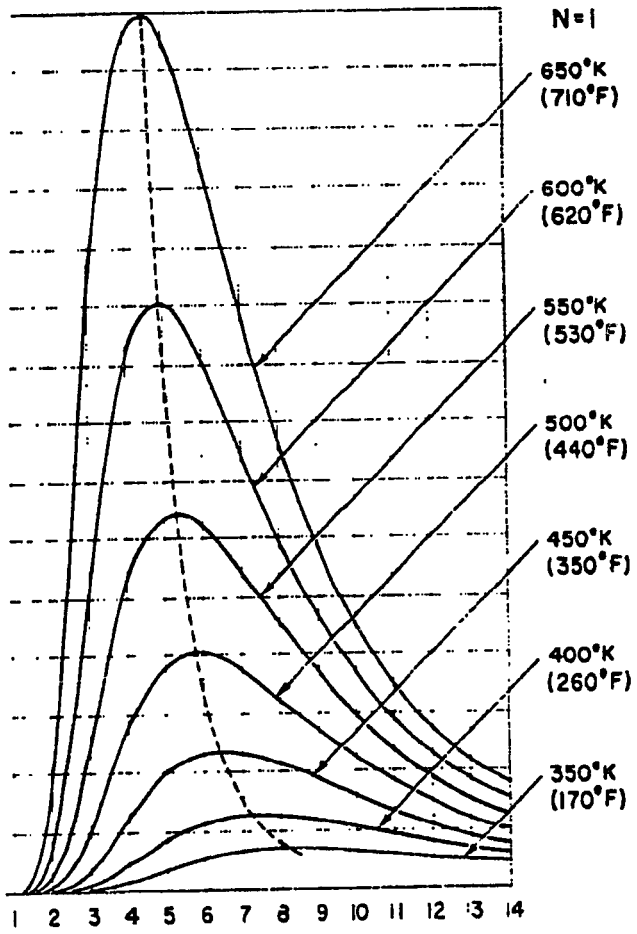

FIGURE 2.2.1 Planck's Black Body Emission Curves. Planck curves over wavelength (in microns) at selected temperatures.

where reflectance, R, is the fraction of incident radiation reflected by the sample, transmittance, T, is the fraction transmitted and absorptance, A, is the fraction absorbed. This will be true for any wavelength of radiation observed. Note that the A used here is not the same as absorbance which is defined as -log T.

The fact that different samples interact differently with radiation of varying wavelengths is used to advantage in the various forms of spectroscopy. The infrared region has been especially useful in transmission or absorbance experiments for the identification and characterization of organic compounds in which certain functional groups absorb radiation predictably in characteristic wavelength regions.

A black body is also an ideal emitter of radiation. But again real samples are generally not ideal emitters. If a sample is in temperature equilibrium with its surroundings, the second law of thermodynamics requires that there can be no net exchange of energy, thus the energy absorbed by a sample will equal the amount emitted by it, and it can be said that

$$A = \varepsilon$$

where ε (emittance) is defined as the emission of the sample divided by the emission expected at that wavelength and temperature for a true black body. This relationship is Kirchhoff's law. If this relationship were not true, and a sample was able to absorb radiation more efficiently than it emitted, it could spontaneously increase in temperature from its surroundings, which obviously is not the case.

The fact that there can be no net exchange of radiation between objects at thermal equilibrium applies to all objects, including radiation detectors. For radiation to be detected, the source of radiation and the detector must be at different temperatures.

If the value of ε is relatively constant at all wavelengths for an object, it is called a gray body, which is the case for many metals. Otherwise samples tend to have characteristic emittance values which change over wavelength.

True black body radiation does exist in any black body cavity, which is any enclosed area whose walls are at thermal equilibrium and have a transmittance of zero. Multiple reflections along with the balanced absorption and emission result in a black body distribution of radiation within the cavity. Thus a small hole into such a cavity is the best approximation to a black body radiator that is available. For the same reason, the texture of the surface of an object will affect its emittance, with a rough or pitted surface generally having higher emittance values.

The relationship between absorptance and emittance is shown in figure 2.2.2. The bottom trace is the emittance spectrum of a polyethylene film which is ratioed against the emission of a black body at the same temperature. The top trace is the transmission spectrum of the same sample. Bands of emission and absorption occur in the same positions in the spectra. Thus the same information used for qualitative and quantitative analysis in transmission spectroscopy should also be present in emission spectra.

2.2.3 Advantages of using Infrared Emission Spectroscopy

Any heated sample, then, will be an emitter of radiation in the infrared region. The detection of that emitted radiation as a function of wavelength (or wavenember or frequency) is referred to as infrared emission spectroscopy (IES). The more commonly used forms of spectroscopy consist of the various methods which study the way a sample interacts with an incident beam of radiation, by transmission and absorbance, reflectance, scattering, fluorescence, etc. Since IES simply detects emission radiated by the sample itself, it has a number of advantages over the more traditional spectroscopies.

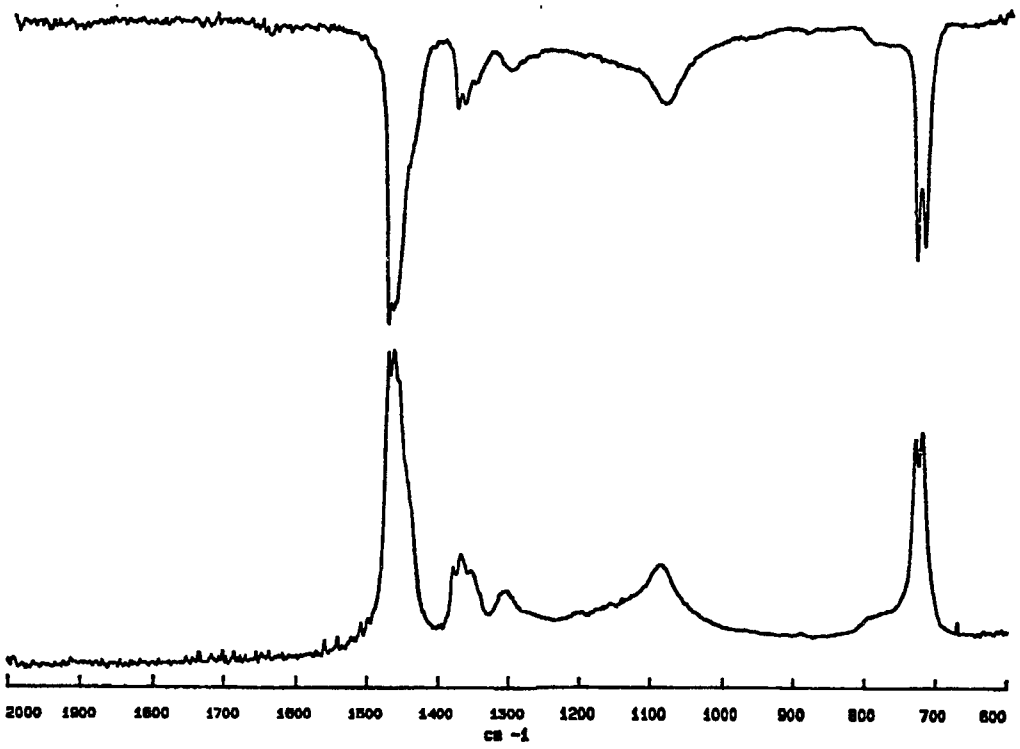

FIGURE 2.2.2 Polyethylene spectra. Transmission and emission spectra of a polyethylene film ratioed to a black body of the same temperature.

These advantages will be discussed specifically with the situation of process analysis in mind, that is, chemical analysis as a product is being manufactured in an industrial plant setting.

The most obvious advantage is that there is no need to use an external source of radiation to see how the sample absorbs, reflects, scatters it, etc. The hot sample acts as its own source. Thus there are no concerns about instability or drift of the radiation source to be compensated for in the design of the experiment.

This also means that requirements for optical alignment are minimized in IES. In the other spectroscopies, great care must be taken to see that the radiation interacts with the sample and strikes the detector exactly as desired to minimize uncertainties in the measurement. This often requires precise alignment of source, sample, detector and optical components such as reflectors and lenses on a very stable optical table. But vibrations, temperature fluctuations, electromagnetic fields, corrosive chemicals in the atmosphere or other hazards in the plant environment may make it difficult to maintain the conditions necessary for such instruments.

The simpler optical requirements in IES apply to the sample itself as well. IES is less sensitive to effects such as reflections or diffractions which may occur at the surface of the sample than other spectroscopies. In addition, emission methods do not require a planar or smoothly curved surface. This means greater flexibility in the shapes of samples that can be used in emission. Also the optical system used to collect the emitted radiation can be chosen to fit the needs of the measurement. Emission from a large area can be collected to provide additional radiance resulting in an average spectrum for that portion of the sample. Alternatively, emission can be collected from samples or portions of samples as small as one millimeter in diameter. Where intensities are small,

additional radiation can be detected by collection over a wide solid angle from the small spot.

The more lenient optical alignment requirements also mean that IES can be done more remotely from the sample. In other spectroscopies, the instrument is generally within a few inches of the sample. Even in the case of fiber optics where the source and detector are removed from the sample, the optical fiber is usually very near, if not in contact with, the sample. But for IES the distance from the sample to the instrument and detector can be anywhere from a few inches to several feet--or miles if the sample is large enough, as is the case in atmospheric studies, for example. This ability to measure remotely could be especially useful in cases when the sample is difficult to approach, such as very hot or radioactive samples.

The remoteness of the measurement also means that it is very non-invasive. The sample may not need to be removed from the process or affected in any way by the measurement. This is in contrast to most current chemical measurements for quality control or quality assurance which require taking a sample from the process to the analytical laboratory for measurement. IES is also therefore a non-destructive measurement of the sample; no sample is used up or lost in getting the measurement.

Eventually, if a two-dimensional chemical image or "map" is desired, this may also be easier done with emission spectroscopy, as is done currently for thermal imaging ("night vision"). Emission from the entire sample could be detected simultaneously for a given wavelength, then scanned over the desired wavelengths. Again the optical system required would be much simpler than a device to scan absorption or reflection spectra over a given region of the sample.

While IES will probably not be useful in most cases for trace analysis in complex mixtures, it can be used for trace analysis on reflective surfaces. Some examples of this

are analyses of trace impurities on magnetic media or corrosion on metal. Where transmission experiments on these samples would require measuring minute differences between large signals caused by small absorbances due the sample in the large signal from the high temperature source, emission studies involve measuring small emissions from the sample against the relatively small background emission of the substrate.

And since emission spectra are dependent on temperature, they will contain information about the temperature of the sample which may also be useful. This assumes that the raw emission spectrum is used. Where the emittance spectrum of the sample is desired, the actual temperature of the sample must be known so that the spectrum can be ratioed to that of a black body of the same temperature. Once this ratioing is done, the temperature information is removed from the spectrum.

2.2.4 Disadvantages of using IES

Of course, emission spectroscopy has a number of disadvantages as well, which have resulted in its minimal usage to date. When deciding the method to be used for a given analysis the advantages and disadvantages of each method must be carefully weighed to find which will provide the superior method of analysis.

The main disadvantage of IES is given by the Planck equation. The lower the temperature of the radiation source is, the less radiation will be available for detection. Therefore a sample between 30 and 200° C will emit much less radiation than the usual instrument glowbar source at several hundred or more degrees. This effect is much more severe at higher energies or shorter wavelengths where emission intensities drop off sharply, so wavelength range is limited in emission experiments. Cooled detectors are available which give reasonable responses over a portion of the IR spectrum for emission from samples at moderate temperature. Figure 2.2.3 shows the Planck curves

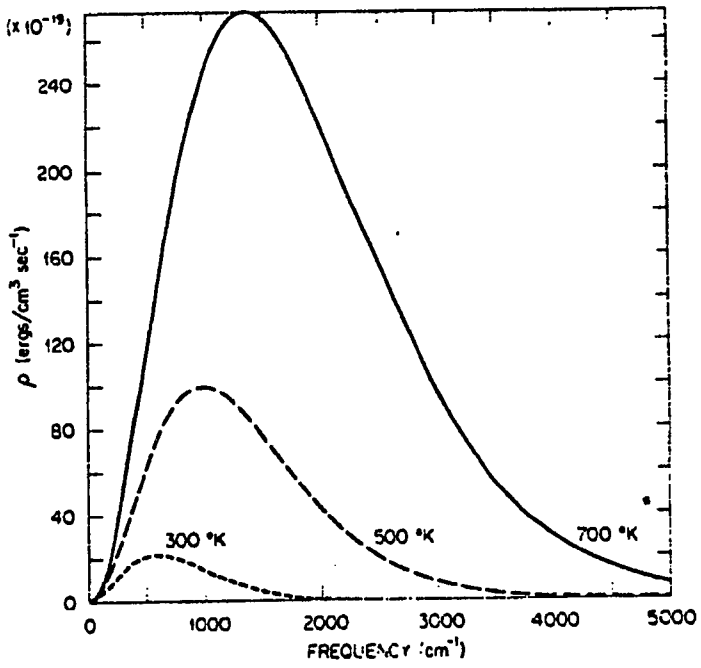

FIGURE 2.2.3 Planck curves over wavenumber. Planck black body emission curves over wavenumber at selected temperatures.

over wavenumber for selected temperatures. Samples below 200° C, for example, will generally give spectra of adequate intensity up to 2000 cm^{-1}, but signal-to-noise ratios will often be too low to be of use above about 2000 cm^{-1}. Of course, for samples at much higher temperature this will not be a limitation.

And in order to observe a spectrum, the sample must be at a different temperature than the detector as noted earlier. It also should preferably be at a different than its surroundings. A sample at the same temperature as its surroundings essentially acts as a sample within a black body cavity, so only the black body temperature information will be observed in the spectrum. Thus observation of a sample in an enclosed vessel, or at room temperature in an open room, will provide little spectral information other than temperature.

As sample thickness increases, its transmittance decreases and absorptance (and thus emittance) increases. The sample eventually becomes essentially opaque. Thus no information will be available in a transmission experiment. In emission it will appear as a black body unless spectral variation is produced at the surface of the sample due to the presense of either (a) reflective properties of the surface or (b) a temperature gradient at the surface of the sample which affect relative absorption and emission in the surface layer. However, since most samples have emittance values less than one, there will generally be some information left in emission spectra.

An additional disadvantage of emission spectroscopy is that temperature information is present in the spectrum. The presence of temperature information in the spectrum has been listed as both an advantage and a disadvantage. If temperature information in the spectra is not useful, it only serves to make the spectra more complex. In fact, the lack of the ability to appropriately interpret complex emission spectra has greatly hindered its application.

2.2.5 Possible Applications of IES

These advantages and disadvantages of the use of emission spectroscopy give an indication of the types of samples and situations for which emission spectroscopy may or may not be useful.

Emission spectra will show the greatest variation and therefore be expected to contain the most information for samples which have the largest variation of emittance over wavelength. Due to the relationship between emittance and absorptance, any sample for which a suitable transmission spectrum can be obtained should provide a reasonable emission spectrum if it can be held at an appropriate temperature. These samples will have low absorptivities or low optical thicknesses at some wavelengths, and high absorptivities at others.

If reflection is ignored so that we can assume

$$A + T = 1$$

and the sample thickness is increased to the point of being optically thick (opaque), transmission approaches 0 and A approaches 1. Since $\varepsilon = A$, the sample will appear to be a black body in emission. Materials with rough or textured surfaces generally have low reflectance, so if they are optically thick very little information other than temperature will remain in the spectra. An exception might be if a temperature gradient could be induced at the surface; since the total amount of radiation emitted is dependent on temperature while the fraction of incident radiation absorbed is relatively independent of temperature, some spectral features might be observed. This has been done, for example, by exciting surface emission using lasers.[43] This effect also is observed as line reversal in samples with temperature gradient which are cooler at the surface.

It is difficult, however, to find samples which act as perfect black bodies because of reflection effects at the surface. If we now look at an opaque sample where the transmission approaches zero,

$$R + A = 1$$

and since $\varepsilon = A$

$$\varepsilon = 1 - R$$

so the information in an emission spectrum of an opaque sample should be roughly the same as in a reflection experiment. Since reflectance is dependent on refractive index, which often varies with the wavelength of radiation based on absorption bands, some chemical information may be available in the emission spectra even of opaque samples. This can be understood intuitively by viewing the bulk of the sample as a black body emitter, while some of this radiation is internally reflected so that it does not escape the surface. IES might therefore be useful on samples with smooth or reflective surfaces such as glasses, polymer extrusions and bulk liquids.

2.2.6 Modeling Emission Spectra

There have been attempts to explicitly model what should be expected from IR emission spectra. These generally are of two types. The first is the accounting or ray tracing method.[44, 45] For a slab of partially transparent material with parallel surfaces, an expression is developed for emission perpendicular to the surface. Emission from a given point is calculated in the forward and reverse directions, and

each ray is followed through the absorptions as it travels through the material and reflections at the two parallel surfaces to find the total emission intensity which escapes the surface. The application of this method is restricted to flat slabs with smooth surfaces which are homogeneous not only in composition, but also in temperature; if temperature gradients are present this method cannot be used. It also, of course, requires a knowledge of the absorptive and reflective properties of the material used.

The second is to solve the equation for radiative transfer.[46, 47, 48] The equation of transfer in the direction s is

$$\mathbf{s} \bullet \nabla I_\nu = \kappa_\nu \left[n_\nu^2 I_{b\nu} (T) - I_\nu \right]$$

where κ_ν is the spectral absorption coefficient, n_ν is the spectral index of refraction and $I_{b\nu}$ (T) is Planck's function. For a slab with parallel surfaces as discussed earlier this is expressed as

$$\cos\theta \frac{dI_\nu}{dy} = \kappa_\nu \left[n_\nu^2 I_{b\nu} (T) - I_\nu \right].$$

The first term on the right accounts for emission, and the second for absorption. As with the earlier method, knowledge of the properties of the material is required.

Both of these methods involve calculations to predict the emission expected based on the known properties of the sample material. They have not been used for the inverse problem of predicting the properties or composition of the material given the observed spectra, which would be a much more complex problem. Therefore neither of these have been found to be especially useful for quantitative analysis.

In this study, on the other hand, an implicit calibration model is developed using the PLS regression method to relate the information in the spectra with the desired parameters by means of a calibration procedure using known samples. This will be discussed in greater detail in section 2.4.

2.3 Previous Applications

Infrared emission spectroscopy has been used in a number of different applications in the past. Most of these applications relate to temperature measurements by optical pyrometry, or qualitative analysis of optically thin samples, although there have been attempts to use IES quantitatively. Quantitative applications of IES in the chemistry literature generally are done on optically thin samples under carefully controlled laboratory conditions, usually with known temperature.

A number of reviews or general papers are available of applications of IES in the chemistry literature [44, 49, 50] or reviews of infrared spectroscopy which include sections on emission [51, 39]

2.3.1 Temperature estimation

IES has been used extensively for temperature measurements in various forms of optical pyrometry or thermal imaging. These methods assume that either the object is a black body, or that its emittance is known for the type of sample being studied in order to calculate temperatures.[52] The emission intensity from the sample is then related to temperature by means of the known emittance and the Planck black body curves. Effects of reflective properties of the surface, atmospheric absorption and emission including dust and vapors, reflected background radiation, etc. must also be considered.[53]

The method was used initially most widely for high temperature measurement due to the requirements of detectors at the time for higher intensity radiation. One common application was temperature measurement of molten glasses.[54] It was realized that the semi-transparency of glass complicated the measurement when temperature gradients were present in the sample,[55] but that this effect could also be used to provide a depth profile of temperature.[56, 57] Infrared emission has also been used for imaging of warm objects ("night vision"), and has been used on objects as small as components of circuit boards.[58]

2.3.2 Molten Salts

Infrared emission and absorption spectra were known to theoretically give the same spectral information, but high temperature samples were required for collecting emission spectra on dispersive instruments initially used. One class of samples which fit this need well was molten salts. Absorption spectra for these samples were difficult to obtain since appropriate window materials for sample cells were not easily found for working at such high temperature which would still transmit in the desired spectral regions.[59] However, emission spectra could be collected on thin films of these samples relatively easily. A thin film of the sample must be obtained on a substrate of relatively low emittance, usually a polished metal surface. A variety of sample preparation methods have been devised for taking these measurements.[60, 61, 40]

2.3.3 Thin Films

As infrared technology improved, emission spectra could be taken at lower temperatures, and thus could be used on a wider variety of samples. The greatest improvements have been the use of cooled detectors, and the use of interferometrically based Fourier transform instruments which are capable of a much higher throughput of

radiation.[62, 63] The technique has been most useful for very thin films of samples on a reflecting backplate. As samples become thicker, self-reabsorption and temperature gradients make the spectral features less distinct and more difficult to interpret.[38, 64]

Interest has therefore been shown in using IES as a surface analysis technique. A number of species of interest occur as thin films or layers on materials of low emittance. For example, numerous IES studies have been made of oxide coatings on metals.[65, 66, 67] These oxide films are generally so thin that it is difficult to obtain reasonable spectra from transmission/reflectance methods due to the small absorptivities. Emission spectra, on the other hand, can be collected efficiently by averaging multiple scans, and contain essentially the same information. Often such oxide coatings serve as catalysts, and emission spectroscopy can be used effectively to study both the oxides and the adsorbed reactant and product species.[68, 69, 70]

A variety of other films have been formed on metal surfaces for analysis by IES. Emission from films of heated oils were reported by Kapff as early as 1948.[71] Due to the temperatures used in emission experiments, studies of liquid samples have generally been limited to materials of low vapor pressure. Lauer has been one of the most prolific workers in the area of IES, and has done extensive studies of lubricants [72] and fuel deposits after combustion.[73] Solid samples analyzed in this way include pesticides [74] and polymers.[75] Blanke *et al.* have compared the potential of emission and reflection/absorption spectroscopies for the analysis of monolayers or samples of known numbers of molecular layers.[76]

Additional effects that have been considered include multiple passing of radiation through the interferometer due to the reflecting backplate [77] and the angular dependence of emission.[78] Polarization techniques have also been used,[79] including studies of molecular alignment.[80] The spectral distortions attributed to

temperature gradients in liquids and molten salts have also been explained by reflectance at the surface and modelled using an isothermal harmonic oscillator.[40] These studies have led to the use of opaque (thick) samples as reference giving undistorted spectra.

2.3.4 Gases

Other samples which are generally found to be optically thin are those in the gas phase.[81] Spectral detail is quite sharp in gas phase IR spectra. Emission spectroscopy is used in the laboratory as a means of studying energy levels in molecules.[82] Such spectra are of special interest in the study of combustion products.[83] This method has also been used for remote monitoring of stack gases in smokestack emissions using a telescope as part of the optical collection system.[84, 85]

Another area where gas phase IR emission spectroscopy has been especially useful is in studies of the atmosphere.[86] With a system of study as large as the earth's atmosphere, obviously a remote sensing method such as IES is most useful. Such systems may be ground, air or satellite based, with a number of satellite based systems used for continuous monitoring. A number of data analysis methods have been developed to extract meaningful information from the spectra in spite of the changing density and temperature of the atmosphere with altitude.[87, 88, 89] Small et al. have developed a method for detecting specific atmospheric constituents whose spectral features are known by means of digital filtering of the interferograms.[90]

2.3.5 Solids

Since emittance values vary with different material, IR emission has been used in geological studies of various rocks and minerals.[91] These studies of the composition

of the earth and oceans can also be done from satellite data.[92, 93]

A variety of other types of solid samples have been studied as well. Emission studies can give additional information on the lattice structure of solid materials such as single crystals [94] and semiconductors.[95] Folberth and Heim have even found that the emission from human skin can be useful in the diagnosis of certain chronic diseases.[96]

2.3.6 Stimulated Emission

IR emission spectra are usually taken from samples which are normally found at elevated temperatures, or heated with traditional heat sources such as electrical heating elements. However, there have been a few studies which used lasers to induce local heating of the sample. This method was initially used on gas phase samples,[97, 98, 99, 100] and is often referred to as infrared fluorescence. The spectra obtained in this manner, especially from gases at low pressure, may not be the same as spectra from samples excited by heat alone, since the lasers initially excite selected vibrational states.

Laser-induced thermal emission has also been used on condensed phases such as solid polymers.[101] When higher pressure gas samples or condensed phases are studied, vibrational energy is rapidly redistributed by collisions to heat energy, and observed spectra are essentially from systems at thermal equilibrium.

2.4 Partial Least Squares

It is clear from the number of previous applications and attempts to use IR emission that it shows great potential as an analytical method and has generated a great deal of interest in the analytical chemistry community over the years. Nevertheless, the majority of applications have been only qualitative in nature, and other than the

atmospheric and geological applications, have generally been limited to carefully controlled laboratory conditions with samples of known temperature.

Yet Griffiths has pointed out that if a general method for quantitative analysis by IES could be formulated it would be a powerful method for monitoring the concentrations of reactants, products and even intermediates in industrial processes.[49] Hirschfeld also mentions that the greatest need is in improving algorithms for rendering emission data more useful quantitatively.[39]

Multivariate calibration methods, and specifically the Partial Least Squares (PLS) method, have been found useful for quantitative analysis in a number of spectroscopic techniques.[102] The most common applications are absorbance or reflectance methods in the mid- and near-IR regions.[103, 104] Infrared emission spectra differ from these methods in that when the spectra are not referenced to a black body of the same temperature emission spectra are quite non-linear in relation to concentration. It is shown later in this work that in spite of these non-linearities the PLS method can be used for prediction in IES.

The PLS regression method and algorithm have been described in the literature.[105, 106] A summary of the method will be given here, along with a short discussion of principal components analysis and principal components regression as a basis for understanding PLS.

PLS regression is an extension of the multiple linear regression problem. The initial assumption is that there is a linear (first order) relationship between a set of measured quantities called independent variables and another quantity called a dependent variable which is to be predicted for unknown samples from the independent variables. In the case of spectroscopy with m wavelengths, the response at each wavelength is an

independent variable which can be denoted x_j for j = 1 to m. If the dependent variable to be predicted, for example concentration, is denoted as y, then

$$y = b_1x_1 + b_2x_2 + b_3x_3 + \ldots + b_mx_m + e$$

or

$$y = \sum_{j=1}^{m} b_jx_j + e$$

or in vector notation

$$y = \mathbf{x'b} + e$$

where the b_j's are the coefficients to be determined while minimizing the error, e. (All vectors are column vectors; row vectors are denoted by " ' ".) Once the appropriate **b** vector is found, the y value for an unknown sample can be estimated by measuring $\mathbf{x'}$ (spectrum) and multiplying by **b**. Since the same b_j values should apply to all samples in the range to be tested, if n calibration samples are found with known y values (by some other reference analysis method), the spectra can be expressed as rows in an n x m data matrix **X** and the n y's and m b's as column vector elements so

$$\mathbf{y = Xb + e.}$$

There are now three possible situations:

If m = n, the number of samples equals the number of variables (wavelengths), a unique solution for **b** can easily be found if **X** has full rank. In this case **e** = 0.

If m > n, there are more variables than samples, an infinite number of solutions can be found for **b**, which is not useful. In this case variables can be deleted, but any information from the deleted variable is lost.

If m < n, there are more samples than variables, no exact solution can be found. A solution can be determined, however, by minimizing the residual, **e**. The most commonly used method to accomplish this is the "least-squares method", where

$$\mathbf{b} = (\mathbf{X}'\mathbf{X})^{-1}\mathbf{X}'\mathbf{y}.$$

A problem occurs where the inverse of **X'X** does not exist due to collinearity.

The situations where MLR alone will be useful is therefore somewhat restricted. Some additional methods have been developed to overcome the problems of collinearity and more variables than samples.

Principal components analysis (PCA) allows an **X** matrix of rank r to be written as the sum of r matrices of rank one. The rank is the intrinsic dimensionality of the matrix. Thus

$$\mathbf{X} = \mathbf{M}_1 + \mathbf{M}_2 + \mathbf{M}_3 + \ldots + \mathbf{M}_r = \mathbf{t}_1\mathbf{p}_1' + \mathbf{t}_2\mathbf{p}_2' + \mathbf{t}_3\mathbf{p}_3' + \ldots + \mathbf{t}_r\mathbf{p}_r'$$

where each **M** is the outer product of two vectors: a score vector **t** and a loading vector

p'. The **p'** vectors in this case are the principal components of the matrix, that is, $\mathbf{p}_1'$ is the first principal component and is a unit vector in the direction that explains the greatest variance in **X**; $\mathbf{p}_2'$ is an orthogonal vector which explains the greatest variance left after $\mathbf{p}_1'$ is removed, etc. The **t** vectors are then the projections of the individual samples onto each of the **p**'s. These results can be found either by the eigenvector formulae, or on computer by the iterative NIPALS (nonlinear iterative partial least squares) algorithm.

At this point principal components regression (PCR) can be used to build the model for prediction. The n x m **X** matrix is first transformed by representing it as its n x a scores matrix **T** consisting of the first a scores vectors. Dimensions having small eigenvalues are excluded to prevent collinearity problems, and the **T** matix has rank a. The MLR formula now becomes

$$\mathbf{y} = \mathbf{Tb} + \mathbf{e}$$

and since the inverse of **T'T** does exist the estimate of **b** is

$$\hat{\mathbf{b}} = (\mathbf{T'T})^{-1}\mathbf{T'y}.$$

PCR thus solves the collinearity problem, and the problem of having more variables than samples by reducing the rank while retaining information from all of the variables. In addition, there may be some noise reduction by eliminating the smaller principal components. However, the principal components are chosen only based on their ability

to model **X**, so some information which could be helpful to predict **y** may also be lost when the smaller principal components are removed.

The Partial Least Squares (PLS) method is built around the NIPALS algorithm. Rather than finding principal components based only on their ability to model **X**, PLS finds its latent variables based on their ability to model **X** and their ability to predict **y**. This is done by an interchange of information between the **X** and **y** data.

In simplified form, for prediction of a single y variable the PLS algorithm can be expressed as

(1) take $\mathbf{u} = \mathbf{y}$

(2) $\mathbf{p}' = \mathbf{u}'\mathbf{X} / \mathbf{u}'\mathbf{u}$

(3) $\mathbf{p}'_{new} = \mathbf{p}'_{old} / \| \mathbf{p}'_{old} \|$

(4) $\mathbf{t} = \mathbf{X}\mathbf{p} / \mathbf{p}'\mathbf{p}$

(5) $\mathbf{X}_{residual} = \mathbf{X} - \mathbf{t}\mathbf{p}'$

(6) repeat.

It is possible to calculate as many PLS components as the rank of **X**, however they are normally not all used. A method must therefore be chosen to determine the number of latent variables or factors to be retained for the model. Since our main concern is the ability of the model to predict unknown samples, predictive ability will be determined using a cross-validation procedure. One sample at a time is removed from the data set and the model is built using the remaining samples. This model is then used to predict the y value of the sample that was left out, and the predicted value is compared the known reference value.

From these predictions, a couple of statistics are calculated to help us evaluate the

method. The first is the PRESS (prediction residual error sum of squares) [107] which is the sum of the squares of the prediction errors over the n samples:

$$\text{PRESS} = \sum_{i=1}^{n} (y_i - \hat{y}_i)^2 \ .$$

where the y_i 's are the reference values obtained by an independent method of analysis and the $\hat{y}_i$'s are the values predicted by cross-validation. The number of factors retained is the lowest number of factors with a PRESS within the uncertainties of the lowest PRESS obtained, that is, the lowest number of factors with a prediction which is not significantly worse than the best PRESS obtained.

Secondly, the SEP (standard error of prediction, or average prediction error) [108] is calculated to give us a meaningful expression of how well the method is able to predict relative to the true values:

$$\text{SEP} = \left(\sum_{i=1}^{n} (y_i - \hat{y}_i)^2 / n \right)^{1/2} = \left(\text{PRESS}/ n \right)^{1/2}$$

The SEP, then, gives an indication of how well the model will predict a sample not contained in the calibration set. The ability of a method to predict as measured by SEP can be no better than the uncertainty of the reference analysis method. While the PLS prediction may actually be better than the reference values from a certain amount of signal averaging due to the number of calibration samples and variables used, the "scatter" in the reference data will remain in the SEP.

Note also that any unknown samples must be adequately represented in the calibration set for accurate prediction. A number of diagnostics are used with the

algorithm to detect samples which are outliers relative to the calibration (which will not be discussed here).

2.5 Polymer Experiments

The samples chosen for the initial experiments in infrared emission spectroscopy were a series of ethylene/vinyl acetate copolymers of varying composition. These samples were chosen as a model system which would have great industrial interest for process analysis. Many polymers are found at elevated temperatures as they are produced, and a method for monitoring their composition and thickness as well as temperature is of great interest. These samples are also easy to work with in an emission type experiment, as they can pressed into films of the desired thickness and heated in an appropriate sample holder.

2.5.1 Experimental

Samples used in this study consisted of commercially available ethylene/vinyl acetate copolymers formed from 9.0, 9.5, 15, 18 and 28% of the vinyl acetate monomer, corresponding to Dupont product numbers Elvax(trademark) 750, 770, 550, 450 and 265. Figure 2.5.1 (A and B) shows the chemical structure of the monomers used to form the polymers, and (C) the repeating units which would be expected in the polymer after reaction. Vinyl acetate concentrations are mean values for the monomer before polymerization from the published nominal values with a range of +/- 1 % absolute. The sample pellets were pressed into films of varying thickness from 0.1 to 0.5 mm using a Carver press with heated plate attachment. Thicknesses were selected

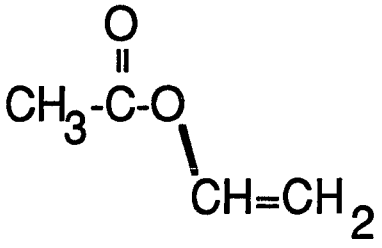

Vinyl acetate

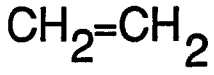

"Ethylene"

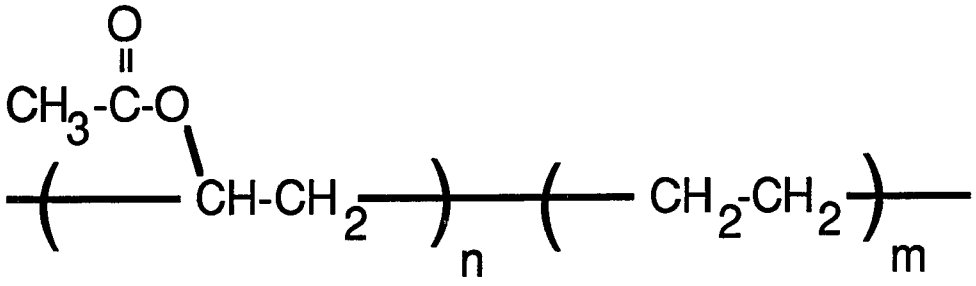

Copolymer

FIGURE 2.5.1 Ethylene/vinyl acetate copolymer structure. Chemical structures of monomers and copolymer product. A. Vinyl acetate. B. Ethylene. C. Repeating units found in copolymer product.

by calibrated metal shims. Samples were pressed for approximately 5 minutes at about 1000 psi, at 10°C below the published softening point of the particular polymer.

Data were collected on a Perkin-Elmer model 1800 FTIR spectrometer equipped with a wide band MCT detector in which the normal source was replaced by a heated sample holder containing the sample. Samples were held in the sample holder as polymer films. In contrast to most other studies, no reflecting backplate was employed. Single beam emission spectra were measured from 4000 to 450 cm^{-1} at 2 cm^{-1} intervals by the coaddition of 16 to 32 scans at 4 cm^{-1} resolution. Data were collected on samples made from the five different concentration of vinyl acetate (9.0, 9.5, 15, 18 and 28%) at four thicknesses (0.1, 0.2, 0.3, 0.5 mm) and three temperatures (100, 110, and 120° C). Temperature was controlled using a Perkin-Elmer temperature controller nominally to +/- 1° C. Each concentration and thickness was a physically different pressing of the sample pellets, while temperature variations were induced in a systematic fashion from 100 to 120° C on each pressed sample.

The single beam emission spectra of each of the 20 sample films (five concentrations at four thicknesses) were measured at three temperatures (100, 110 and 120 °C). This gave a total of 60 possible spectra, seven of which had to be eliminated due to experimental difficulties (such as melting or tearing during heating) leaving 53 for the calibration set. These 53 single beam spectra were used to build a model using PLS analysis. The region from 2000 to 450 cm^{-1} at 1 cm^{-1} intervals of the single beam emission spectra was used in all cases giving 1550 data points per spectrum. The data were mean centered before application of PLS. The 4000 to 2000 cm^{-1} region was eliminated due to poor signal to noise ratio caused by low emission intensities from the samples at the relatively low temperatures used in the study.

2.5.2 Results and Discussion

Figure 2.5.2 shows the single beam emission spectrum of a 15% sample at 0.1 mm thickness taken at 120° C compared with the transmission spectrum of a sample of the same composition. No attempt has been made to correct the emission spectrum based on response of the instrument, background or temperature--which could be done, for example, by ratioing to a black body. It therefore retains the shape of the black body curve superimposed on the spectrum; this also means that the temperature information should still be available in the spectrum. The positions of emission bands correspond directly with bands seen in the reference transmission spectrum in figure 2.5.2 B; however due to the multiple radiation transfer events in emission from thick films the band shapes in the emission spectrum are distorted. Nevertheless specific group frequencies and indicator (fingerprint) bands can be readily identified in the emission spectrum of this sample. Specifically, the C=O stretch at 1740 cm^{-1} along with the 1240 cm^{-1} band, and the 1375 cm^{-1} band due to the methyl group protons indicate the CH_3-(C=O) (acetate) group. Also the 1450 and 720 cm^{-1} bands are clearly identifiable, indicating deformation and rocking of CH_2 groups arising from the (poly)ethylene contribution.

Figure 2.5.3 shows a series of spectra of the same thickness and temperature at different concentrations. Note that as the relative concentration of vinyl acetate groups increases, the optical density of the sample at many wavelengths increases and structure in the spectral bands become less distinct as more wavelengths approach saturation. No single wavelength that could be directly correlated with concentration over the entire set of 53 samples. Therefore multivariate methods were used for the calibration.

The single beam spectra show a considerable variation with thickness: while a fair amount of structure including identifiable bands (as noted above) is seen in thinner

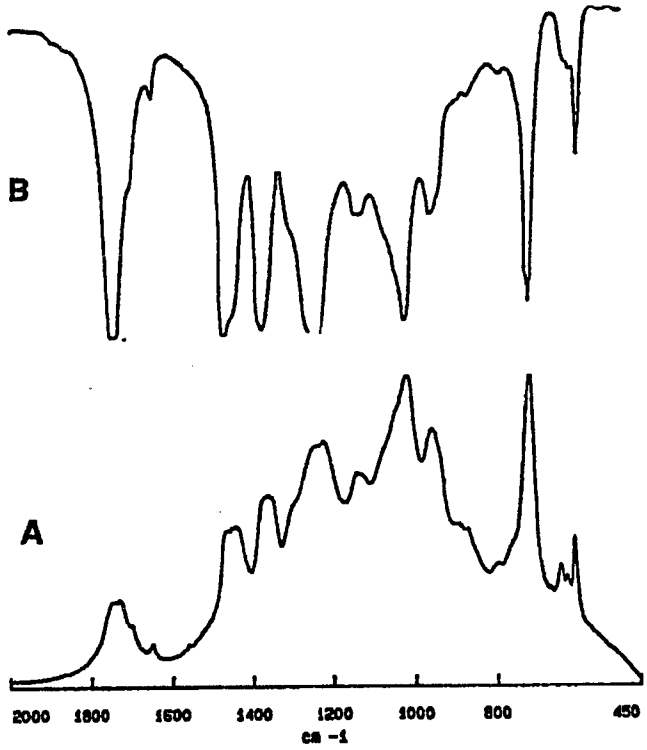

FIGURE 2.5.2 15% Vinyl acetate. Spectra of 15% vinyl acetate sample. A. Emission spectrum of 0.3 mm sample. B. Reference transmission spectrum.

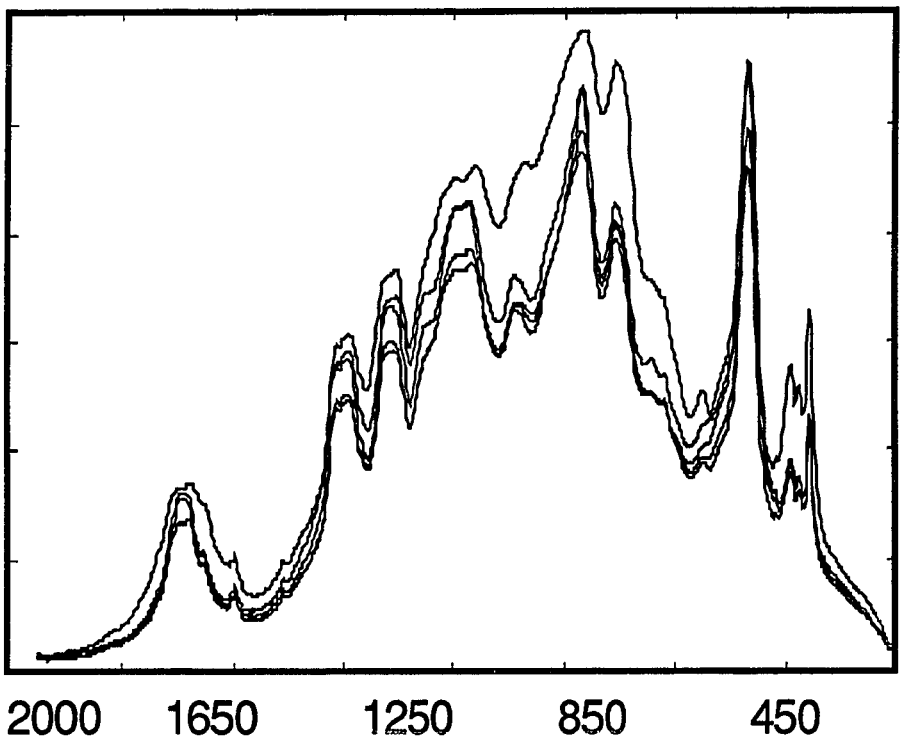

FIGURE 2.5.3 Varying concentration. Emission spectra of samples with concentrations 9.0, 9.5, 15, 18 and 28% vinyl acetate with thickness constant at 0.1 mm and temperature at 120° C.

samples, these bands are broadened and the amount of visible structure decreases as thickness, and therefore optical density, increases as seen in figure 2.5.4 Sample thickness has an effect in that radiation emitted deeper in the sample will be reabsorbed before it can escape the surface, since as we saw earlier the bands at which a sample absorbs will be in the same position as emission bands. As the sample gets thicker, it eventually becomes opaqe at a given wavelength meaning that transmittance approaches zero. If surface reflectance is minimal, the sample approaches a black body radiator.

Because uncorrected single beam data were used, the spectra also contained temperature information. Spectra of a sample show an increase in intensity with increasing temperature seen in figure 2.5.5. This indicates that attempting to directly correlate concentration with emission intensity at a single wavelength will be impossible, since intensities for identical samples will vary with temperature. However, since temperature information is present in the spectrum, temperature prediction may also be possible.

As discussed earlier, temperature obviously affects the spectrum in that a hotter sample is able to radiate more in the IR region. But this is not simply a linear effect on intensity; it is dependent on Planck's equation, so intensity is shifted to higher energies as temperature increases. This causes the effect to be non-linear.

Temperature gradients also will have an effect on how much of the radiation is reabsorbed relative to the amount of emission. For example, if the surface layer of a sample is cooler than subsurface sample, it will absorb approximately the same fraction of radiation coming from the sample interior as it would if it were all the same temperature, but it will emit less, giving lower emission intensities overall, especially at highly absorbing wavelengths.

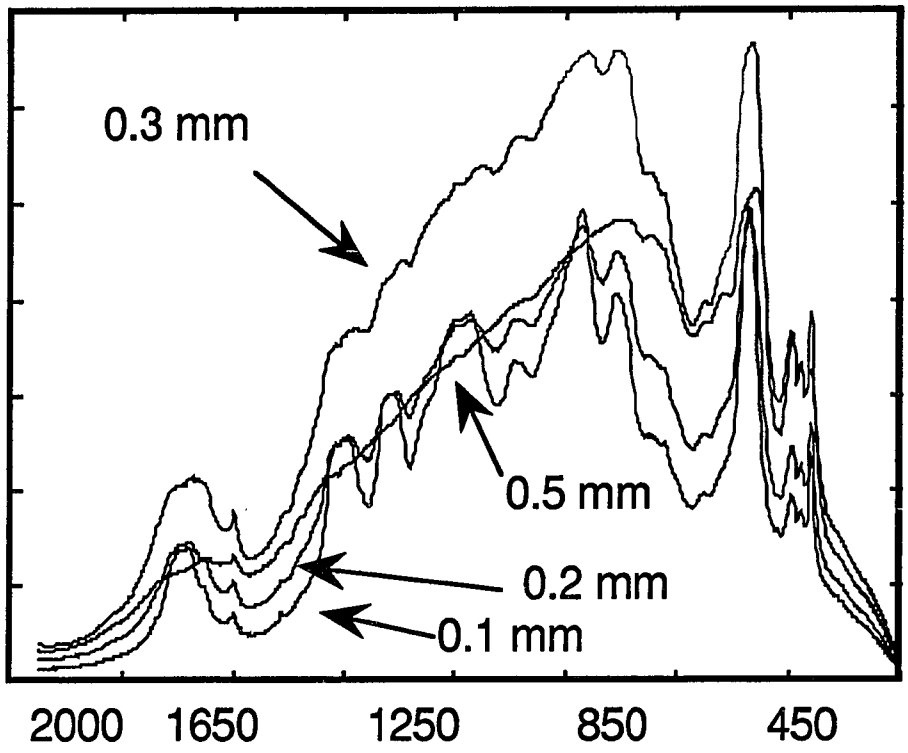

FIGURE 2.5.4 Thickness variation. Emission spectra of 0.1, 0.2, 0.3 and 0.5 mm thick 15% vinyl acetate sample at 120° C.

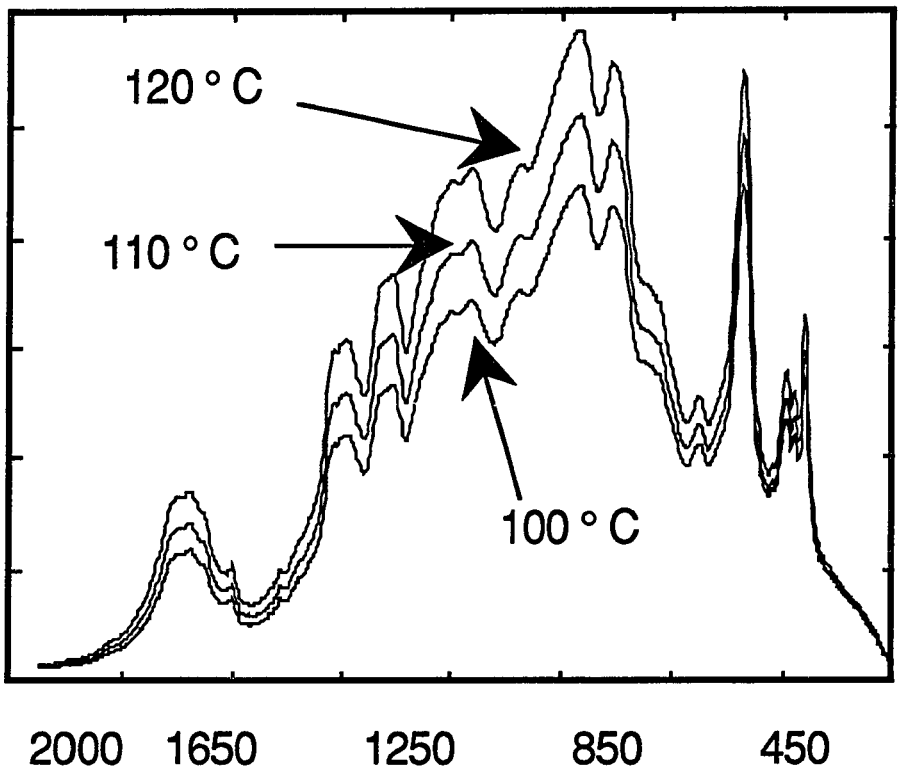

FIGURE 2.5.5 Temperature variation. Emission spectra at 100, 110 and 120° C of 0.1 mm thick 28% vinyl acetate sample.

The drop in emission intensity in the spectrum of the highest concentration sample in figure 2.5.3 and for the thickest sample in figure 2.5.4 is quite unexpected. However it is consistantly seen for the highest concentration sample in any similar series of spectra of samples with the same thickness and temperature but changing concentration except in a series of the thinnest (0.1mm) samples; it is also seen for the thickest sample in all such series for samples of a given temperature and composition but changing in thickness. The most likely explanation for this effect is that temperature gradients were present across the sample due to the method of sample heating. The sample film is held around its circumference within a heated cylinder, but its surface on both sides is exposed to the atmosphere of the instrument. The side toward the interferometer is closest to one end of the cylinder and is therefore likely to be slightly cooler. This cooler surface layer will then absorb more radiation emitted from the subsurface material than it emits itself, since absorption occurs at the same wavelength as emission. This effect would be expected to be most noticeable with increasing thickness where larger temperature gradients might be formed, or with increasing vinyl acetate concentration which would cause the surface layer to be more highly absorbing; these are exactly the situations where it is observed. This is supported by the fact that the concentration effect is not observed in the thinnest samples, where temperature gradients will be minimized. Alternative explanations for the composition effect would include the possibility that changing composition alters the thermal conductivity properties of the material creating larger temperature gradients, or that changing composition alters the refractive index and thus the reflective properties at the material surface. However, the exact cause of this effect is irrelevant to this study. What is important to note is that certain spectral irregularities may be expected in real samples in a process analysis situation. The question is whether multivariate methods will be capable of extracting the

desired information from the spectra in spite of the irregularities.

If spectra are collected in absorbance units, the effects of concentration and thickness are linearized by the relationship

$$\text{Absorbance} = -\log T.$$

But in emission spectroscopy the only way to make a similar transformation of the data is if the temperature of the sample is known so that one can ratio to a black body at the same temperature, convert from emittance to transmittance by

$$\varepsilon + T + R = 1$$

and then calculate back to absorbance units. However this means the benefit of predicting temperature of unknown samples is lost, and requires that temperature must be known precisely for all unknown samples. It also does not correct for other non-linear effects such as temperature gradients. Therefore, rather than attempting to transform the data in an attempt to fit an explicit linear model, an implicit model is developed from the data using PLS which is able to account for some of the non-linearities by using additional linear factors.

From the variance of the spectra with respect to composition, PLS analysis was able to construct a biased model for the prediction of vinyl acetate concentration. It should be noted that the model is being constructed with spectral data from the 53 samples that also have variance and non-linearities due to thickness and temperature. A 12 latent variable model was found to be optimal based on cross validation calculations of PRESS and the associated standard error of PRESS as detailed in section 2.4. This model provides a SEP of 1.1% absolute in vinyl acetate concentration over the 9 - 27% range. Restriction of the calibration set to 44 samples by the removal of all the samples

at 28 % vinyl acetate provided an improvement in the predictive power of the method giving a SEP of 0.5% absolute vinyl acetate concentration. This result may actually be approaching the uncertainty of the reference values, which is the limit of the predictive ability of a method based on SEP. The results are summarized in table 2.5.1, and plots of predicted vs. reference % vinyl acetate for the full calibration and the restricted calibration set are shown in figures 2.5.6 and 2.5.7. Improvement with restriction of the calibration set has been observed by Fredericks et al. with respect to the factor analysis of FT-IR transmission spectra of coals.[109] This may also be an appropriate approach for quality control applications where values are expected to fall within a limited range.

Note that composition has been predicted in spite of changing sample thickness and the additional non-linearity that it causes. Given this variance with respect to thickness a calibration model was developed to predict thickness with varying vinyl acetate concentration and temperature using the same spectral data. The results of the predicted vs. reference thickness are shown in Figure 2.5.8. The SEP for thickness is 0.02 mm. These results are particularly interesting as non-invasive methods for sample thickness measurements are in demand for continuous process monitoring.

Again a calibration model was developed to predict temperature with varying composition and thickness using the same spectral data. The results of this analysis produced an SEP of 4 °C while the total temperature range was only 20 °C. These results are not nearly as satisfying as the previous predictions of vinyl acetate concentration and thickness especially in light of the fact that remote temperature measurements are routinely made using infrared methods. A probable explanation for this is that temperature control in these experiments was not precise. This was later

TABLE 2.5.1 Summary of predictions for polymer samples.

Data Type	Standard Error of Prediction					
	Conc. (%)	Factors	Thickness (mm)	Factors	Temp. (°C)	Factors
9, 9.5, 15, 18, 26% "Leave one out" Cross validation	1.1	12	0.02	12	4	10
Remove all of one conc.; predict 9.5, 15, 18%	1.4	6	0.03	6	5.2	7
9, 9.5, 15, 18% "Leave one out" Cross validation	0.5	12	0.02	10	4	9
Remove all of one conc.; predict 9.5, 15, 18%	1.0	10	0.02	8	6.4	6

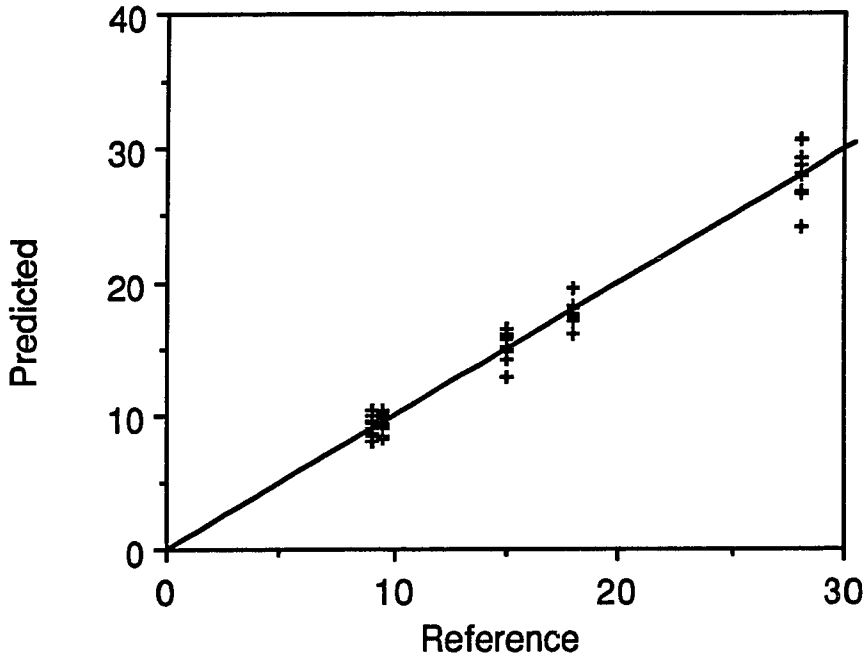

FIGURE 2.5.6 Predicted versus reference concentration values--polymers.

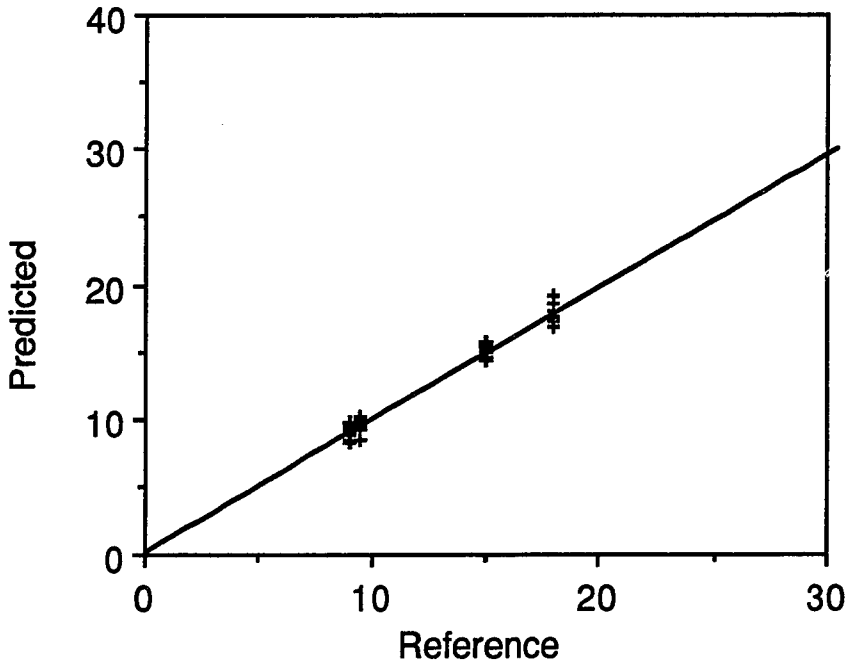

FIGURE 2.5.7 Predicted vs. reference concentration--reduced data set. Predicted vs. reference concentration values for data set using only 9.0, 9.5, 15 and 18% samples.

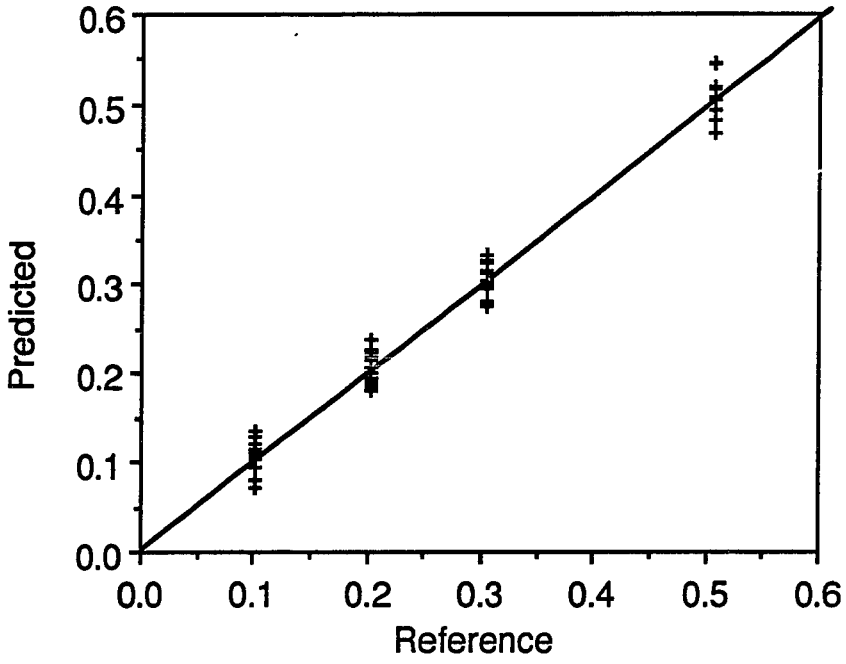

FIGURE 2.5.8 Predicted vs. reference thickness values.

found to be the case in that the temperature controller used was not very reproducible, indicating that the reference values were probably not very precise. And as noted earlier, temperature gradients may have been present across the sample. The poor prediction may therefore be due to poor reference values for sample temperature.

It is commonly said that multivariate calibrations can not do better than the reference method. What this means in practice is that while predicted values may actually be better than the reference values resulting from a certain amount of signal averaging due to the number of samples in the calibration set and the number of wavelengths used, the precision of the calibration is measured by comparing it with the reference values in the form of SEP. Therefore even if the calibration method was able to predict better than the reference method, the difference between reference and predicted values would reflect the "scatter" due to uncertainty in the reference data. Thus poor reference values necessarily result in (apparently) poor prediction.

Normally temperature prediction methods using IES assume a known or constant emittance of the sample; since emittance is changing with concentration and sample thickness, temperature will be more difficult to predict in this case than if emittance values were constant. However, since composition and thickness were predicted well it seemed reasonable to assume that temperature could also be predicted. Additional experiments were necessary (see section 2.6) to verify that temperature may be predicted better if reference values are known with greater precision, and to discount the other possibility that PLS was not able to separate the variation due to temperature from that due to composition and thickness

This set of data has been analyzed extensively in an attempt to better understand how the method works and how the predictive ability might be improved. For example, using second derivative spectra was found to improve the composition prediction

slightly. This might be expected since composition information is mainly contained in the spectral variation found on top of the broad black body background. The predictions were also made using selected wavelength regions of the spectra; however, no subportion of the spectra was found which predicted better than using the entire spectral region, and each portion had some predictive ability indicating that information is present throughout the spectrum which is used by PLS. Examination of latent variable loading plots gave no conclusive information on the importance of various spectral regions.

Table 2.5.1 summarizes the results from these initial experiments using infrared emission coupled with multivariate data analysis as a quantitative analytical technique. Using IES methods, the challenge of prediction of composition of samples which are not simple mixtures of the components of interest, but the products of polymerization reactions, has been met within precision limits reasonable for process analysis situations.

The ethylene/vinyl acetate copolymer system used was chosen due to the interest in process analysis applications. These experiments do not show the ultimate capabilities of the method because the reference values were not known to high precision for either composition or thickness in this data set. The experiments which follow were conducted on better characterized samples.

The number of factors used for the models may seem excessive. But it must be remembered that the uncorrected single beam spectral data were used in which non-linear variations are observed, forcing the model to use more linear factors than one might expect from such a chemically simple system. PLS, being a linear method, must model non-linearities by using additional factors. The major problems arise from the lack of linearity of intensity due to multiple radiation transfer events, which are in turn

dependent on sample temperature and geometry (thickness) as well as the logarithmic nature of the relationship between spectral intensities and concentration or thickness. The method used to choose the number of latent variables to retain is based on the ability of the method to predict a sample not in the calibration set (cross validation) so that the data are not being overfit.

2.6 Liquid Samples--Emission

One of the major limitations of the initial study of the polymer samples is that the true precision of the reference values is either not known (composition and thickness) or known to be poor (temperature). It is therefore difficult to separate the prediction error due to the data analysis method from prediction error due to uncertainty in the reference values; that is, we cannot truly determine how well the calibration method is predicting compared with the best that could be done which is limited by the uncertainty of the reference method. Therefore another study was done using liquid samples in an adjustable pathlength cell so that composition, thickness and temperature values will be known with greater precision to better determine the precision of the calibration method.

2.6.1 Experimental

A Perkin-Elmer model 1720 FTIR spectrometer was modified by Perkin-Elmer to allow use of the instrument for either emission or transmission studies. Changing one reflector allows the emission of a sample outside the instrument to be detected (figure 2.6.1). A medium band MCT (Hg-Cd-Te) detector is used to provide the required sensitivity.

The samples studied are binary mixtures of organic liquids commonly used as stationary phases in gas-liquid chromatography: squalene and di(2-ethylhexyl)sebacate,

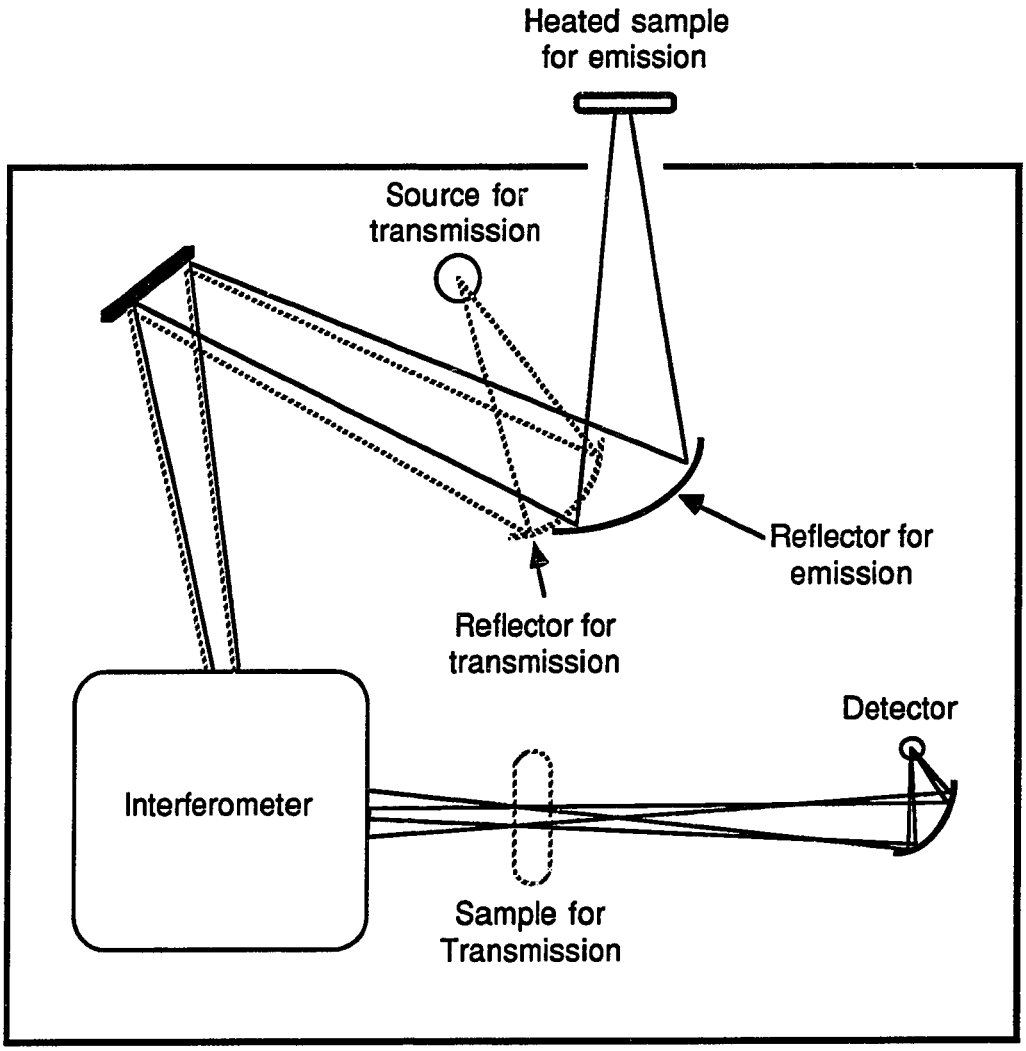

FIGURE 2.6.1 Perkin-Elmer 1720. Block optical diagram of the Perkin-Elmer model 1720 Fourier transform infrared spectrometer. Replacement of one reflector converts the optical system from transmission to emission mode.

seen in figure 2.6.2. These compounds were chosen for their low vapor pressures and high boiling points and therefore thermal stability over a wide range of temperatures. Since they are very complex molecules, they have a large number of strongly absorbing bands in the infrared. They may also serve as a model of organic systems that might be encountered in process analysis situations. Mixtures of 60, 70, 80 and 90% squalene were prepared by weight on an analytical balance.

Samples were placed in a variable pathlength liquid cell. Cell windows are KBr, and again no reflecting backplate is used. The cell pathlength is adjustable from 50 micrometers to 5 mm, and pathlengths of 0.1, 0.2, 0.4, 0.6, 1, 3 and 5 mm were used.

The circumference of the cell was wrapped in a heating tape whose temperature was controlled by a variable voltage power supply. Sample temperature was accurately measured by an RTD temperature sensor placed against the back window of the cell. For longer pathlength samples, a thermocouple could also be placed inside the cell to verify the measurement, and temperatures were in agreement within 1° C. The raw emission spectrum, 2nd derivative of the emission spectrum and raw interferogram from the instrument were recorded for each concentration and thickness at 4 random temperatures in the range between 45 and 80° C. A 500 point spectrum was used for the PLS analysis from 3000 - 500 cm^{-1} at 5 cm^{-1} intervals for emission and derivative spectra; the entire 200 point interferogram was used for interferogram predictions.

2.6.2 Results and Discussion

A typical spectrum is shown in figure 2.6.3. Although the interferometer portion of the instrument may be purged and sealed, a significant portion of the beam's path is through room atmosphere (between the sample and the instrument, and through the normal sample compartment to the detector). This results in observable fine structure

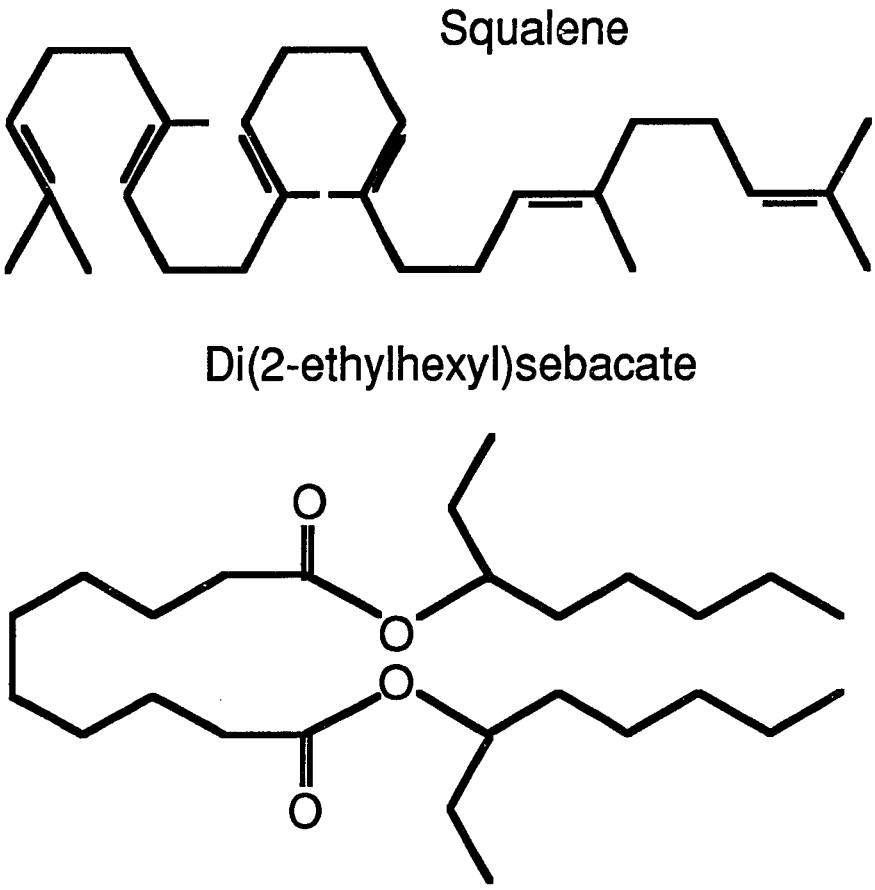

FIGURE 2.6.2 Chemical structures. Chemical structures for squalene and di(2-ethylhexyl)sebacate.

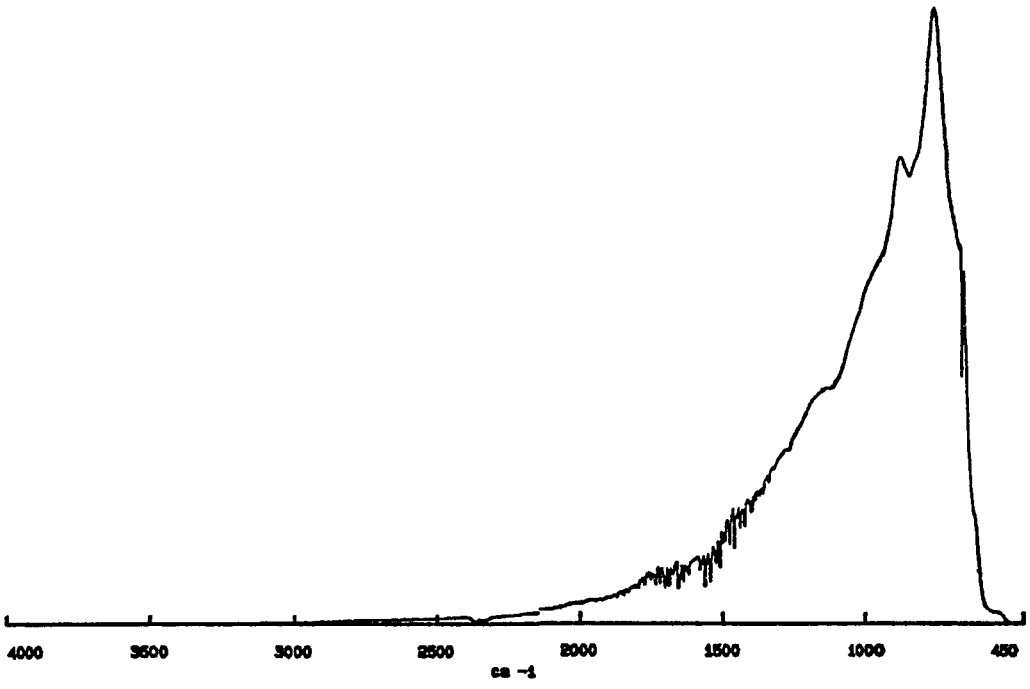

FIGURE 2.6.3 Liquid emission spectrum. Emission spectrum of 80% squalene sample at 0.2 mm and 78° C.

due to absorption by atmospheric H_2O and CO_2, especially between 1350 and 1800 and between 2300 and 2400 cm^{-1}. The sharp drop in intensity from 550 to 450 cm^{-1} is due to instrument and detector response. The low intensities above 2000 cm^{-1} are due to the relatively low temperature of the samples related to Planck's equation. Some of the additional apparent "structure" in the spectrum is actually due to variable instrument response over the wavelength range. No attempt is made to correct for these various response factors; they are assumed to be constant or random enough that they will not affect the calibration from PLS which bases its prediction on variance in the spectra that is actually related to the property being calibrated.

The response at a given wavelength is therefore the product of the instrument response functions and atmospheric transmittance with the room temperature background behind the sample minus the portion of the background absorbed by the sample plus the amount emitted by the sample. The room containing the instrument approximates a black body cavity at room temperature. Therefore a room temperature sample will not be visible, since its emittance equals its absorptance. For example, a 25° sample in a 25° room with $A = \varepsilon = 0.5$ at a given wavelength will absorb half of the 25° background black body radiation and emit half of what a 25° black body would emit, resulting in no net change of the signal. Assuming emittance is constant over temperature, however, the same sample at 50° will absorb half of the 25° background black body radiation and emit half of what a 50° black body would emit, so the increased emission will result in spectral variance which can be observed for higher (or lower) temperature samples against a room temperature background.

Figure 2.6.4 shows a series of spectra of varying concentration for a single thickness at approximately the same temperature (since temperatures were chosen randomly over the 45 - 80 ° C range, they do not match exactly). The changes in

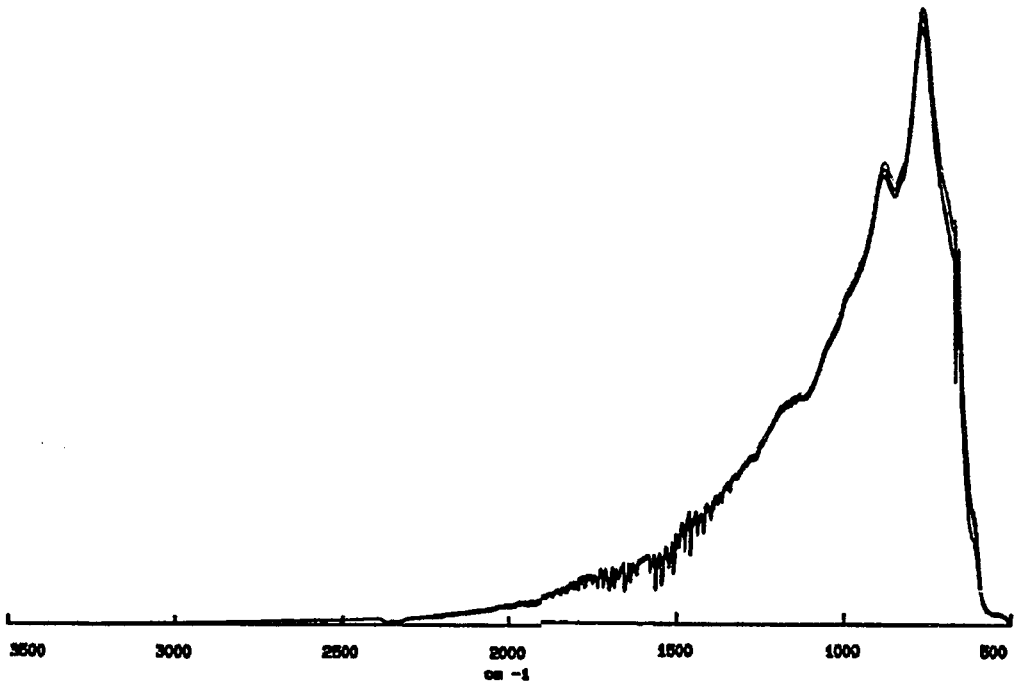

FIGURE 2.6.4 Concentration variation--liquid emission. Emission spectra of 0.4 mm thick samples: 60% at 75° C, 70% at 79° C, 80% at 77° C, and 90% at 75° C.

intensity from one sample to the next are fairly small over much of the spectrum, indicating that emittance values are fairly consistant between samples, with the greatest change visible between 600 and 700 cm^{-1}. A view of the transmission spectra of samples with these same concentrations and thickness in figure 2.6.5 indicates that the samples are nearly opaque at many wavelengths, and at other wavelengths the variation in absorptivities is relatively small.

The effect of temperature on the spectra is seen in figure 2.6.6, with intensities increasing with temperature over the entire spectral range and proportionally larger increases at higher energies. Of the three parameters studied, temperature has the greatest effect on the intensities in the spectra.

Figure 2.6.7 shows spectra at a constant composition and approximately the same temperature with thickness varying. Variation in the emission in the 600 to 700 cm^{-1} region is much more pronounced, as well as the region between 1750 and 2300 cm^{-1} in spite of the relatively low intensities in that portion of the spectrum. Transmission spectra for samples of the same concentration and thicknesses in figure 2.6.8 confirm that the greatest variation in absorptivities/emittance values occur in these regions. Again, many wavelengths are nearly opaque even for the very thin samples. Thus although the thinner samples are in a similar range of thicknesses to the polymer samples used in the earlier study, the optical densities are much higher. The thickest sample transmits less than 3% of the incident radiation over the entire IR region, indicating that one would expect it to approach black body emission.

However, when the PLS algorithm is used as before to predict sample concentration from the emission spectra, sufficient information remains in the spectra to allow reasonable concentration prediction. Table 2.6.1 summarizes the predictive ability

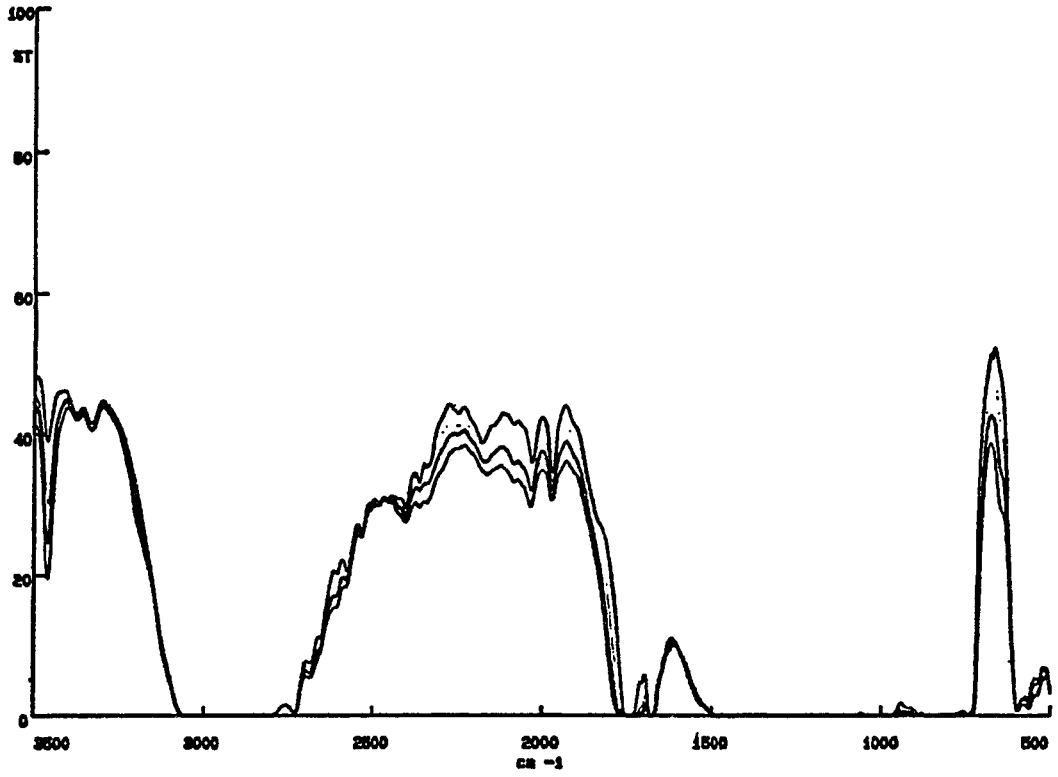

FIGURE 2.6.5 Concentration variation--transmission. Transmission spectra of 60, 70, 80 and 90% squalene samples 0.4 mm thick.

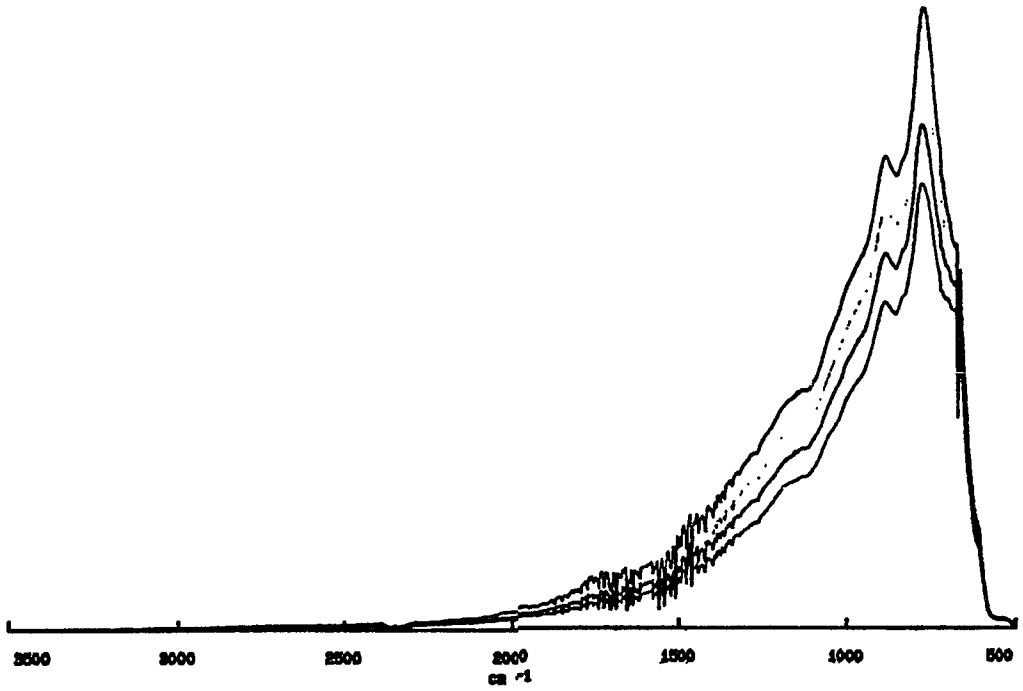

FIGURE 2.6.6 Temperature variation--liquid emission. Emission spectra taken at 50, 60, 68 and 78° C of 0.2 mm thick 80% squalene sample.

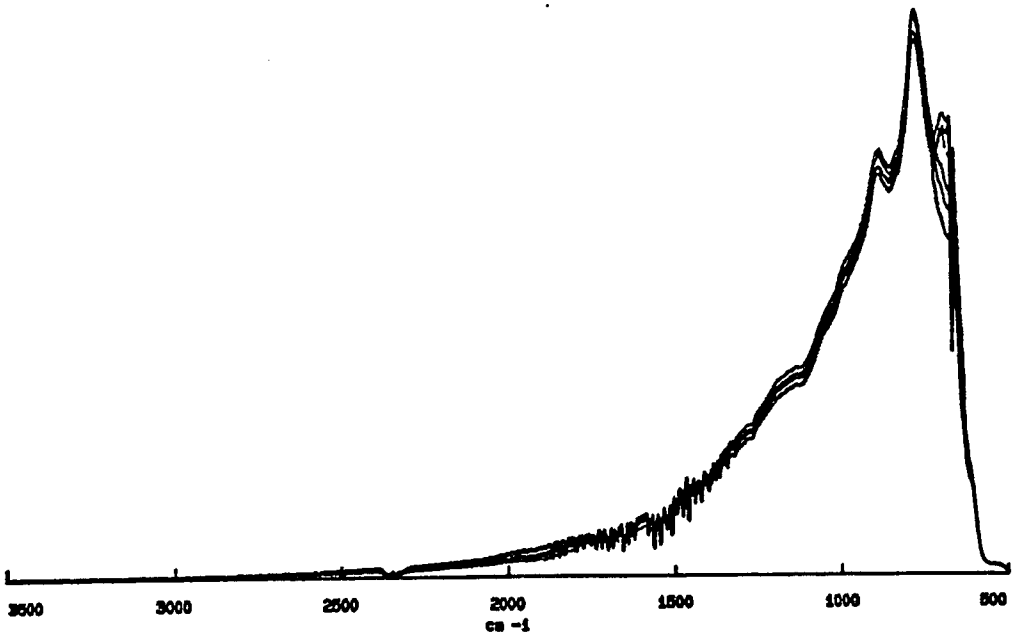

FIGURE 2.6.7 Thickness variation--liquid emission. Emission spectra of 80% squalene sample taken at: 0.1 mm and 66° C, 0.2 mm and 68° C, 0.4 mm and 69° C, 0.6 mm and 67° C, 1.0 mm and 67° C, 3.0 mm and 68° C, and 5.0 mm and 65° C.

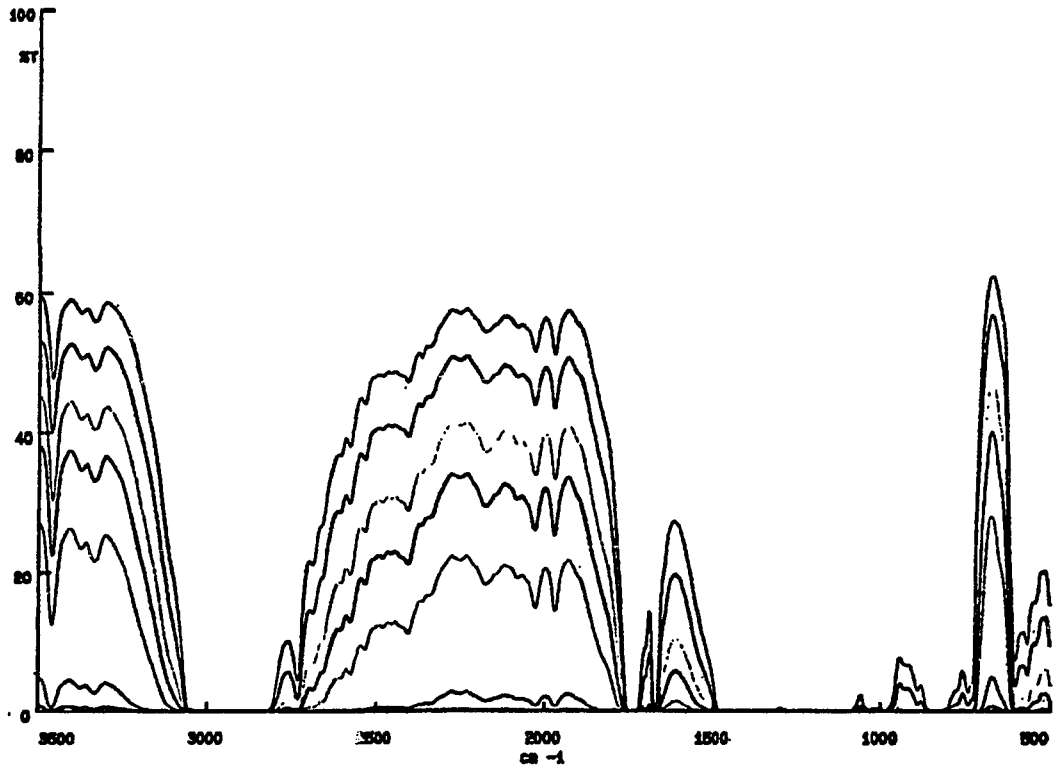

FIGURE 2.6.8 Thickness variation--liquid transmission. Transmission spectra of 80% squalene sample taken at 0.1, 0.2, 0.4, 0.6, 1.0, 3.0 and 5.0 mm.

TABLE 2.6.1 Prediction results for liquid emission. Summary of prediction results for emission spectra of liquids.

Data Type	Standard Error of Prediction					
	Conc. (%)	Factors	Thickness (mm)	Factors	Temp. (°C)	Factors
Thick (0.6-5mm) samples Emission spectra	3.4	10	0.43	11	0.7	14
Thin (0.1-0.6mm) samples Emission spectra	1.6	16	0.03	15	0.9	13
Thin (0.1-0.6mm) samples 2nd deriv. spectra	3.0	11	0.05	10	1.0	9
Thin (0.1-0.6mm) samples Interferograms	2.8	10	0.05	14	0.7	12

of the method for certain subsets of the data, along with the number of latent variables (factors) found to be significant in the calibration.

When samples with thicknesses in the 0.6 - 5 mm range are used, the SEP for concentration predictions is 3.4% absolute over the 60 - 90% range. While such results may not seem impressive in a day of high precision measurements, they may be adequate for many process analysis applications and are certainly impressive results considering the complexity of the spectra used in the measurement.

Prediction of the thickness of these samples gives a SEP of 0.43 mm over the 0.6 - 5 mm range.

Temperature in this case is predicted quite well, with a SEP of 0.7° C over the 45 - 80° range. This verifies that temperature prediction is possible from emission spectra using PLS when temperature values are known to sufficient precision in the calibration set.

For thinner samples in the 0.1 - 0.6 mm range, concentration and thickness predictions are much better. Of the 64 possible spectra, 3 were removed due to experimental problems. An additional 3 were found statistically to be spectral outliers by an F-test. These six samples were removed from the calibration set. Concentration predictions showed a SEP of 1.6% absolute over the 60 -90% range. Sample thickness had SEP of 0.03 over the 0.1 - 0.6 mm range.

Temperature was predicted with a SEP of 0.9°, still impressive being within one degree. While 13 factors were used for this prediction, it should be noted that a single factor predicted temperature with a SEP of 1.6, so it appears that the main temperature effect is easily modeled while additional factors make slight corrections for the non-linearities.

Table 2.6.1 also shows that the use of second derivative spectra for the prediction resulted in slightly poorer prediction for the samples for all three parameters, although it used 4 or 5 fewer latent variables to make its optimal prediction. Second derivative spectra tend to remove broad baseline variations to bring out the fine structure of the spectrum; this may help explain the decrease in the number of latent variables used in prediction.

It is interesting to note that the prediction can also be made directly from the interferogram, without transforming to the spectral domain. The concentration and thickness predictions are again slightly worse than the prediction from the emission spectra, but still as good or better than the second derivative predictions. Temperature for these samples was actually predicted better by using the interferograms than either emission or derivative spectra, with a SEP of 0.7° C. Thus the prediction is not dependent on responses at individual wavelengths, but on the information which is present in the entire spectrum whether transformed into the spectral domain or left in the original time (interferogram) domain.

The success of the PLS method in predicting composition, sample thickness and sample temperature with these liquid samples verifies the validity of the results of the earlier polymer studies that IR emission shows great promise as an analytical tool for certain process situations.

2.7 Liquid Samples--Transmission and Absorbance

One concern expressed about the results in both the polymer and liquid studies above is the number of latent variables retained in developing the models, which generally run from 10-16. The validity of the results can so far be supported by two facts. First of all, in cross validation the predicted sample is not used in the calibration

set, which assures that the data is not being overfit. Secondly, the large number of latent variables retained might be expected from the complexity of the spectra. The three major effects on the spectra of composition, thickness and temperature are all also non-linear in emission spectra. Therefore if each of these effects requires 3 or 4 factors to describe its non-linearities, 10 or more factors might easily be expected.

In the more typical transmission experiments, response is linearized for concentration and thickness effects by converting data to absorbance units. In this section, spectra of the liquid samples are taken in the transmission mode and a comparison is made in the number of factors retained and predictive ability for transmission, absorbance and emission spectra of these samples.

2.7.1 Experimental

Squalene/di(2-ethylhexyl) sebacate mixture samples are prepared as in section 2.6.1 with concentrations 60, 65, 70, 75, 80, 85 and 90% squalene; the three additional concentrations have been added to assure a sufficiently large calibration data set will be obtained. Temperature will not be varied or predicted, since it has minimal effect on transmission spectra. Transmission spectra are obtained for these samples in the variable pathlength cell for the thicknesses used earlier from 0.1 to 5.0 mm on the same PE 1720 FTIR using the instrument source and DTGS detector (figure 2.6.1). Transmission spectra are also transformed to absorbance units, and spectra are saved in both transmission and absorbance units. The Perkin-Elmer instrument truncates absorbance values greater than 5; these data points were given the value 5.

Data analysis was done using PLS as before, dividing each set into thin samples between 0.1 and 0.6 mm and thicker samples between 0.6 and 5 mm, and using 500 point spectra from 3000 - 500 cm^{-1} at 5 cm^{-1} intervals.

2.7.2 Results and Discussion

Typical spectra of samples with changing concentration are shown in figures 2.7.1 and 2.7.2 in transmission and absorbance units respectively. As concentration changes, spectral intensities may increase or decrease, depending on whether squalene or di(2-ethylhexyl)sebacate is more absorbing at a given wavelength. Intensities at certain wavelengths remain nearly unchanged with concentration, indicating that the transmittance values of the two components are nearly the same at those wavelengths.

Figures 2.7.3 and 2.7.4 show spectra with changing thickness at constant composition. Absorbance increases and transmission decreases as the sample thickness increases. The thickest sample transmits less than 3% of the incident radiation over the entire spectrum; however in absorbance units some spectral features are still clearly visible indicating that spectral information is still available.

Results from the PLS analysis are summarized in table 2.7.1, along with the earlier results from the emission experiments. For thicker samples, the emission spectra showed the best prediction of sample concentration with a SEP of 3.4 vs. 6.6 for absorbance and 4.0 for transmission. Thus there is an indication that emission spectroscopy may have an advantage over transmission spectroscopy in some instances. Thickness, however, was predicted better by absorbance (SEP of 0.21) than emission (0.43), and better yet by transmission (0.1).

As expected, the absorbance spectra require fewer latent variables to make the predictions, requiring only 3 for concentration and 2 for thickness. Emission and transmission both require 10 for concentration and 11 for thickness for their optimal predictions. This implies that the number of factors retained for prediction for emission spectra are reasonable, using about the same number as the less complex transmission spectra. Figure 2.7.5 shows the SEP vs. number of factors used in prediction for the

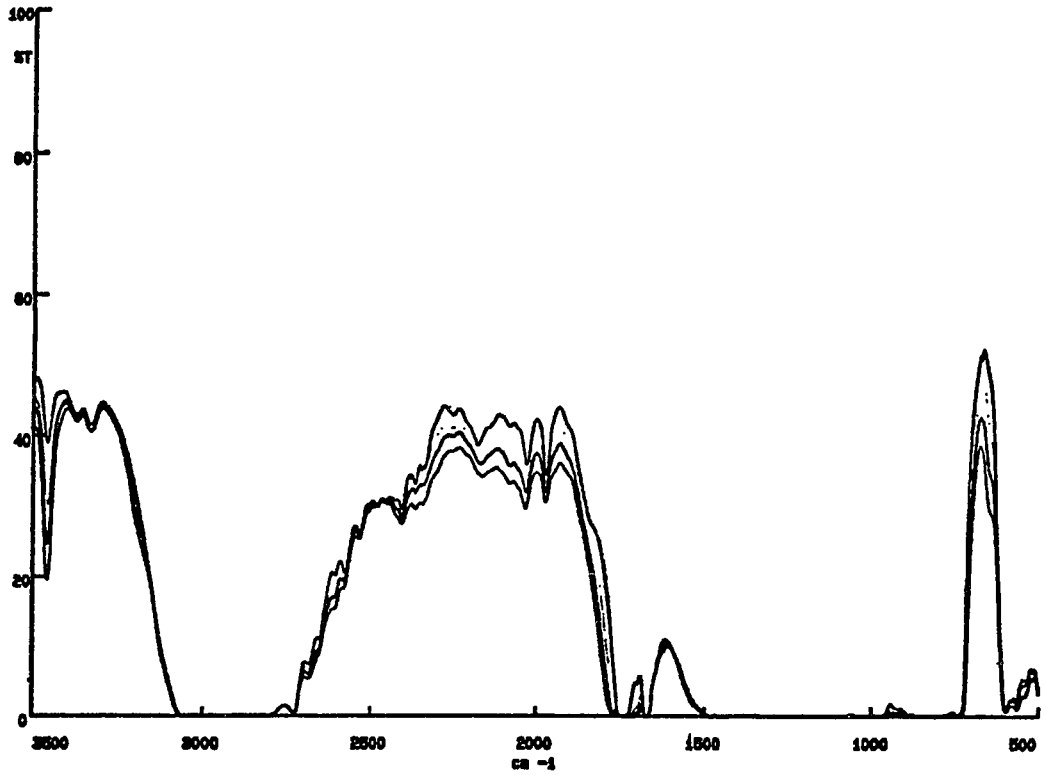

FIGURE 2.7.1 Concentration variation--liquid transmission.

Transmission spectra taken of 0.4 mm thick 60, 70, 80 and 90% squalene samples.

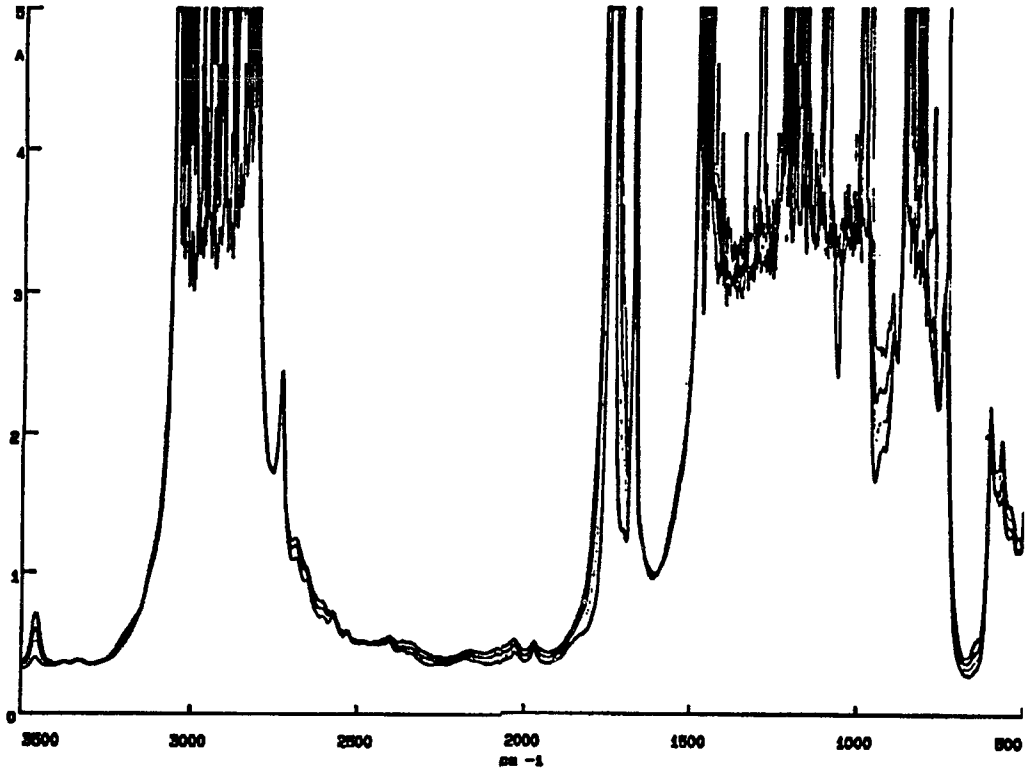

FIGURE 2.7.2 Concentration variation--liquid absorbance.

Absorbance spectra taken of 0.4 mm thick 60, 70, 80 and 90% squalene samples.

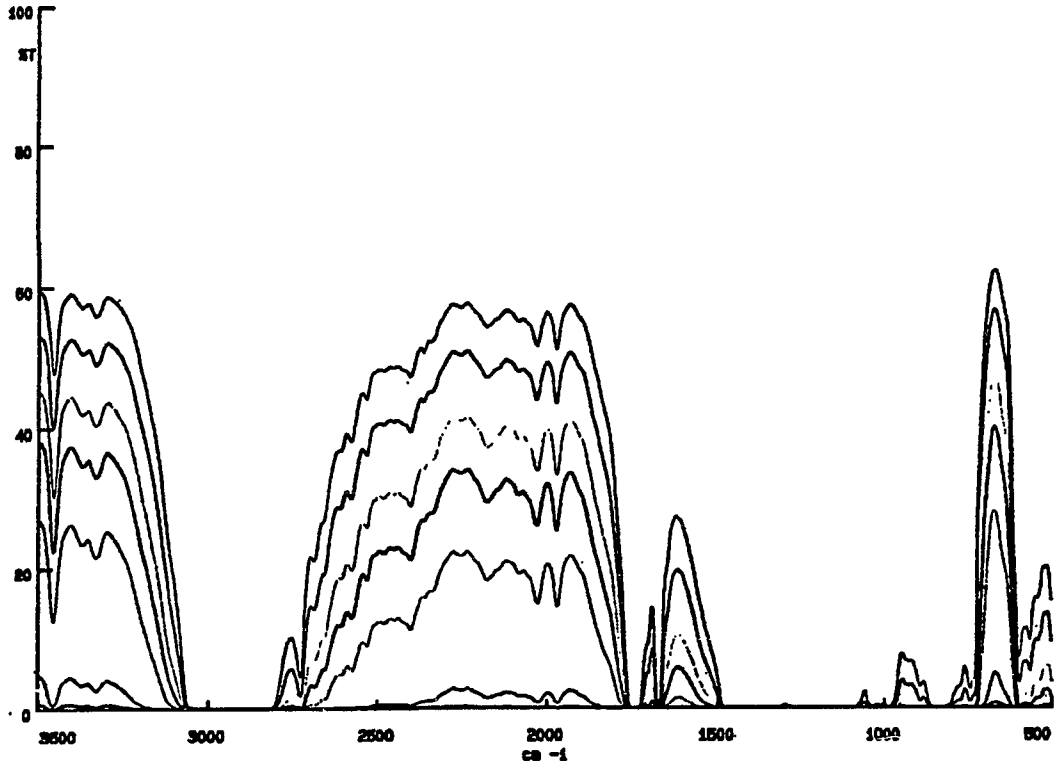

FIGURE 2.7.3 Thickness variation--liquid transmission. Transmission spectra of 80% squalene sample taken at 0.1, 0.2, 0.4, 0.6, 1.0, 3.0 and 5.0 mm.

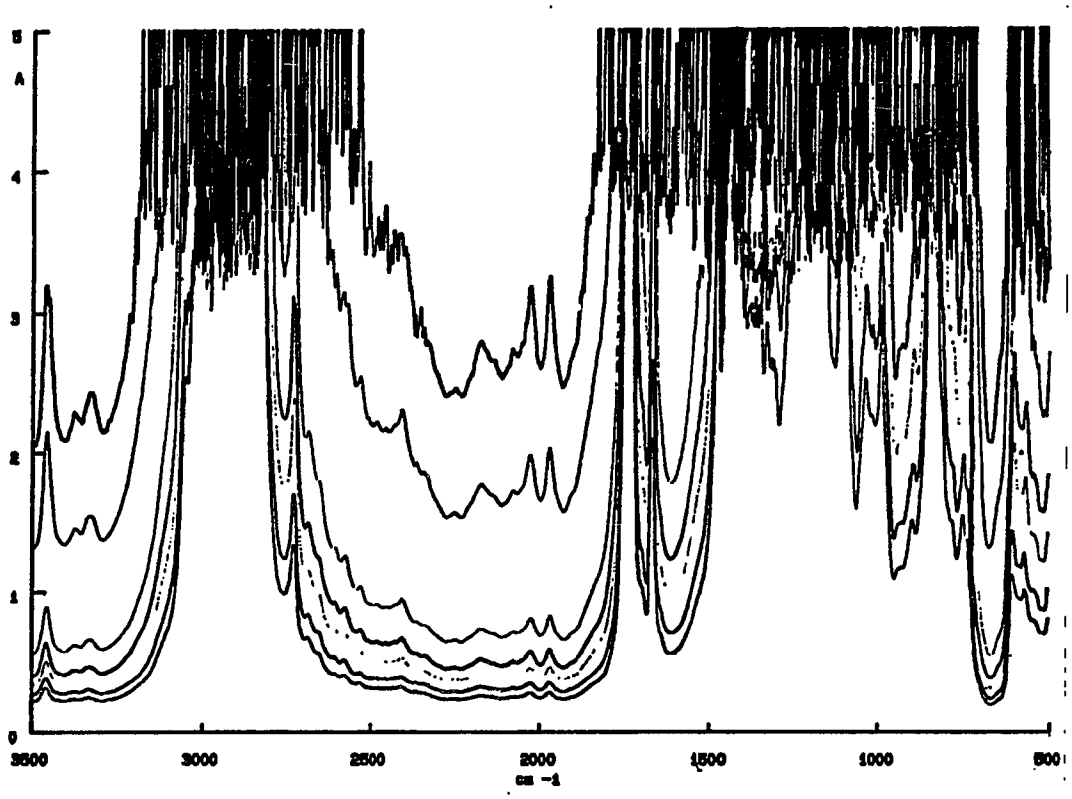

FIGURE 2.7.4 Thickness variation--liquid absorbance. Absorbance spectra of 80% squalene sample taken at 0.1, 0.2, 0.4, 0.6, 1.0, 3.0 and 5.0 mm.

TABLE 2.7.1 Prediction results--liquids. Summary of prediction results for emission, transmission and absorbance spectra of liquid samples.

Data Type	Standard Error of Prediction			
	Concentration (%)	Factors	Thickness (mm)	Factors
Thick (0.6-5mm) samples Emission spectra	3.4	10	0.43	11
Thick (0.6-5mm) samples Transmission spectra	4.0	10	0.1	11
Thick (0.6-5mm) samples Absorbance spectra	6.6	3	0.21	2
Thin (0.1-0.6mm) samples Emission spectra	1.6	16	0.03	15
Thin (0.1-0.6mm) samples Transmission spectra	0.1	13	0.002	12
Thin (0.1-0.6mm) samples Absorbance spectra	2.5	5	0.02	4
Thin (0.1-0.6mm) samples Absorbance trunc. at 3	0.77	9	0.003	11
Thin (0.1-0.6mm) samples Absorbance trunc. at 2	0.51	10	0.002	13

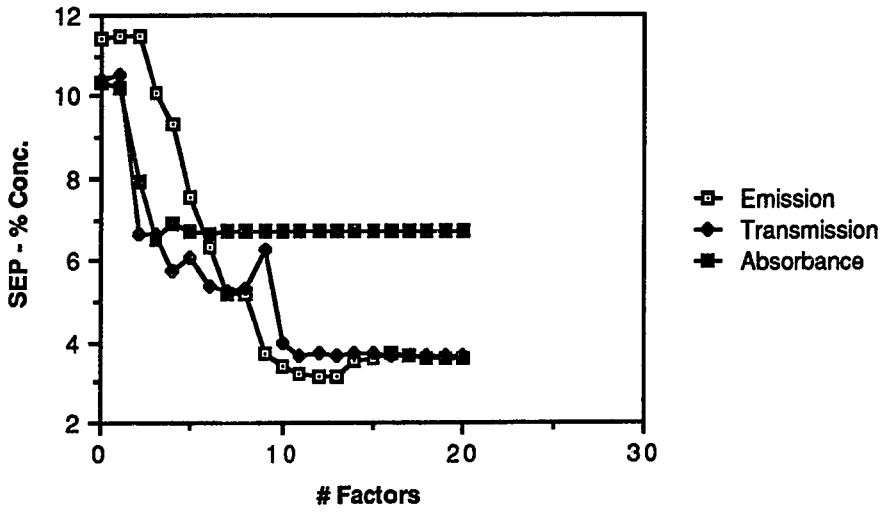

FIGURE 2.7.5 SEP--concentration of thick samples. SEP vs. number of factors retained in the model used for predicting concentration in samples 0.6 - 5 mm thick.

three methods. The optimal prediction is reached quickly by absorbance calibration, and predictive ability levels off as additional factors are added. Emission and transmission predictions continue to improve until they reach their optimal predictions between 10 and 15 factors. A similar trend is seen in figure 2.7.6 for thickness predictions.

For the thinner set of samples, the emission spectra (SEP = 1.6) still have an advantage over absorbance spectra (2.5) in predicting concentration, but surprisingly the transmission calibration (0.1) is an order of magnitude better than both. For thickness prediction absorbance (SEP = 0.02) is slightly better than emission (0.03), but again transmission (0.002) is an order of magnitude better than both. Again, absorbance calibrations use far fewer factors for prediction.

It is not too surprising that transmission measurements are able to predict much better than emission data considering the relatively low temperature samples used in emission. The amount of energy available and therefore signal to noise in the transmission experiment from the high temperature source is obviously much greater. The transmission spectrum is ratioed against the empty sample compartment to help account for any variation due to the atmosphere, instrument drift, etc. The sample emission spectra, on the other hand, are seen as small changes on top of the black body radiation background from the environment surrounding the sample, with much lower intensities of radiation available for detection.

What is especially surprising in this case is that the transmission data predict so much better than absorbance data, when the absorbance values are simply transformations of the transmission data expected to make it more linear which would be expected to improve the predictive power. This can be explained by observing that the transformation of data from transmission to absorbance by the relationship

$$\text{Absorbance} = -\log T$$

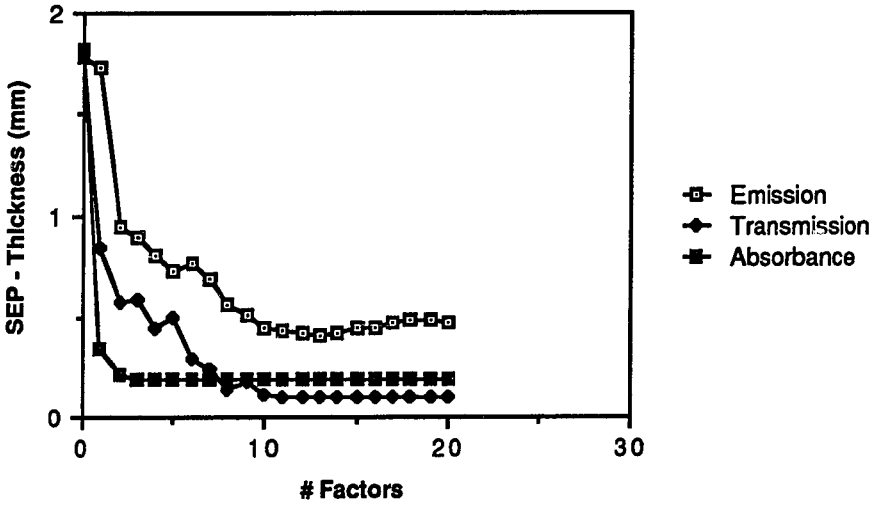

FIGURE 2.7.6 SEP--thickness of thick samples. SEP vs. number of factors retained in the model used for predicting thickness in samples 0.6 - 5 mm thick.

greatly expands the noise in the regions of the spectrum which have low T values. For example, the difference between T values of .0001 and .00001 may be within the noise level of the instrument, and will have little effect on prediction since the difference is miniscule in relation to the total range from 0 to 100. But those same values in absorbance units become 4 and 5, which cover 20% of the range from 0 to 5 absorbance units. Since the samples used have high optical densities over much of the wavelength range, a significant portion of the spectrum now essentially contains only "noise", which apparently degrades the predictive ability of the method. This is clearly visible in the absorbance spectra in figures 2.7.2 and 2.7.4 where spectra appear quite noisy in the 3-5 absorbance unit range. This is also seen in the % of variance in the spectra which has been explained by the model. For the emission and transmission spectra, over 99% of the spectral variance has been explained by the factors retained for prediction. For absorbance, only 75% of the variance is explained by the model.

To further check this assumption, values in the absorbance data set were truncated at 3 absorbance units (which corresponds to 0.001 transmission units or 0.1 %T); that is, all values greater than 3 were reassigned the value 3. The prediction for concentration was improved from a SEP of 2.5 to about 0.8, and thickness from 0.02 to 0.003. Thus removing those values suspected of being in a "noisy" portion of the spectrum greatly improves the predictive ability of the calibration. Truncating the data at 2 absorbance units results in slightly better prediction with a SEP of 0.51 for concentration and 0.002 for thickness. In addition, over 98% of the spectral variance is now explained by the model for data with absorbances truncated at 3, and over 99% for data truncated at 2. The absorbance calibration now retains a larger number of factors. This may be caused by the additional non-linearities imposed on the absorbance data by truncating values, creating a plateau value for each wavelength.

While interference fringes are not obvious in either the transmission or aborbance spectra, it is possible that they are present and this information used by the PLS calibration to give the high precision thickness estimates.

Figures 2.7.7 and 2.7.8 show the trends in the SEP for emission, transmission, absorbance and absorbance truncated (at 3) data over number of factors retained in the model for thin samples. The original absorbance calibration shows the rapid optimization of predictive ability in a few factors, while the truncated absorbance data continues to improve.

This result is very significant for the entire area of multivariate calibration in that it implies that great care must be taken in preprocessing of data to be sure that the transformation used does not scale the noise level of the data up to intolerable levels. This rather unique result may be due in part to the fact that many of these wavelengths do contain useful predictive information over part of their range (for example, for the thinnest samples), but as their value increases the "noise" or uncertainty associated with the value increases due to the -logarithmic relationship.

While transmission and absorbance spectra do predict better than emission for thin samples, this does not imply that emission will not be useful. The reasons cited earlier for using IES methods in process situations have more to do with other considerations which make emission methods more attractive than transmission methods. As long as predictive ability is sufficient for the application, IES should remain a viable tool. And the better prediction by emission on the thicker samples indicates that it may in fact be the best method for prediction in some situations.

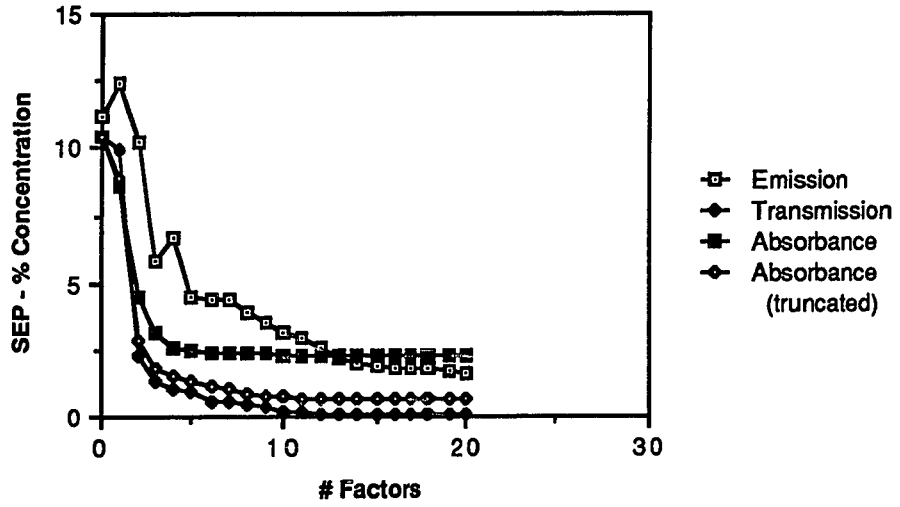

FIGURE 2.7.7 SEP--concentration of thin samples. SEP vs. number of factors retained in the model used for predicting concentration in samples 0.1 - 0.6 mm thick.

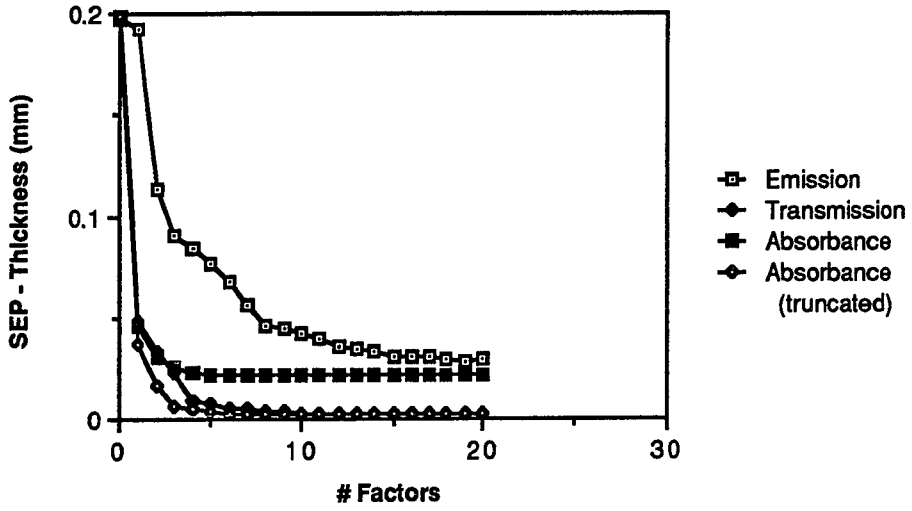

FIGURE 2.7.8 SEP--thickness of thin samples. SEP vs. number of factors retained in the model used for predicting thickness in samples 0.1 - 0.6 mm thick.

References

1. I. E. Frank and B. R. Kowalski, *Anal. Chem.*, **1982**, *54*, 232R - 243R.

2. J. Ruzicka and E. H. Hansen, *Anal. Chim. Acta*, **1975**, *78*, 145-157.

3. F. Zhaolun, J. M. Harris, J. Ruzicka and E. H. Hansen, *Anal. Chem.*, **1985**, *57*, 1457-1461.

4. S. D. Hartenstein, J. Ruzicka and G. D. Christian, *Anal. Chem.*, **1985**, *57*, 21-25.

5. F.Lazaro, A. Rios, M. D. Luque de Castro and M Valcarcel, *Anal Chim. Acta*, **1986**, *179*, 279-287.

6. A. T. Haj-Hussein and A. T. Christian, *Analyst*, **1986**, *111*, 65-68.

7. L. T. Skeggs, *Am. J. Clin. Pathol.*, **1957**, *28*, 311-322.

8. J. Ruzicka and E. H. Hansen, *Anal. Chim. Acta*, **1978**, *99*, 37-76.

9. J. Ruzicka and E. H. Hansen, *Flow Injection Analysis*, **1988**, Wiley-Interscience, New York.

10. J. Hungerford, *Thesis*, University of Washington, **1986**.

11. J. T. Vanderslice, A. G. Rosenfeld and G. R. Beecher, *Anal. Chim. Acta*, **1986**, *179*, 119-129.

12. G. Taylor, *Proc. Roy. Soc.*, **1953**, *A219*, 186-203.

13. R. Aris, *Proc. Roy. Soc.*, **1956**, *A235*, 67-77.

14. H. S. Fogler, *Elements of Chemical Reaction Engineering*, **1986**, Prentice-Hall, Englewood Cliffs, NJ.

15. J. C.Sternberg, *Advances in Chromatography, vol. 2*, ed. J. C. Giddings and R.A. Keller, Marcel Dekker, New York, **1966**, 205-270.

16. R. S. Schifreen, D. A. Hanna, L. D. Bowers and P. W. Carr, *Anal. Chem.*, **1977**, *49*, 1929-1939.

17. J. Ruzicka and E. H. Hansen, *Anal. Chim. Acta*, **1984**, *161*, 1.

18. B. C. Erickson, B. R. Kowalski and J. Ruzicka, *Anal. Chem.*, **1987**, *59*, 1246-1248.

19. J. Ruzicka and E. H. Hansen, *Anal. Chim. Acta*, **1986**, *179*, 1-58.

20. J. Ruzicka, *Anal. Chem.*, **1983**, *55*, 1040A-1053A.

21. J. Mindegaard, *Anal. Chim. Acta*, **1979**, *104*, 185-189.

22. H. Bergamin F., E. A. G. Zagatto, F. J. Krug and B. F. Reis, *Anal. Chim. Acta*, **1978**, *101*, 17-23.

23. J. Toei and N. Baba, *Anal. Chem.*, **1986**, *58*, 2348-2350.

24. A. Rios, M. D. Luque de Castro and M Valcarcel , *Anal. Chem.*, **1986**, *58*, 663-664.

25. D. Betteridge and B. Fields, *Anal. Chem.*, **1978**, *50*, 654-656.

26. E. H. Hansen, J. Ruzicka, F. J. Krug and E. A. G. Zagatto, *Anal. Chim. Acta*, **1983**, *148*, 111-125.

27. J. Ruzicka, J. W. B. Stewart and E. A. Zagatto, *Anal. Chim. Acta*, **1976**, *81*, 387-396.

28. L. Anderson, *Anal. Chim. Acta*, **1979**, *110*, 123-128.

29. L. S. Ramos, *et al.*, *Anal. Chem.*, **1986**, *58*, 294R-315R.

30. J. B. Dawson and D. C. Chilvers, *Analyst* , **1984**, *109* , 473-475.

31. J. P. Foley and J. G. Dorsey, *J. Chromatogr. Sci.* , **1984**, *22*, 40-46.

32. R. A. Vaidya and R. D. Hester, *J. Chromatogr.*, **1984**, *287*, 231-244.

33. W. H. Lawton and E. A. Sylvestre, *Technometrics*, **1971**, *13*, 617-633.

34. M. A. Sharaf and B. R. Kowalski, *Anal. Chem.*, **1982**, *54*, 1291-1296.

35. D. W. Osten and B. R. Kowalski, *Anal. Chem.*, **1984**, *56*, 991-995.

36. D. W. Osten and B. R. Kowalski, "Multivariate Self-Modeling Curve Resolution Program", Laboratory for Chemometrics, Department of Chemistry, University of Washington, Seattle, WA 98195.

37. D. W. Osten and B. R. Kowalski, *Anal. Chem.*, **1985**, *57*, 908-917.

38. P. R. Griffiths, *Appl. Spectrosc.* **1972**, *26(1)*, 73-76.

39. T. Hirschfeld, *Appl. Opt.* **1978**, *17(9)*, 1400-1412.

40. J. Hvistendahl, E. Rytter, H.A. Oye, *Appl. Spectrosc.* **1983**, *37*, 182-187.

41. J. B. Callis, D. L.Illman, B. R. Kowalski, *Anal. Chem.*, **1987**, *59*, 624A-637A.

42. A. Hadni, *Essentials of Modern Physics Applied to the Study of the Infrared*, Pergamon Press, New York, **1967**.

43. L. T. Lin, D. D. Archibald and D. E. Honigs, *Appl. Spectrosc.*, **1988**, *42(3)*, 477-483.

44. J. B. Bates, in *Fourier Transform Infrared Spectroscopy: Applications to Chemical Systems. Vol. 1.* ed. J. R. Ferraro and L. J. Basile, Academic Press, **1978**, pp.99-142.

45. H. O. McMahon, *J. Opt. Soc. Am.*, **1950**, *40(6)*, 376-380.

46. R. Viskanta and E. E. Anderson, in *Advances in Heat Transfer. Vol. 11.* ed. T. F. Irvine, Jr. and J. P. Harnett, Academic Press, **1975**, 318-441.

47. E. E. Anderson, *J. Quant. Spectrosc. Radiat. Transfer*, **1979**, *21*, 183-192.

48. S. T. Thynell and M. N. Ozisik, *J. Quant. Spectrosc. Radiat. Transfer*, **1986**, *36(1)*, 39-50.

49. P. R. Griffiths, *Am. Lab.*, **1975** (March), 37-45.

50. N. Sheppard, in *Analytical Applications of FT-IR to Molecular and Biological Systems*, ed. J. R. Durig, D. Reidel Publishing, Boston, **1980**, 125-140./

51. P. R. Griffiths and J. A. deHaseth, *Fourier Transform Infrared Spectrometry*, John Wiley & Sons, **1986**, 202-208.

52. A. S. Tenney, *Res. & Dev.*, **1988** (Feb.) 122-126.

53. G. D. Nutter, in *Applications of Radiation Thermometry*, ed. J. C. Richmond and D. P. DeWitt, ASTM Special Technical Publication 895, Philadelphia, **1984**,3-23.

54. J. R. Beattie, *Brit. J. Appl. Phys.*, **1960**, *11*, 151-157.

55. R. Gardon, J. Am Ceramic Soc., **1956**, *39(8)*, 278-287.

56. R. Viskant, P. J. Hommert and G. L. Groninger, Appl. Opt., **1975**, *14(2)*, 428-437.

57. I. H. Farag and R. L. Curran, *Chem. Eng. Comm.*, **1987**, *52*, 291-300.

58. M. L. Rauhe and H. E. Randall, *Solid State Technology*, **1970** (March), 67-87.

59. J. K. Wilmshurst, *J. Chem. Phys.*, **1963**, *39(10)*, 2545-2548.

60. T. R. Kozlowski, *Appl. Opt.*, **1968**, *7(5)*, 795-800.

61. J. B. Bates, *Appl. Spectrosc.*, **1973**, *27(3)*, 204-208.

62. M.J.D. Low and I. Coleman, *Spectrochim. Acta* , **1966**, *22*, 369-376.

63. J. K. Barr, *Infrared Physics*, **1969**, *9*, 97-108.

64. P. H. G. Van Kasteren and L. H. Smeets, *SPIE--Fourier Transform Infrared Spectroscopy*, **1981**, *289*, 83-86.

65. G. E. Guazzoni, *Appl. Spectrosc.*, **1972**, *26(1)*, 60-65.

66. D. Kember and N. Sheppard, *Appl. Spectrosc.*, **1975**, *29(6)*, 496-500.

67. L. M. Gratton, S. Paglia, F. Scattaglia and M. Cavallini, *Appl. Spectrosc.*, **1978**, *32(3)*, 310.

68. G. Fabbri and P. Baraldi, *Appl. Spectrosc.*, **1972**, *26(6)*, 593-599.

69. B. Jonson, B. Rebenstorf, R. Larsson and M. Primet, *Appl. Spectrosc.*, **1986**, *40(6)*, 798-803.

70. P. C. M. van Woerkom and R. L. de Groot, *Appl. Opt.*, **1982**, *21(17)*, 3114-3118.

71. S. F. Kapff, *J. Chem. Phys.*, **1948**, *16(5)*, 446-453.

72. J. L. Lauer and V. W. King, *Infrared Phys.*, **1979**, *19*, 395-412.

73. J. L. Lauer, P. Vogel and G. T. Seng, *Appl. Spectrosc.*, **1985**, *39(6)*, 997-1004.

74. I Coleman and M. J. D. Low, *Spectrochim. Acta*, **1966**, *22*, 1293-1298.

75. N. Harrison, C. S. Bilen and D. J. Morantz, *Polymer Comm.*, **1984**, *25(1)*, 15-17.

76. J. F. Blanke, S. E. Vincent and J. Overend, *Spectrochimica Acta*, **1976**, *32A*, 163-173.

77. D. B. Chase, *Appl. Spectrosc.*, **1981**, *35(1)*, 77-81.

78. R. G. Greenler, *J. Chem. Phys.*, **1969**, *50(5)*, 1963-1968.

79. K. Wagatsume, K. Monma and W. Suetaka, *Appl. Surf. Sci.*, **1981**, *7*, 281-285.

80. V. W. King and J. L. Lauer, *J. Lubrication Technology*, **1981**, *103*, 65-73.

81. S. S. Penner, *Quantitative Molecular Spectroscopy and Gas Emissivities*, Addison-Wesley Publishing, Reading, Mass., 1959.

82. G. N. Plass, *J. Opt. Soc. Am.*, **1959**, *49(8)*, 821-828.

83. C. C. Limbaugh and K. R. Kneile, *J. Quant. Spectrosc. Radiat. Transfer*, **1984**, *31(2)*, 161-171.

84. M. J. D. Low and F. K. Clancy, *Env. Sci. Technol.*, **1967**, *1(1)*, 73-74.

85. H. W. Prengle, Jr., C. A. Morgan, C. Fang and L. Huang, *Env. Sci. Technol.*, **1973**, *7(5)*, 417-423.

86. H. W. Yates, *Appl Opt.*, **1970**, *9(9)*, 1971-1975.

87. W. L. Smith, *Appl. Opt.*, **1970**, *9(9)*, 1993-1999.

88. D. J. W. Kendall and T. A. Clark, *Int. J. Infrared and Millimeter Waves*, **1981**, *2(4)*, 783.

89. J. H. Park, *Appl. Opt.*, **1986**, *25(19)*, 3490-3501.

90. G. W. Small, R. T. Kroutil, J. T. Ditiloo and W. R. Loerop, *Anal. Chem.*, **1988**, *60*, 264-269.

91. M. J. D. Low and I. Coleman, *Appl. Opt.*, **1966**, *5(9)*, 1453-1455.

92. F. Nerry, J. Labed and M. Stoll, *Appl Opt.*, **1988**, *27(4)*, 758-764.

93. K. Masuda, T. Takashima and Y. Takayama, *Remote Sensing of the Environment*, **1988**, *24*, 313-329.

94. R. Frech and J. B. Bates, *Spectrochim. Acta*, **1979**, *35A*, 685-694.

95. D. L. Stierwalt and R. F. Potter, in *Report of the International Conference on the Physics of Semiconductors*, July **1962**, 513-520.

96. W. Folberth and G. Heim, *SPIE - Fourier and Computerized Infrared Spectroscopy*, **1985**, *553*, 129-130.

97. J. W. Robinson, H. M. Barnes, C. Woodward and J. W. Robinson, *Anal. Chim. Acta* , **1968**, *43*, 119-128.

98. D. M. Hailey, H. M. Barnes, C. Woodward and J. W. Robinson, *Anal. Chim. Acta*, **1971**, *56*, 161-174.

99. D. M. Hailey, H. M. Barnes and J. W. Robinson, *Anal. Chim. Acta*, **1971**, *56*, 175-183.

100. H. H. Belz, H. Gutberlet, B. Schallert and B. Schrader, *Appl. Spectrosc.*, **1987**, *41(6)*, 1009-1019.

101. L. T. Lin, D. D. Archibald and D. E. Honigs, *Appl. Spectrosc.*, **1988**, *42(3)*, 477-483.

102. D. M. Haaland and E. V. Thomas, *Anal. Chem.*, **1988**, *60(11)*, 1193-1202.

103. B. R. Buchanan and D. E. Honigs, *Spectrosc.*, **1986**(July), *1(7)*, 40-42.

104. D. M. Haaland, *Anal. Chem.*, **1988**, *60(11)*, 1208-1217.

105. P. Geladi and B. R. Kowalski, *Anal. Chim. Acta*, **1986**, *185*, 1-17.

106. M. A. Sharaf, D. L. Illman and B. R. Kowalski, *Chemometrics*, John Wiley & Sons, New York, **1986**, 281-295.

107. L. Breiman, J. H. Friedman, R. A. Olshen and C. J. Stone, *Classification and Regression Trees* , Wadsworth, Belmont, CA, **1984**.

108. S. Wold, *Technometrics*, **1978**, *20*, 397-405.

109. P. M. Fredericks, J. B. Lee, P. R. Osborn and D. A. J. Swinkels, *Appl. Spectrosc.* **1985**, *39*, 303-310.

VITA

Brice Carl Erickson was born on December 12, 1957 in Mora, Minnesota to Reynold and Marian Erickson. He lived in White Bear Lake, Minnesota where he graduated from Mariner High School in 1976. He attended Concordia College in Moorhead, Minnesota, and participated in a summer internship with the 3M company in St. Paul following his junior year. He received a B.A. in chemistry from Concordia in December of 1979.

He held positions at North Dakota State University in Fargo under Dr. Philip Boudjouk in research on organosilicon compounds, and with Henkel Corp. in Minneapolis in analytical methods development for polymers. From 1981 to 1984 he worked for the State of North Dakota Department of Health in the analysis of environmental samples using a variety of analytical techniques. In 1983, Brice married Shirley Howe.

In 1984 he entered graduate school at the University of Washington. He completed the Ph. D. degree in Analytical Chemistry in August of 1988.

He has accepted a position at Macalester College in St. Paul, Minnesota.